FORSCHUNGSZENTRUM JÜLICH GmbH

Institut für Kernphysik

Beta Decay Studies of Shell Model Aspects of N = 83 and 84 Nuclei

Roberto Menegazzo

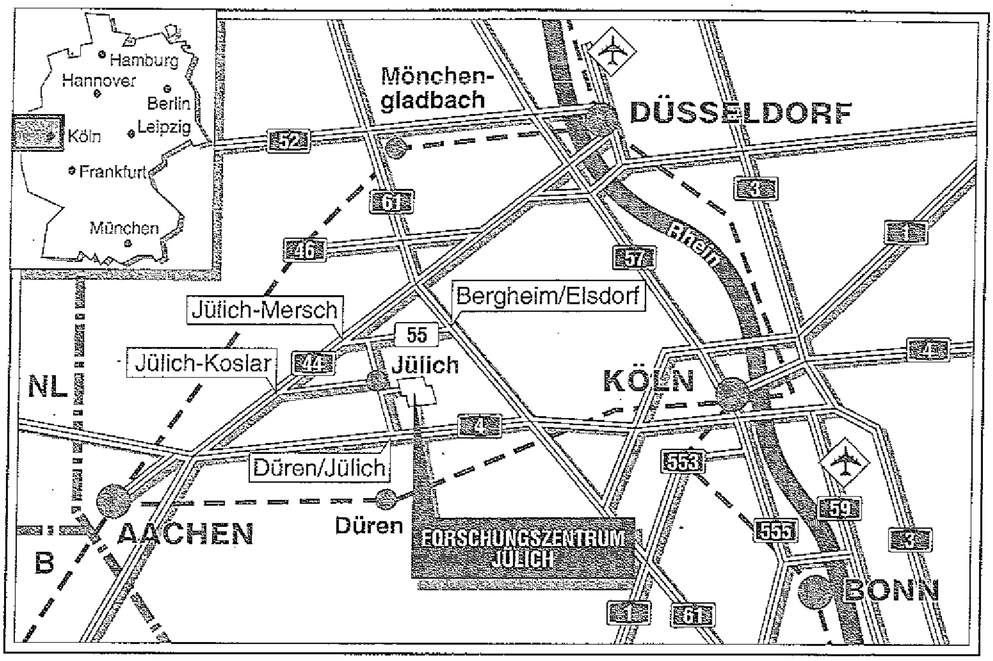

Berichte des Forschungszentrums Jülich ; 2529
ISSN 0366-0885
Institut für Kernphysik Jül-2529
D 38 (Diss. Universität Köln)

Zu beziehen durch: Forschungszentrum Jülich GmbH · Zentralbibliothek
Postfach 1913 · D-5170 Jülich · Bundesrepublik Deutschland
Telefon: 02461/61-6102 · Telefax: 02461/61-6103 · Telex: 833556-70 kfa d

Beta Decay Studies of Shell Model Aspects of N = 83 and 84 Nuclei

Roberto Menegazzo

TABLE OF CONTENTS

CHAPTER 1 : Introduction.

It is known since some time that the $^{146}_{64}Gd_{82}$ nucleus displays several features characteristic of a doubly closed nucleus, in some respects similar as ^{208}Pb. The nuclei in the neighbourhood of such doubly closed cores are well described in terms of the spherical shell model. Shell model analyses in heavy nuclei have originally been developed in the ^{208}Pb region, and they were particularly successful when the single particle energies and the two-body nucleon-nucleon interactions were extracted from experimental data. More recently, the empirical shell model has also been applied with good success to the nuclei around ^{146}Gd.

In contrast to ^{208}Pb, which is a stable nucleus, the neutron deficient ^{146}Gd lies far off the stability valley. Consequently, the spectroscopic data on the nuclei around ^{146}Gd originate to a large extend from in-beam γ-ray measurements following fusion-evaporation reactions where preferably the levels at the yrast line are excited. This often presents a limitation since many specific basic excitations that are needed as input for the shell model analysis lie above the yrast line and therefore are still largely unknown.

The only means to identify above-yrast levels in these nuclei is to excite them in β-decay. For allowed transitions, the β-decay directly locates specific configurations in the daughter nucleus, which in their γ-decay will often populate other above-yrast configurations.

In the present thesis I will report results obtained from β-decay studies of nuclei above ^{146}Gd, namely the decays of the $1/2^+$ and $11/2^-$ activities of the N=82 nuclei ^{147}Tb and ^{149}Ho, and the β-decay branch of the $27/2^-$ 3-quasiparticle isomer at 3 MeV excitation in ^{149}Dy. These decay studies have been carried out at accelerators with a separator on-line, where the activity, after extraction from the production target, is mass separated in a magnetic sector field and in general deposited on a transport tape that is periodically moved to the measuring position.

The data reported here have been obtained at the GSI-, the ISOCELE II- at Orsay, and the ISOLDE-CERN on-line mass separators.

The mass separators and also the γ-detection equipment used in these experiments are quite similar at the three installations, but significantly different activity production processes are employed in the three laboratories. By far the highest yields are achieved at ISOLDE where the activity is produced through spallation of Tantalum with a 600 MeV proton beam, but here long isobaric chains are collected giving rise to a higher γ-ray background in the spectra. At GSI, fusion-evaporation reactions close to the Coulomb barrier of Ni-ions on various $\sim 1\,mg/cm^2$ thick metallic target foils with $Z \sim 40$ produce much purer activities but with significantly lower yield. At ISOCELE, proton- or ^{3}He-beams of ~ 200 MeV on selected targets producing the activity through xn-reactions provide high yields of a particular isotope free of the preceeding decays.

The present β-decay studies provide new results on valence-particle-phonon coupling in the $N = 83$ nuclei which relate in a conclusive manner to the quadrupole moment of the core phohon. Moreover, the data quite accurately determine the hitherto unknown $\pi h_{11/2} \rightarrow \nu h_{9/2}$ Gamow-Teller single particle transition strength, and identify important empirical input information for theoretical analyis of the GT-transition strength reduction. Finally the results have provided an empirical determination of the $\pi h_{11/2} \nu h_{9/2}$ two-body residual interaction. With these results is now possible to carry out more comprehensive shell model calculations for nuclei with several valence particles. In the last chapter I will present examples of such parameter-free predictions for yrast energies in $N = 83$ and 84 nuclei with up to ten valence particles. The $\pi h_{11/2} \nu h_{9/2}$ residual interaction is also needed for analysis of the GT-decays in this region. As an example I will discuss the strength functions for the decays of doubly even $N = 82$ nuclei which provide basic data for the attenuation of the Gamow-Teller transition strength.

CHAPTER 2 : ^{147}Gd from $11/2^-$ and $1/2^+$ ^{147}Tb decays.

2.1 Introduction and previous studies.

The ^{147}Gd nucleus with N=83 and Z=64 has one neutron outside the ^{146}Gd closed core. At low excitation energy (E_x< 2 MeV) one expects only a limited number of levels which can be devided into three categories :

(i) the single neutron states with the valence neutron occupying the $f_{7/2}$, $p_{3/2}$, $h_{9/2}$, $p_{1/2}$ (, $f_{5/2}$, and $i_{13/2}$) shell model orbitals (where the latter two might lie somewhat above 2 MeV);

(ii) the two-particle one-hole states $\nu d^{-1}_{3/2} j^2_0$, $\nu s^{-1}_{1/2} j^2_0$ (, and $\nu h^{-1}_{11/2} j^2_0$) where one neutron is lifted above the N=82 energy gap;

(iii) the twelve states formed by the couplings of the $f_{7/2}$ valence neutron with the ^{146}Gd 3^- and 2^+ core excitations at 1.6 and 2.0 MeV.

Although ^{147}Gd has been intensively studied through radioactivity and in-beam experiments, a number of the expected low-lying states are still missing. Largely, these states lie well above the yrast line and are therefore not populated in in-beam experiments. On the other hand most of them may well be indirectly excited after β-decay, and the combination of high detection sensitivity and the use of mass separated samples should then allow to see these states in the decay of the ^{147}Tb $1/2^+$ and $11/2^-$ isomers.

The β-decay pattern of these two isomers should be significantly different. The $h_{11/2}$ valence proton of the high-spin isomer has an ideal β-decay partner in the completely empty $\nu h_{9/2}$ shell into which it can decay via a fast Gamow-Teller (GT) transition while above N=82 there is no partner for allowed decay of the $s_{1/2}$ valence proton.

The description of ^{147}Tb as a pure one-valence-proton nucleus could be, however, too simplified. It is well known that pairing forces smear the sharp boundary between occupied and unoccupied orbitals which corresponds to a probability of pair scattering across the respective shell closure. This effect is dominant in deformed nuclei where the single particle energy separations are smaller than the pairing interaction. In (doubly closed) spherical nuclei, this is in general not the case, but in ^{146}Gd the proton energy gap is comparable to the strength of the pairing interaction and therefore pair scattering into the $h_{11/2}$ orbital above Z=64 cannot a priori be excluded. The decay of a proton from such a scattered pair will proceed as $(\pi h^2_{11/2})_{0^+} \xrightarrow{GT} (\pi h_{11/2} \nu h_{9/2})_{1^+}$ and populate high-lying 3-quasiparticle levels in the daughter nucleus which, in ^{147}Tb $11/2^-$ decay, have the configurations $[(\pi h_{11/2} \nu h_{9/2})_{1^+} \; \pi h_{11/2}]_{9/2^-, 11/2^-, 13/2^-}$.

As mentioned the $\pi s_{1/2}$ valence particle has no allowed decay partner in orbitals above N=82 and therefore very little strength is expected in its decay, as suggested already by the long half life. The decay pattern of the ^{147}Tb $1/2^+$ isomer, which so far was not well investigated, should however change drastically if pair scattering across Z=64 would occur. In this case, decay of a paired $h_{11/2}$ proton should lead to population of 3-quasiparticle states with configurations $[(\pi h_{11/2} \nu h_{9/2})_{1^+} \pi s_{1/2}]_{1/2^+, 3/2^+}$, which should lie at similar energies and be fed with comparable strength as in the $11/2^-$ decay.

The comparison of ^{147}Tb $11/2^-$ and $1/2^+$ decays is therefore of crucial importance to elucidate the question of pair scattering across the Z=64 energy gap, which is one motivation for the measurements described below.

The presence of two decay isomers in ^{147}Tb has since long been recognized [CHU 69], and the decay of the long-lived low-spin isomer was originally investigated by Afanasev et al. [AFA 71] who observed fifteen ^{147}Gd γ-transitions and could place most of them in a ^{147}Gd level scheme from their analysis of summing peaks in singles γ-ray spectra. They assigned the lowest observed excited state, at 1.153 MeV (see Fig.2.3), as the $\nu p_{3/2}$ single particle level from the systematics in the lower-Z N=83 nuclei. Conversion electron measurements [AFA 71, VYL 72] enabled them to specify even parity to levels at 1.293, 1.413 and 1.700 MeV and odd parity to the level at 1.848 MeV. A high-lying level, at 3.977 MeV, has been tentatively proposed from γ-ray energy differences. The interpretation of these states was however harmed by the early incorrect $5/2^+$ $(3/2^+)$ assignement of the ^{147}Tb parent state. These results have been essentially confirmed in a later $\gamma\gamma$-coincidence measurement [NEW 74] except for the level at 3.977 MeV. The authors placed a new low-lying level at 1.759 MeV and measured as 1.6(1) h the half life of the ^{147}Tb low-spin isomer.

Only ten years later 1.6 h ^{147}Tb has been assigned as $1/2^+$ [NAG 81] with the odd proton occupying the $s_{1/2}$ single particle orbital. This result led to a reinterpretation [STY 81] of the ^{147}Gd levels; neutron two–particle one–hole character was proposed for the $1/2^+$ and $3/2^+$ states at 1.292 and 1.412 MeV while the $1/2^-$ state at 1.847 MeV was assigned as the $\nu p_{1/2}$ single particle state.

The 1.83(6) min ^{147}Tb $11/2^-$ decay (see Fig.2.1) proceeds primarily to states in ^{147}Gd at 1.397 and 1.798 MeV [BOW 73, NEW 74]. The small log ft–values establish their $\nu h_{9/2}$ character. A weakly populated 0.997 MeV level was later assigned as $13/2^+$ [KLE 75, KLE 79A] from in–beam γ–measurements.

Many non yrast low– and intermediate – spin states in ^{147}Gd have been identified in a later in–beam experiment [KOM 83], including all the ^{147}Gd states known from the ^{147}Tb $11/2^-$ and $1/2^+$ decays. Spins and parities could be assigned from conversion electron and angular distribution measurements and level configurations have been discussed in terms of the spherical shell model. Five levels close to 1.7 MeV excitation, with spins $11/2^+$ (1.702 MeV), $9/2^+$ (1.643 MeV), $7/2^+$ (1.628 MeV), $3/2^+$ (1,699 MeV) and $1/2^+$ (1.759 MeV), have been interpreted as $\nu f_{7/2} \times 3^-$ levels where the 0.997 MeV state is the lowest–lying septuplet member.

In later neutron pick–up measurements [KAD 89] predominant $s_{1/2}$ and $d_{3/2}$ neutron–hole character has been specified for the states at 1.699 and 1.759 MeV which reassigned the low–lying 1.292 and 1.412 MeV levels as the $1/2^+$ and $3/2^+$ members of the $\nu f_{7/2} \times 3^-$ family.

Independent in–beam data [YAT 86] located an additional low–lying state in ^{147}Gd at 1.944 MeV which has been assigned as $11/2^-$ and interpreted as a $\nu f_{7/2} \times 2^+$ particle–phonon coupling.

2.2 Measurements and experimental results.

2.2.1 ^{147}Tb $11/2^-$ decay.

The 1.8 min ^{147}Tb $11/2^-$ decay has been studied at the GSI on–line mass separator. The A=147 isobars have been produced in a fusion–evaporation reaction with 5 MeV/A ^{58}Ni beam on a ^{93}Nb target. The tape transport cycle of 2 min + 2 min collection + measuring time was optimised for investigation of the

54 sec ^{147}Dy decay, but also gave excellent data for 1.8 min ^{147}Tb decay. Two large volume (>25%) coaxial and 1 planar Ge detectors have been used to measure γγ– and γX– coincidences. Singles spectra have also been recorded in multiscaling mode. Results of a first analysis of these data have been reported in an Annual Report [PII 84].

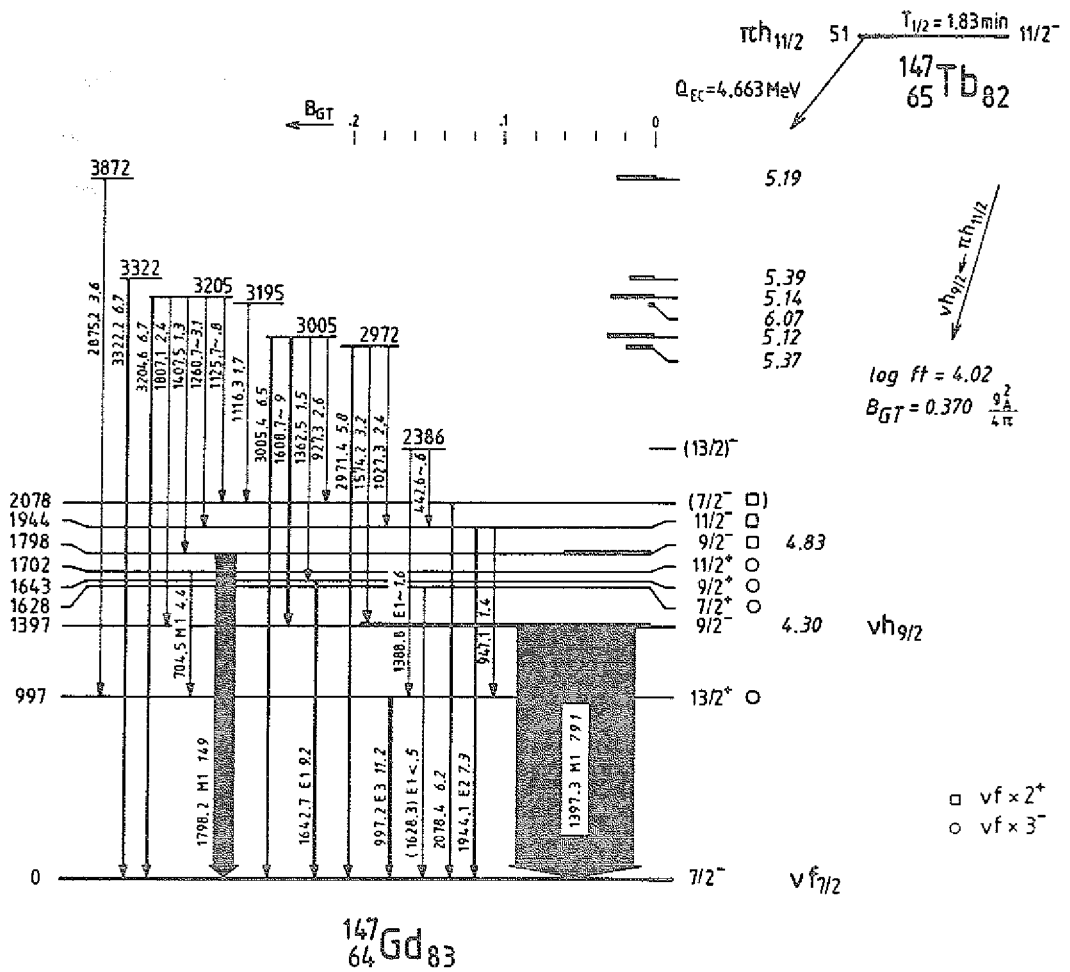

Fig.2.1 Decay scheme of 1.8 min ^{147}Tb 11/2$^-$. Total transition intensities are given per 10^3 parent decays. Specified transition multipolarities are from conversion electron data [STY 81, KOM 83, YAT 86]. The GT–strength in units of $g_A^2/4\pi$ is indicated to the right of the levels.

We have obtained independent data from a separate measurement of ^{147}Dy decay at ISOLDE–CERN, with 600 MeV protons on a Ta target, and have also reanalised the data from the previous experiment. We confirm the earlier reported results, and could extend the decay scheme above 2.5 MeV. All $\gamma\gamma$–coincidence relations required in the level scheme shown in Fig.2.1 are established in the coincidence spectra, and essentially all γ–transitions are observed in coincidence with ^{147}Gd X–rays (Fig.2.2 and Table 2.1). Multipolarities used to calculate the total intensity of transitions in Fig.2.1 from theoretical conversion coefficients [RÖS 78] are from [KOM 83, YAT 86].

Table 2.1: Gamma transitions in ^{147}Gd observed in decay of 1.83 min ^{147}Tb(11/2$^-$).

E_γ (keV)	I_γ^a	Observed coincident transitions[b]	E_i (keV)	$I_i^\pi \rightarrow I_f^\pi$
442.6(5)	~.6	1944	2386.3	(13/2)$^-$ → 11/2$^-$
704.5(3)	4.4(8)	(Gd X),997	1701.7	11/2$^+$ → 13/2$^+$
927.3(9)	2.6(8)	2078	3005.4	(9/2$^-$) → (7/2$^-$)
947.1(4)	1.4(8)	997,(1027,1261)	1944.1	11/2$^-$ → 13/2$^+$
997.2(2)	11.1(16)	Gd X,704,2875,947,1261	997.2	13/2$^+$ → 7/2$^-$
1027.3(3)	2.4(8)	1944	2971.4	(9/2$^-$) → 11/2$^-$
1116.3(5)	1.7(8)	2078	3194.7	(9/2$^-$) → (7/2$^-$)
1125.7(5)	~.8	(2078)	3204.6	(9/2$^-$) → (7/2$^-$)
1260.7(4)	~3.1	Gd(Tb) X,1944,947,997	3204.6	(9/2$^-$) → 11/2$^-$
1362.5(9)	1.5(8)	1643	3005.4	(9/2$^-$) → 9/2$^+$
1388.8(5)	~1.6	Gd(Tb)X,(997)	2386.3	(13/2)$^-$ → 13/2$^+$
1397.3(2)	790(40)	Gd X,1609,1807,1547	1397.3	9/2$^-$ → 7/2$^-$
1407.5(9)	1.3(6)	1798	3204.6	(9/2$^-$) → 9/2$^-$
1574.2(3)	3.2(8)	1397	2971.4	(9/2$^-$) → 9/2$^-$
1608.7(5)	~9	Gd(Tb)X,1397	3005.4	(9/2$^-$) → 9/2$^-$
1628.3(4)	<.5	(Gd X,Tb X)	1628.3	7/2$^+$ → 7/2$^-$
1642.7(3)	9.2(24)	Gd(Tb)X,1363	1642.7	9/2$^+$ → 7/2$^-$
1798.2(2)	149(9)	Gd X,1407	1798.2	9/2$^-$ → 7/2$^-$
1807.1(4)	2.4(8)	1397	3204.6	(9/2$^-$) → 9/2$^-$
1944.1(3)	7.3(16)	(Gd X),1027,1261	1944.1	11/2 → 7/2
2078.4(4)	6.2(16)	927,1116,1126	2078.4	(7/2$^-$) → 7/2$^-$
2875.2(5)	3.6(8)	(Gd X, Tb X),997	3872.4	(11,13/2$^-$) → 13/2$^+$
2971.4(4)	5.8(16)	Gd X	2971.4	(9/2$^-$) → 7/2$^-$
3005.4(4)	6.5(16)		3005.4	(9/2$^-$) → 7/2$^-$
3204.6(4)	6.7(16)	(Gd X)	3204.6	(9/2$^-$) → 7/2$^-$
3322.2(4)	6.7(16)	(Gd X,Tb X)	3322.2	(9/2$^-$) → 7/2$^-$

a) Normalized to 10^3 ^{147}Tb(11/2$^-$) decays; statistical errors quoted.

b) For contaminated gate transitions only the X – rays coincident with the degenerate gate doublet partner are listed; the contaminant γ – rays are omitted.

A summary of the levels populated in this decay is given in Table 2.3. Their spin assignements, and the strength distribution will be discussed in the sections 2.3 and 2.4 .

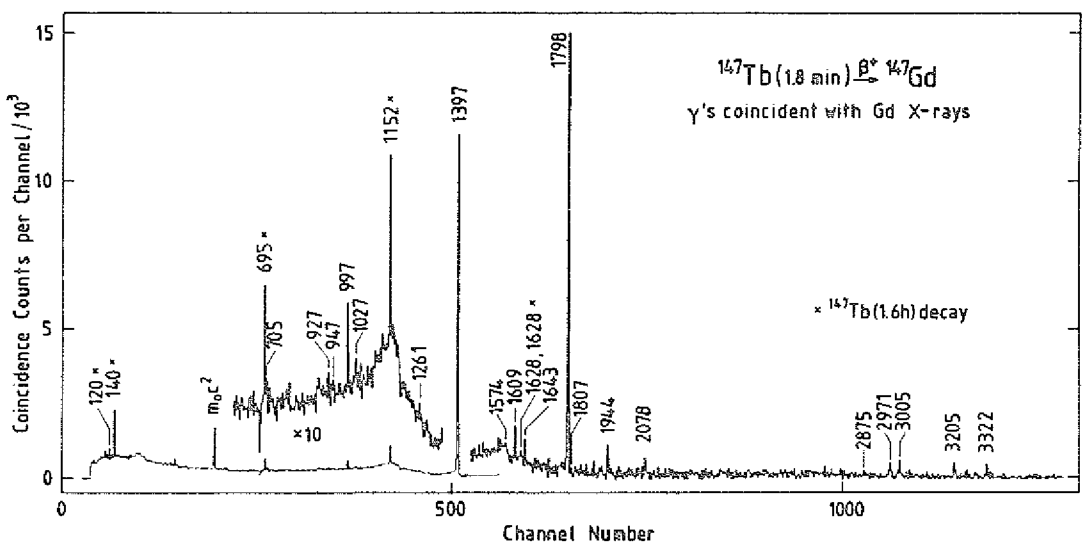

Fig.2.2 Gamma–ray spectrum of 1.8 min ^{147}Tb decay measured in coincidence with Gd X–rays.

2.2.2 ^{147}Tb 1/2$^+$ decay.

The ^{147}Tb activity for investigation of the 1.6 h 1/2$^+$ decay was produced at the ISOCELE II on–line mass separator with a 200 MeV proton beam focussed on a massive (~ 7 gr.) molten ^{nat}Gd target in the separator ion source. The ^{147}Tb was thus obtained free of preceeding activities, but the sources were polluted with 24 d ^{147}Eu, which is more efficiently released from the ion source. It was suppressed through the tape transport cycle with 80 min collection– and 80 min measuring–time. Two large–volume coaxial detectors recorded γγ–coincidences in list mode and γ–singles spectra split in four 20 min subgroups for decay–time evaluation.

Our data confirm the previously known [LED 78] decay scheme including the nine γ–transitions with energies below 2 MeV. In addition we could place many weak high–energy transitions (Fig.2.3), part of them previously identified but unplaced [AFA 71, NEW 74], which establish levels up to 4.2 MeV excitation (Table 2.3).

Table 2.2: Gamma transitions in ^{147}Gd observed in decay of 1.6 h ^{147}Tb(1/2$^+$).

E_γ (keV)	I_γ^{a}	Observed coincident transitions[b]	E_i (keV)	$I_i^\pi \rightarrow I_f^\pi$
119.7(2)	69(7)	SmX,140,1152,348,435,1466,1534, 2423[d],2733	1412.1	$3/2^+ \rightarrow 1/2^+$
140.0(2)	352(14)	Gd X,1152,120,555,348,407,435,1466, 2759,2840,2561,2789,2033,2329,2423, 1534,(2733)	1292.4	$1/2^+ \rightarrow 3/2^-$
347.9(4)	24.1(28)	Eu (Gd) X,140,120,1152	1760.0	$1/2^+ \rightarrow 3/2^+$
407.2(3)[c]	19(4)	Gd(Eu,Sm) X,140,1152	1699.5	$3/2^+ \rightarrow 1/2^+$
434.9(4)[c]	6.5(19)	Eu(Gd) X,1152,140,120	1847.0	$1/2^- \rightarrow 3/2^+$
547.1(3)[c]	22(4)	Gd (Eu) X,1152	1699.5	$3/2^+ \rightarrow 3/2^-$
554.6(2)	47(5)	Gd X,140,1152	1847.0	$1/2^- \rightarrow 1/2^+$
694.6(2)	403(11)	Gd X,1152,2006	1847.0	$1/2^- \rightarrow 3/2^-$
1152.4(2)	928(19)	Gd X,695,140,120,554,2681,2563,547, 348,407,1285,2759,2840,1658,1709, 2733,1534,2423,2329,2006,(1466,2033)	1152.4	$3/2^- \rightarrow 7/2^-$
1285.0(3)	4.7(13)	Gd X,1152	2437.8	$(3/2^-) \rightarrow 3/2^-$
1466.2(2)	11.4(23)	Gd X,140,1152,120	2878.3	$\rightarrow 3/2^+$
1533.7(3)	4.0(13)	Gd (Eu) X,1152,140,120	2945.8	$\rightarrow 3/2^+$
1627.9(4)	34(4)	Gd X	1627.9	$(5/2^+) \rightarrow 7/2^-$
1658.1(3)	4.6(11)	Gd X,1152	2810.5	$\rightarrow 3/2^-$
1708.7(3)	7.2(13)	Gd X,1152	2861.1	$\rightarrow 3/2^-$
1947.6(2)	21.9(28)	Gd X	1947.6	$(5/2^-) \rightarrow 7/2^-$
1970.0(4)	3.2(11)	Gd X,(120[d],1152[d])	(1970.0	$(7/2^-) \rightarrow 7/2^-)$
2006.1(3)	5.2(11)	Gd X,695,1152	3853.1	$\rightarrow 1/2^-$
2033.4(3)	5.5(15)	Gd X,140,1152	3325.8	$\rightarrow 1/2^+$
2329.0(3)	6.4(12)	Gd X,(140,1152)	(3621.4	$\rightarrow 1/2^+)$
2422.6(4)[e]	6.0(15)	Gd X,(140,1152,120[d])	(3715.2	$\rightarrow 1/2^+)$
2438.0(3)	10.8(24)	Gd X	2437.8	$(3/2^-) \rightarrow 7/2^-$
2560.8(4)	5.4(13)	Gd X,1152,(140)	3853.1	$\rightarrow 1/2^+$
2562.9(4)	17.2(24)	Gd X,1152	3715.2	$\rightarrow 3/2^-$
2680.6(2)	36(4)	Gd X,1152	3833.0	$(1/2^-) \rightarrow 3/2^-$
2732.5(3)	2.8(12)	Gd X,1152,(140)	(4144.6	$\rightarrow 3/2^+)$
2758.8(3)	4.7(13)	Gd X,140,1152	4051.2	$\rightarrow 1/2^+$
2788.6(3)	3.9(15)	Gd X,140,1152	4081.0	$\rightarrow 1/2^+$
2840.0(3)	5.2(16)	Gd X,140,1152	4132.4	$\rightarrow 1/2^+$

a) Normalized to 10^3 ^{147}Tb(1/2$^+$) decays; statistical errors quoted.

b) For contaminated gate transitions only the X-rays coincident with the degenerate gate doublet partner are listed; the contaminant γ-rays are omitted.

c) Line obscured in the Orsay spectra by transitions in Sm or Eu. Energies and intensities from: J. Styczen et al., Proc. 4th Int. Conf. of Nuclei far from Stability, Helsingor, p.548, and J. Styczen, private comunication,1983.

d) Weak coincidence relationship inconsistent with adopted placement. Transition placement tentative.

e) Possibly doublet.

The observed coincidence relations are summarised in Table 2.2. Coincidence spectra with Gd X–rays (Fig.2.4) give clear identification for all the ground state transitions.

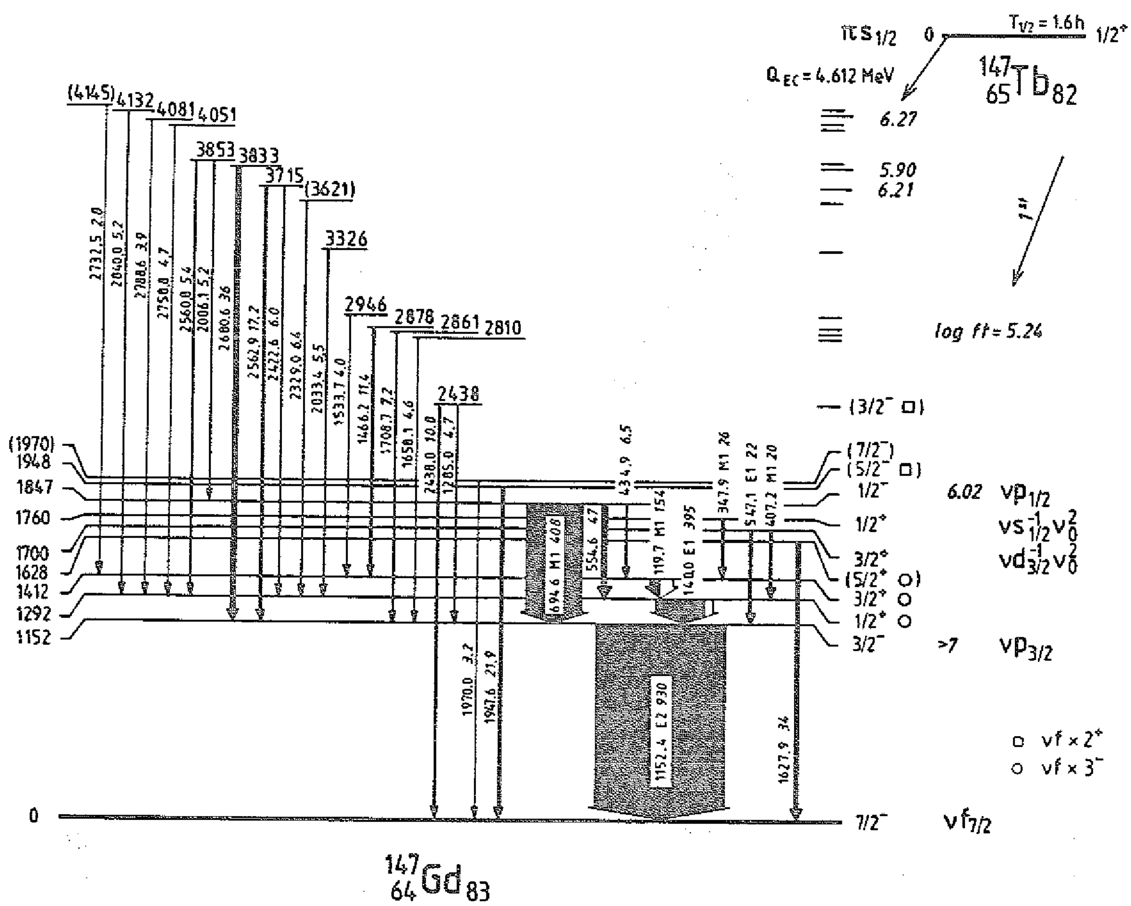

Fig2.3 Decay scheme of 1.6 h ^{147}Tb 1/2+. Total intensities are given per 10^3 parent decays. Specified transition multipolarities are from electron conversion data [AFA 71, VYL 72].

Below 2 MeV excitation we observe three new levels, at 1.628, 1.948, and (1.970) MeV, which deexcite exclusively to the $\nu f_{7/2}$ ground state, have no connection with higher–lying states and are only weakly fed in the decay.

For the 1.628 MeV level there is a difficulty, since a ground state transition of that energy observed in the in–beam data [KOM 83] establishes a $7/2^+$ level within less than 1 keV of our 1.628 MeV state. In the GSI data, devoted to investigation of ^{147}Tb $11/2^-$ decay, we observe in coincidence with Gd X–rays a 1628 keV transition which in the singles spectra is obscured by a stronger 1629.4 keV line in ^{147}Tb. From the coincidence spectrum with Gd X-rays (Fig.2.2) we estimate its intensity as ~ 0.2% that of the 1397 keV line. In the Orsay data, free of preceeding decays, we also find a 1627.9 keV line , in coincidence with Gd X-rays. Its intensity is however by far too big to be assigned exclusively to the $11/2^-$ decay. In these spectra the $11/2^-$ parent decays represent about 12% of all ^{147}Tb decays and therefore the intensity of the 1628 keV transition, if assigned only to the $11/2^-$ decay, should only be $\sim 3 \cdot 10^{-4}$ that of the 1152 keV line. In contrast we find a value of $3.7 \cdot 10^{-2}$ which firmly assigns the transition to ^{147}Tb $1/2^+$ decay. This conclusion is also confirmed by the decay-time analysis, where the 1628 and 1152 keV lines are clearly seen to decay with the same half life.

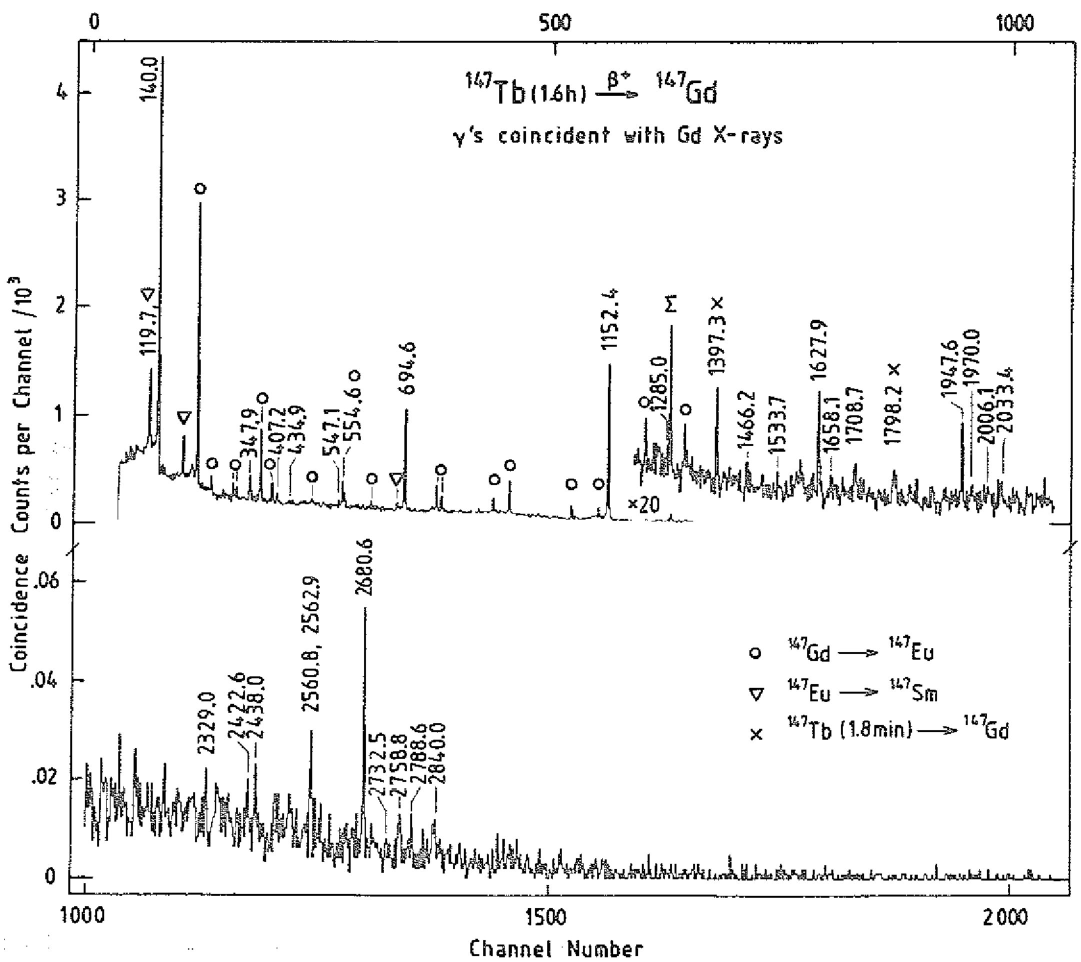

Fig.2.4 Gamma-ray spectrum of 1.6 h ^{147}Tb $1/2^+$ decay measured in coincidence with Gd X-rays.

Table 2.3 : Levels in ^{147}Gd populated in decay of the ^{147}Tb 1/2$^+$ and 11/2$^-$ isomers.

	^{147}Tb 1/2$^+$				^{147}Tb 11/2$^-$			
E_x (keV)	I^π	‰feed	log ft [a]	E_x (keV)	I^π	‰feed	log ft [b]	B_{GT} [b,c]
				997	13/2$^+$	~.2	8.09	—
1152	3/2$^-$	36(26)	7.46					
1292	1/2$^+$	136(17)	6.81					
				1397	9/2$^-$	777(40)	4.30	19.3(13)
1412	3/2$^+$	103 (8)	6.87					
1628	(5/2$^+$)	34(4)	7.25					
				1628	7/2$^-$	< .5	> 7.39	—
				1643	9/2$^+$	8(3)	6.19	—
1700	3/2$^+$	44(5)	7.12					
				1702	11/2$^+$	4.4(8)	6.41	—
1760	1/2$^+$	26(3)	7.31					
				1798	9/2$^-$	148(9)	4.83	5.7(4)
1847	1/2$^-$	456 (12)	6.02					
				1944	11/2$^-$	~2.6	6.52	—
1948	(5/2$^-$)	22(3)	7.29					
1970	(7/2$^-$)	3(1)	8.12					
				2078	(7/2$^-$)	~1.0	6.88	—
				2386	(13/2)$^-$	~2.2	6.39	—
2438	(3/2$^-$)	16(3)	7.21					
2810		5(1)	7.55					
2861		7(1)	7.32					
2878		11(2)	7.11					
2946		4(1)	7.53					
				2972	(9/2$^-$)	11(2)	5.37	1.7(3)
				3005	(9/2$^-$)	20(4)	5.12	3.0(6)
				3195	(9/2$^-$)	1.7(8)	6.07	.33(16)
				3205	(9/2$^-$)	14(2)	5.14	2.8(5)
				3322	(9/2$^-$)	7(2)	5.39	1.6(4)
3326		6(2)	7.16					
3621		6(1)	6.85					
3715		23(3)	6.21					
3833	(1/2$^-$)	36(4)	5.90					
3853		11(2)	6.39					
				3872	(11,13/2$^-$)	3.6(8)	5.19	2.5(6)
4051		5(1)	6.47					
4081		4(2)	6.50					
4132		5(2)	6.27					
4145		3(1)	6.52					

a) $Q_{EC}[^{147}\mathrm{Tb}(1/2^+)]$ = 4.612(15) MeV [RUB 86, SCH 87], $T_{1/2}$=1.6(1) h [NEW 74].
b) $Q_{EC}[^{147}\mathrm{Tb}(11/2^-)]$ = 4.663 (15) MeV [KEL 91] [RUB 86, SCH 87], $T_{1/2}$ = 1.83(6) min [BOW 73].
c) in units of 100 $\cdot g_A^2/4\pi$. Calculated as $B_{GT} = \frac{3880}{ft}\, g_A^2/4\pi$ corresponding to $(g_A/g_V)^2$= 1.26.

From the combined analysis of the two experiments we can only extract an upper limit of 0.05 % per Tb $11/2^-$ decays for the intensity of the 1628.3 keV $7/2^+ \longrightarrow$ ground state transition [KOM 83]. The singles intensity of the unresolved doublet in the Orsay spectra has therefore been assigned to the 1627.9 keV transition fed in $1/2^+$ decay.

As mentioned two high-energy transitions (2562 and 2681 keV) established, in a previous investigation, a level at 3.977 MeV [AFA 71]. From our coincidence data (Table 2.2) we firmly place them deexciting two different levels. We summarize the results of both decays in the ^{147}Gd level list of Table 2.3.

To calculate the log ft- and B_{GT}-values we use for the ^{147}Tb $1/2^+$ and $11/2^-$ decays the half life of 1.6(1) h [NEW 74] and 1.83(6) min [BOW 73] respectively. The $Q_{EC}(1/2^+)$ = 4.612(15) keV and $Q_{EC}(11/2^-)$ = 4.663(15) have been deduced from a recent β-endpoint measurement ($Q_{EC}(11/2^-)$= 4.660(15) MeV) [KEL 91A] and from ^{147}Gd [RUB 86] and ^{147}Tb($1/2^+$) [SCH 87] masses ($Q_{EC}(1/2^+)$= 4.615(19) MeV), and including the 50.6(9) keV excitation energy of the ^{147}Tb $11/2^-$ isomer [LIA 87].

2.2.3 Sensitivity limit.

In a high-resolution γ-spectroscopic study of the β-decay the detection sensitivity is an important factor which must be considered in a quantitative discussion of the observed β-strength. Determination of a sensitivity limit for the β-strength is not straightforward, since the data provide at best an intensity limit for the weakest γ-ray that can be observed in the decay. This limit will depend on the γ-ray energy, via the detector efficiency, and also in a less staightforward manner on the detection limit in coincidence measurements which, in general, depends on the level scheme. To deduce from such experimental limits a β-strength limit must always require assumptions about the decay pattern of the (observed and unobserved) levels, and most crucially on the excitation energy of the unobserved states.

The Fig.2.5a gives the detection sensitivity limit for the experiment on 1.8 min ^{147}Tb decay. In this measurement ^{147}Dy decay was strongly dominant which precluded firm γ-ray assignement to ^{147}Tb decay from singles spectra alone. The curve (A) gives the sensitivity limit for γ's coincident with the intense 1397, 1798 or 997 keV ground state transitions. Primarily fed states decaying only to the ground state would be identified in γ-coincidences with the Gd X-rays from the EC-process which in the present case is >50% for E_x>1 MeV. The curve (B) gives this limit extracted from our Gd X-ray coincidence data.

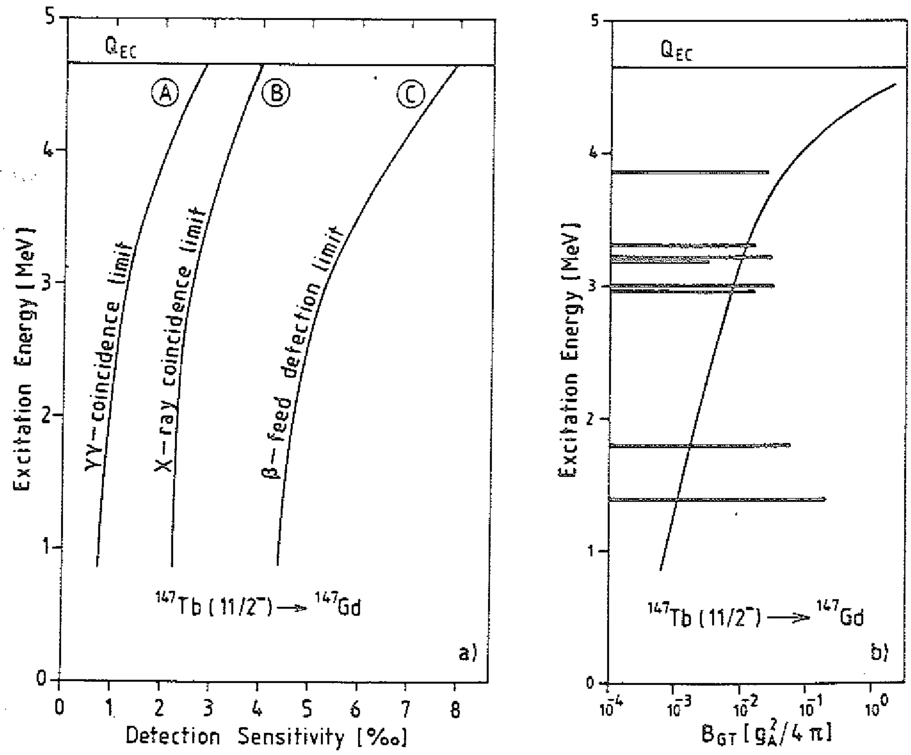

Fig.2.5 Detection limit in the study of 1.8 min ^{147}Tb 11/2$^-$ decay.
(a) Sensitivity limit for γ-ray intensities as deduced from γγ-coincidence spectra (curve A) and from coincidence with Gd X-rays (curve B). From the last observed level, at 3.9 MeV, to higher energy the curves have been estimated from the detector efficiency. The β-feed detection limit (curve C) represents a conservative estimate for detection of an individual state (see discussion in the text).
(b) Sensitivity limit for β-strength detection. Experimental B_{GT}-values in units of $g_A^2/4\pi$ are shown as horizontal bars for levels with $B_{GT}>3\cdot10^{-3}$ $g_A^2/4\pi$. The smooth curve corresponds to curve C in Fig.(a) and specifies the minimum strength in an individual level that can be detected.

If we now assume that the γ-deexcitation of any high-lying state proceeds at least 50% through one transition we deduce the conservative level feed limit of curve (C). This, folded with the Fermi function gives the strength sensitivity limit in Fig.2.5b, referring to a single state. Clearly, significant strength can escape detection if disperged into a large number of states fed with intensities below the limit of curve (C).

In this context it is interesting to compare our present results obtained from high-resolution γ-ray spectroscopy with strength functions measured by an independent method – total absorption γ-ray spectroscopy (TGA) [ALK 89, ALK90].

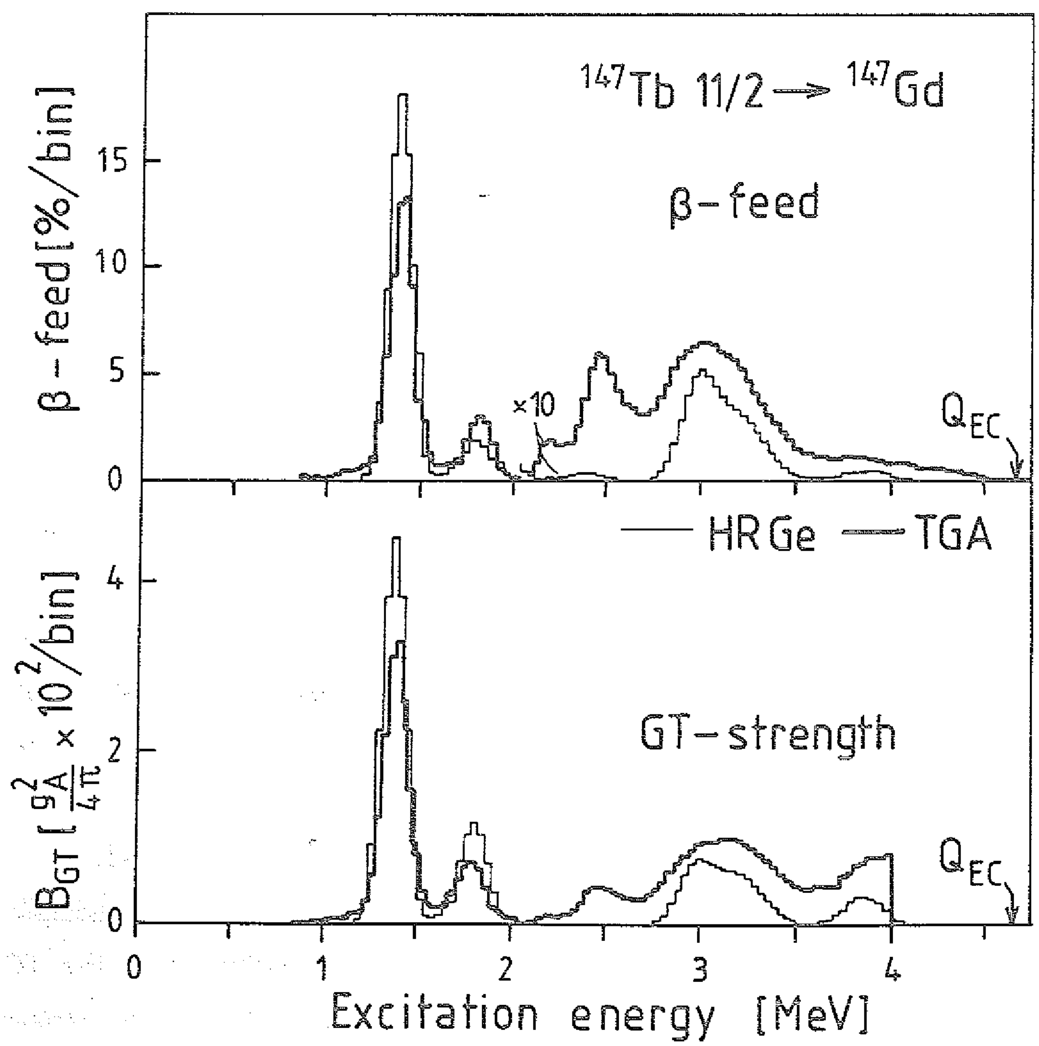

Fig.2.6 Beta-feeding distributions for ^{147}Tb $11/2^-$ decay. Compared are the results obtained in the present high-resolution (HRGe) study with those from a total-absorption γ-ray (TGA) measurement with a large-volume scintillation detector [ALK 90]. As a function of excitation energy the Fig.(a) shows the β-feeding intensity, and the Fig.(b) the β-strength. Energy bin 36.3 keV.

In Fig.2.6a and 2.6b we compare the two measurements, where we have folded our data with the more limited energy resolution (144 keV FWHM at 1397 keV) of the TGA–spectrometer.

The overall agreement is good, the prominent β–feed goes to the low–lying $9/2^-$ states. More close inspection reveals that in the TGA–measurements a higher fraction of the total feed populates states above 2.1 MeV, 19% compared to 6% in our high–resolution measurement. This difference inevitably will lead to a higher total B_{GT} from TGA than we find, namely 0.51 vs 0.37(2) $g_A^2/4\pi$, and accordingly will reduce the strength to the two low–lying $9/2^-$ states (Fig.2.6b).

In principle, of the two techniques the TGA measurement should give a more reliable result, and the fact that the TGA strength value is higher than our would support this. It is always possible, and even likely, that the β–decay weakly feeds a great number of levels at high excitation which in their decay emit only γ–rays below our detection limit. Such unobserved feed can always bring the two results into agreement irrespective whether or not the γ–decay proceeds through lower–lying states.

Nevertheless, we also note in the comparison some features of particular concern. One point is the 2% excess feed found by TGA between 0.87 and 1.1 MeV excitation which clearly should have become evident in our data. Moreover, here all ^{147}Gd levels are identified, which is incompatible with the 2% feed in this energy region.

The 4.7% feed between 2.1 and 2.6 MeV presents a similar problem. In our experiment we detect in this region levels fed with ≥ 0.2 % of the parent decays, which would mean that there should be at least 20 unobserved levels at that excitation that can be directly fed in β–decay of the ^{147}Tb $11/2^-$ parent state. Such a high number of levels with I = 9/2, 11/2 or 13/2 at this low energy is clearly incompatible with the structure of the ^{147}Gd single particle nucleus.

Another aspect which renders detailed comparison of the strength distributions difficult is the limited knowledge of the experimental uncertainties in the TGA results which involve ambitious background subtraction procedures and response function unfolding.

The arguments given above might suggest that the particular discrepancies discussed could be due to experimental errors.

2.3 Spin–parity and configuration assignements.

The only information on the spin and parity of the levels populated in ^{147}Tb decay are their log ft–values and the γ–decay branchings together with the known parent and daughter assignements. In many cases, in particular for weakly fed levels, the information is insufficient to clarify the level spin and parity. However, as discussed above, only a limited number of levels is expected in ^{147}Gd at low excitation energy. Most of them have been identified in previous studies, and many of these states are populated in the decay. But we also observe new levels below 2.1 MeV which can with some confidence be assigned as these missing low–lying configurations. Clearly these assignements are not based on experimental data and are therefore tentative.

The already discussed 1.628 MeV state populated in $1/2^+$ decay must almost certainly be $(\nu f_{7/2} \times 3^-)_{5/2^+}$, the only missing member of the octupole septuplet. It appears surprising that this level should be populated in $1/2^+$ decay, but no other state can ever be conceived in ^{147}Gd at this low excitation. The rather high 3.4% intensity of the 1628 keV line clearly shows that appreciable γ–intensity feeding the state is not observed in our experiment.

Of the three remaining higher–lying states we tentatively assign the 2.078 MeV level as $(\nu f_{7/2} \times 2^+)_{7/2^-}$. We will later discuss that the γ–ray feeding into that state supports this assignement.

The two other states, at 1.948 and 1.970 MeV, observed in $1/2^+$ decay are not fed from higher–lying levels. They decay only by a single transition to the ^{147}Gd ground state and are therefore difficult to distinguish.

The still unassigned low–lying excitations are $(\nu f_{7/2} \times 2^+)_{5/2^-}$ and $(\nu f_{7/2} \times 0_2^+)_{7/2^-}$ which both should decay in this way. Here, however, the closely above expected $\nu f_{5/2}$ state complicates the situation further. Nothing is known in ^{147}Gd about this single particle excitation, but in lower–Z N=83 isotones the $\nu f_{5/2}$ state, from (d,p) studies, is known to be strongly fragmented by coupling to the $\nu f_{7/2} \times 2^+$ and 4^+ N=82 core excitations which, however, in ^{146}Gd lie ~ 0.3 MeV higher in energy. We therefore, on a quite speculative basis, assign the 1.948 MeV level as $(\nu f_{7/2} \times 2^+)_{5/2^-}$, and prefer, on account of its 8 times weaker intensity, $(\nu f_{7/2} \times 0_2^+)_{7/2^-}$ for the 1.970 MeV level on a similar footing.

Another missing low-lying excitation is the $(\nu f_{7/2}\times 2^+)_{3/2^-}$. But this level is expected to mix strongly with the 1.152 MeV $p_{3/2}$ single neutron state and one therefore anticipates that the $(\nu f_{7/2}\times 2^+)_{3/2^-}$ quintet member should be raised in energy well above the 1.97 MeV core 2^+ state. The 2.438 MeV state is a possible candidate for $(\nu f_{7/2}\times 2^+)_{3/2^-}$. The observed γ-decay to the $f_{7/2}$ ground state and to the $p_{3/2}$ level support this suggestion.

Up to about 2 MeV the ^{147}Gd level scheme should be complete since all the expected excitations, listed in the introduction, are now identified.

Before a more detailed discussion of the nuclear structure of these low-lying states we will briefly review the experimental information on the ^{147}Gd levels above 2.4 MeV which have only been observed in the present decay study.

The six high-lying states fed in $11/2^-$ decay receive significant β-strength. Their decay patterns suggest $9/2^-$ or $11/2^-$ assignements except for the highest state at 3.872 MeV, which must be $11/2^-$ or $13/2^-$. Consideration of the β-strength function, to be discussed in section 2.4, will further specify the level spins.

In $1/2^+$ decay all log ft-values are as expected quite large, and here the only spin-parity information are the rather wide bonds implied from the γ-decay branching. The proposed $1/2^-$ assignement for the 3.833 MeV state is based on strength function arguments to be discussed below (section 2.4).

2.3.1 The $\nu f_{7/2}\times 3^-$ particle-phonon multiplet.

The 3^- octupole excitation in ^{146}Gd at 1.579 MeV couples to the well isolated $f_{7/2}$ neutron to give a septuplet of states with I^π from $1/2^+$ to $13/2^+$. For harmonic vibration, the multiplet is expected to occur at the phonon energy but the degeneracy of the multiplet is broken by various interaction processes which mix the particle-phonon states with other excitations. A detailed analysis of the $\nu f_{7/2}\times 3^-$ multiplet in the N=83 nuclei from ^{141}Ce to ^{147}Gd is given in [KAD 89] and [TRA 89]. The authors describe the experimentally observed energy shifts of the multiplet members in terms of a quadrupole-quadrupole $(q\cdot Q)$ interaction [deS 61, BOH 75] of the $\nu f_{7/2}$ valence particle with the 3^- core vibration and of configuration mixing which in ^{147}Gd involves mainly the $\nu i_{13/2}$ single particle state and the $\nu s^{-1}_{1/2}\, j^2_0$ and $\nu d^{-1}_{3/2}\, j^2_0$ two-particle one-hole states.

Our tentative assignement of the 1.628 MeV state as $(\nu f_{7/2}\times 3^-)_{5/2^+}$ agrees within 100 keV with its estimated energy [KAD 89] and completes the $\nu f_{7/2}\times 3^-$ multiplet in ^{147}Gd.

2.3.2 The $\nu f_{7/2}\times 2^+$ particle–phonon multiplet.

The second excited state in ^{146}Gd is the 2^+ collective state wich lies at 1.972 MeV excitation. Its coupling with the $f_{7/2}$ neutron gives in ^{147}Gd a quintet of states with I^π from $3/2^-$ to $11/2^-$, most of them identified for the first time in the present study. We have assigned to this configuration the levels at 2.438 MeV ($3/2^-$), 1.948 MeV ($5/2^-$), and 2.078 MeV ($7/2^-$) which, with the previously suggested $9/2^-$ (1.798 MeV) and $11/2^-$ (1.944 MeV) members, complete the $\nu f_{7/2}\times 2^+$ multiplet in ^{147}Gd. Also in this case, like in the $\nu f_{7/2}\times 3^-$ coupling discussed above, we observe significant deviations from the simple description of a degenerate particle–phonon multiplet. The energy shifts of the $\nu f_{7/2}\times 2^+$ multiplet members can be discussed, within the same framework used for the $\nu f_{7/2}\times 3^-$ septuplet [KAD 89, TRA 89], in terms of configuration mixing with close–lying single particle states and of a $q\cdot Q$ interaction.

For the two phonons there is however an important difference in their couplings with single particle states. For the quadrupole phonon all the multiplet members in ^{147}Gd have a close–lying partner in the $f_{7/2}$, $p_{3/2}$, $h_{9/2}$, and $f_{5/2}$ single neutron states of the N=82–126 shell and also in the close–lying $\nu h^{-1}_{11/2} i^2_0$ two–particle one–hole excitation. In contrast, only the $\nu i_{13/2}$ particle, and less strongly the $\nu s^{-1}_{1/2} i^2_0$ and $\nu d^{-1}_{3/2} i^2_0$ two–particle one–hole states, couple appreciably to the $\nu f_{7/2}\times 3^-$ septuplet.

We use the Fig.2.7 to discuss the coupling effects, where the data are compiled and the coupling matrix elements are indicated.

The most clearcut data are available for the $9/2^-$ member where both the $(\nu f_{7/2}\times 2^+)_{9/2^-}$ and the mixing $\nu h_{9/2}$ are identified from the decay data, and where the B_{GT}–values give their spectroscopic factors. In the approximation of a two–state mixing we can obtain from these data the coupling matrix element (m) and the unperturbed energies (E_1 and E_2) from

$$m = (E_\Lambda - E_V)\,\frac{\sqrt{s_\Lambda \cdot s_V}}{s_\Lambda + s_V} \tag{2.1}$$

$$E_{1,2} = \frac{1}{2}(E_\Lambda + E_V) \pm \frac{1}{2}\sqrt{(E_\Lambda - E_V)^2 - 4m^2} \tag{2.2}$$

where s_Λ and s_V are the spectroscopic factors (B_{GT}-values) of the $\nu h_{9/2}$ component in the two observed $9/2^-$ states with energies E_Λ and E_V.

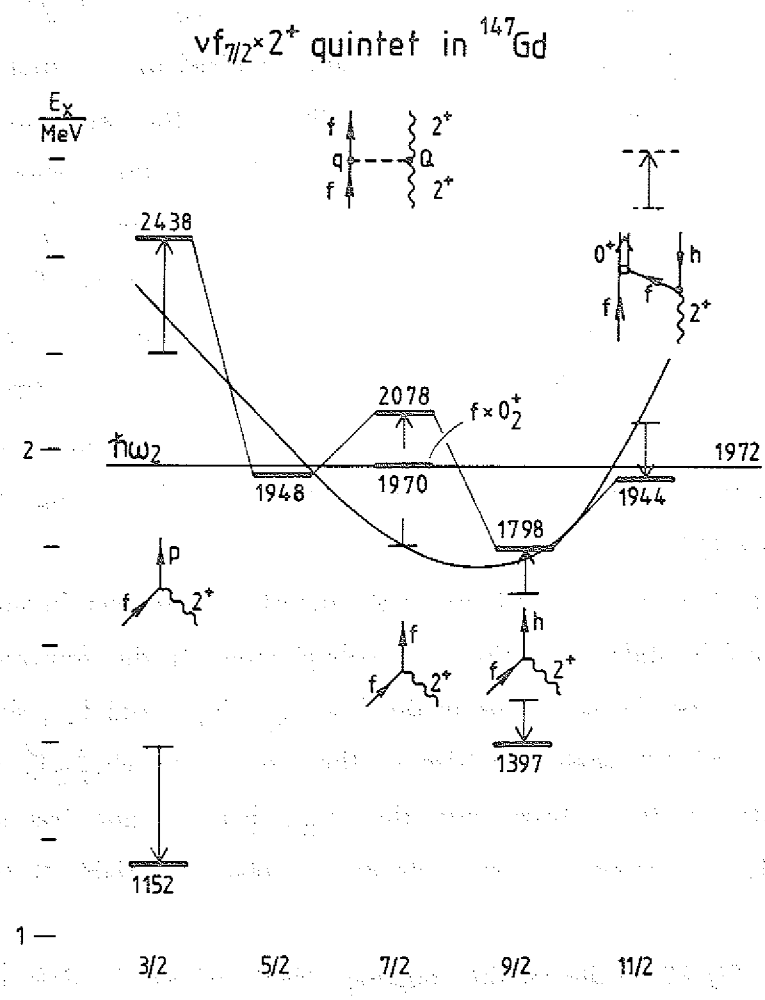

Fig.2.7 Excitation energy versus spin for the odd-parity levels in ^{147}Gd related to the $\nu f_{7/2} \times 2^+$ multiplet, including the single neutron states which couple to the f × 2 levels. The coupling matrix elements are indicated. Experimental states are shown as heavy bars labelled with the energy in keV; states with dominant f × 2 character are connected. Unperturbed energies are drawn as short horizontal lines with arrows (cf. text). The curve shows the spin-dependence of the energy displacement calculated from the center diagram (eq.2.3) with K = + 2.5 MeV.

The calculated mixing matrix element $m(\nu h_{9/2},\nu f_{7/2}\times 2^+) = 0.17$ MeV gives 1.71 MeV for the unperturbed energy of the $(\nu f_{7/2}\times 2^+)_{9/2^-}$ coupling. It is interesting to note that this coupling matrix element is about five times smaller than the known 0.8 MeV $(\nu i_{13/2}, \nu f_{7/2}\times 3^-)$ coupling strength [PII 90] which is responsible for the shift of the $13/2^+$ octupole member at 0.997 MeV. The reduction of our estimated coupling strength is however an expected result which is attributed to the spin–flip nature of the $\nu h_{9/2} \longrightarrow \nu f_{7/2}$ transition.

Further experimental data which give the mixing strength of the quadrupole excitations with close–lying states are available only for the $11/2^-$ multiplet member. This state is expected to mix with the $\nu h^{-1}_{11/2} j^2_0$ two–particle one–hole excitation which in a recent transfer measurement [KLE 91] was located at ~2.62 MeV (given in Fig.2.7 as a dashed line). From this result and the measured spectroscopic factors we have calculated using eqs. (2.1) and (2.2) the $(\nu h^{-1}_{11/2} j^2_0, f_{7/2}\times 2^+)$ coupling matrix element as 0.25 MeV and the unperturbed energy of the $(\nu f_{7/2}\times 2^+)_{11/2^-}$ state as 2.06 MeV. Also here the small matrix element is expected since this 4^{th}–order coupling process involves the exchange of an $f_{7/2}$ neutron between the 2^+ quadrupole– and the 0^+ pair–phonon.

From our data we have indirect information about the $(\nu f_{7/2}, \nu f_{7/2}\times 2^+)$ coupling strength. This matrix element is expected to be quite similar to that of the $(\nu h_{9/2}, \nu h_{9/2}\times 2^+)$ coupling which, anticipating the results discussed in Section 2.4.2, we have determined to be ~ 0.7 MeV. Since the angular part of the two matrix elements are nearly equal we assume that also the two coupling strength are similar and estimate the unperturbed $(\nu f_{7/2}\times 2^+)_{7/2^-}$ energy at 1.81 MeV.

For the $5/2^-$ multiplet member we cannot estimate the unperturbed energy since, as discussed, there is no information in ^{147}Gd about the $\nu f_{5/2}$ (spin–flip) mixing partner.

For the $(\nu f_{7/2}\times 2^+)_{3/2^-}$ state we also expect significant coupling to the $p_{3/2}$ single neutron state but at present there is no experimental information about this coupling strength. The unperturbed $3/2^-$ energies, shown in Fig.2.7, correspond to a 0.5 MeV matrix element, in accord with the approximate magnitude for this coupling.

It is apparent from the figure that even our corrected energies deviate up to several 100 keV from the 2^+ energy, but it is interesting to note that these shifts vary regularly with spin and can be described by a quadrupole–quadrupole interaction [deS 61]. Theory gives the I–dependence of the shift as

$$\delta E(I) = K(-)^{I-1/2} \begin{Bmatrix} 2 & 7/2 & I \\ 7/2 & 2 & 2 \end{Bmatrix}, \qquad (2.3)$$

where K is a strength constant. The curve in Fig.2.7 is obtained with a value of K=2.5 MeV and follows our corrected unperturbed multiplet energies fairly well, although it should be remembered that only the $9/2^-$ and $11/2^-$ unperturbed energies could be determined somewhat reliably, leaving significant uncertainty for the coupling constant. In any case however the sign of the coupling constant is firm. This result, together with the negative quadrupole moment of the $f_{7/2}$ particle definitely specifies the core 2^+ quadrupole moment to be positive which gives repulsive interaction, or positive energy shifts, for the aligned and antialigned couplings. This is an interesting finding and can be directly related to the microscopic structure of the ^{146}Gd 2^+ phonon. That state has dominant contributions from the antialigned $\pi s_{1/2}d_{5/2}^{-1}$ and $\pi d_{3/2}g_{7/2}^{-1}$ particle–hole excitations.

In general the phonon quadrupole moments in doubly–closed nuclei are small since the particles contribute with negative and the holes contribute with positive quadrupole moment to the 2^+ phonon. For the above two dominant proton particle–hole components of the ^{146}Gd 2^+ state however, the quadrupole moments of the holes, $d_{5/2}^{-1}$ and $g_{7/2}^{-1}$, are significantly larger than the $s_{1/2}$ and $d_{3/2}$ particle quadrupole moments, and a positive 2^+ phonon quadrupole moment results, which we recognize in the ^{147}Gd $\nu f_{7/2}\times 2^+$ quintet data.

This is in contrast to the octupole septuplet [KAD 89], where the $\pi h_{11/2}d_{5/2}^{-1}$ dominant phonon contribution has negative quadrupole moment [KLE 81] and where the $\nu f_{7/2}\times 3^-$ multiplet shows attractive interaction for the extreme couplings.

2.4 Beta–decay results.

Data on the β–decay itself elucidate on two important aspects. First, it is of interest to compare the absolute β–transition rates with theoretical predictions. This is of current interest in particular for GT–transitions which are widely found to be significantly reduced compared to fundamental predictions. At the end of this chapter we will discuss new aspects of the $\pi h_{11/2} \longrightarrow \nu h_{9/2}$ transition strength relating to this problem. The second interesting feature is the distribution of the β-strength, as a function of the excitation energy, in the daughter nucleus. Thus an allowed β-transition can provide firm identification of its daughter configuration even at high excitation energy where other means to characterize specific states are limited. This also refers to situations where the daughter configuration is mixed into several states, an aspect which is often of interest in the nuclear structure interpretation.

Before consideration of the GT-results we will briefly discuss the first-forbidden decay of ^{147}Tb(1/2$^+$).

2.4.1 β-decay of ^{147}Tb 1/2$^+$.

Of the low-lying ^{147}Gd levels fed in ^{147}Tb 1/2$^+$ decay only the 1.847 MeV $\nu p_{1/2}$ state receives appreciable intensity, giving log ft = 6.0, while all other levels below 2.5 MeV have at most log ft = 6.8.

The β-transition proceeds as first-forbidden $\pi s_{1/2} \longrightarrow \nu p_{1/2}$. The same pseudoscalar β-transition occurs also in β^--decay of $^{207}_{81}Tl_{126}$ where the $s_{1/2}$ proton-hole of Tl transforms in the $p_{1/2}$ neutron-hole in $^{207}_{82}Pb_{125}$. In both nuclei one would expect similar decay rates, but in ^{207}Tl it is found to be 8 times faster (log ft = 5.1) [LED 78].

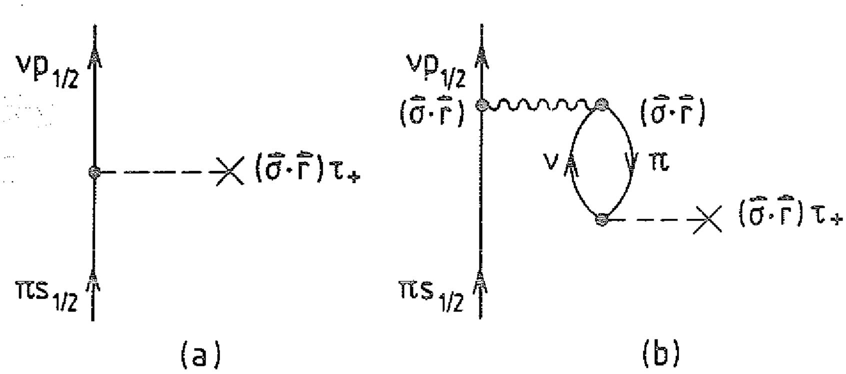

Fig.2.8 First-order core polarization for the $\pi s_{1/2} \longrightarrow \nu p_{1/2}$ transition in ^{147}Tb 1/2$^+$ decay. The $\pi^{-1}\nu$ bubble in graph (b) corresponds to the 0^- core excitations discussed in the text.

A likely explanation for this difference is given by a screening process which can affect the transition rate in ^{147}Tb but is excluded for ^{207}Tl. The transition $\pi s_{1/2} \rightarrow \nu p_{1/2}$, or its equivalent β^--transition $\pi s_{1/2}^{-1} \rightarrow \nu p_{1/2}^{-1}$, can be represented by the diagrams shown in Fig.2.8. Graph (a) represents the single particle matrix element between the initial proton $s_{1/2}$ and the final neutron $p_{1/2}$ state. Graph (b) represents a first-order correction to the decay rate involving 0^- neutron-particle proton-hole excitations. This correction characterizes the screening of the single particle transition since the β-strength is removed from the low-lying single particle state and is shifted to higher-lying 3-quasiparticle states in ^{147}Gd with the configurations $[\pi s_{1/2}(\pi^{-1}\nu^{+1})_{0^-}]$.

The important difference between the β-decays of ^{207}Tl and ^{147}Tb is that in the latter case such ΔN=1 neutron-particle proton-hole 0^- screening excitations are possible, as is shown in Fig.2.9, while in ^{207}Tl they are blocked, due to the specific locations of the proton and neutron Fermi surfaces.

We note that in ^{147}Tb $1/2^+$ decay a state at 3.83 MeV is fed with log ft=5.9, a somewhat higher strength than in the 1.847 MeV $\nu p_{1/2}$ level. That 3.83 MeV state could be such a 3-quasiparticle screening excitation; its exclusive decay to the 1.152 MeV $\nu p_{3/2}$ excitation is in accord with this tentative interpretation.

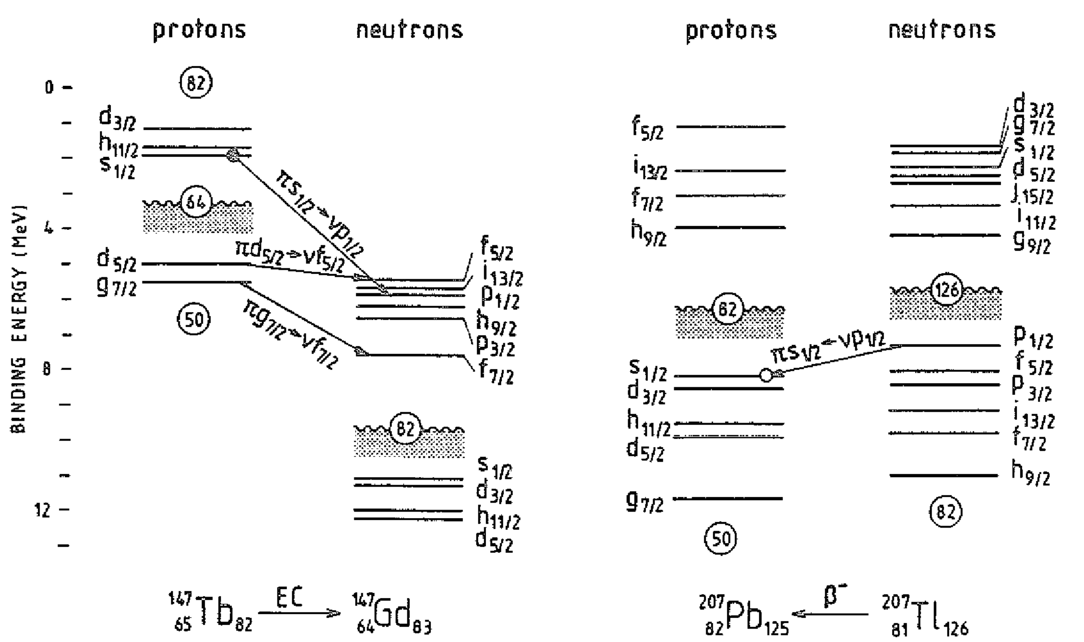

Fig.2.9 The first-forbidden β-transition in ^{147}Tb and ^{207}Tl connecting $\pi s_{1/2}$ and $\nu p_{1/2}$, and the 0^- screening excitations in ^{147}Gd.

The pertinent two 3-quasiparticle configurations, apparent from Fig.2.9, $\pi s_{1/2}(\pi g_{7/2}^{-1} \nu f_{7/2})$ and $\pi s_{1/2}(\pi d_{5/2}^{-1} \nu f_{5/2})$ give rise to four $1/2^-$ states. A shell model calculation, without configuration mixing, predicts the lowest of them slightly above 3.3 MeV. The three remaining $1/2^-$ states are obtained above 4 MeV and evidently should also receive significant strength.

The here discussed core polarization screening of a pseudoscalar β-transition became for the first time evident in the present ^{147}Tb $1/2^+$ decay study.

2.4.2 β-decay of ^{147}Tb $11/2^-$.

2.4.2.1 Decay of the $h_{11/2}$ valence proton and quadrupole core polarization.

The principle result of the ^{147}Tb $11/2^-$ decay study is the identification of significant GT-decay strength to levels above 2.5 MeV in the daughter nucleus, where we observe a group of intensely populated states close to 3 MeV, and an isolated level at 3.9 MeV also with an intensity well above our detection sensitivity limit. Except one, all of these states have log ft < 5.4 and therefore are clearly populated in GT-decay. Their summed strength is about one third of the total ^{147}Tb $11/2^-$ decay strength. From these results alone it would be natural to attribute the high-lying strength to decay of a paired $h_{11/2}$ proton present in ^{147}Tb due to pair scattering across Z = 64 as discussed above.

However, the comparison with the ^{147}Tb $1/2^+$ decay, where the summed strength to levels above 2.5 MeV is nearly 8 times less, definitely excludes that the major high-lying strength in ^{147}Tb $11/2^-$ decay could originate from decay of a core-excited 0^+ proton-pair. We therefore are led to conclude that the high-lying GT-strength must primarily be attributed to decay of the $h_{11/2}$ valence proton. In this case the ^{147}Gd states must have $I^\pi = 9/2^-$, which is compatible with their γ-deexcitation, except for the highest state at 3.872 MeV that we will discuss later.

A mechanism to raise the $\nu h_{9/2}$ strength, which resides mainly in the low-lying 1.397 and 1.798 MeV states, to this high excitation energies is the coupling of the $h_{9/2}$ single neutron to the proton particle-hole 2^+ core excitation in ^{146}Gd at

1.972 MeV. This core–excited configuration lies at an excitation energy where $9/2^-$ states of other configurations are expected. The small energy separation of these $9/2^-$ states allows for configuration mixing and causes the spreading of the β–strength to their $\nu h_{9/2}$ components.

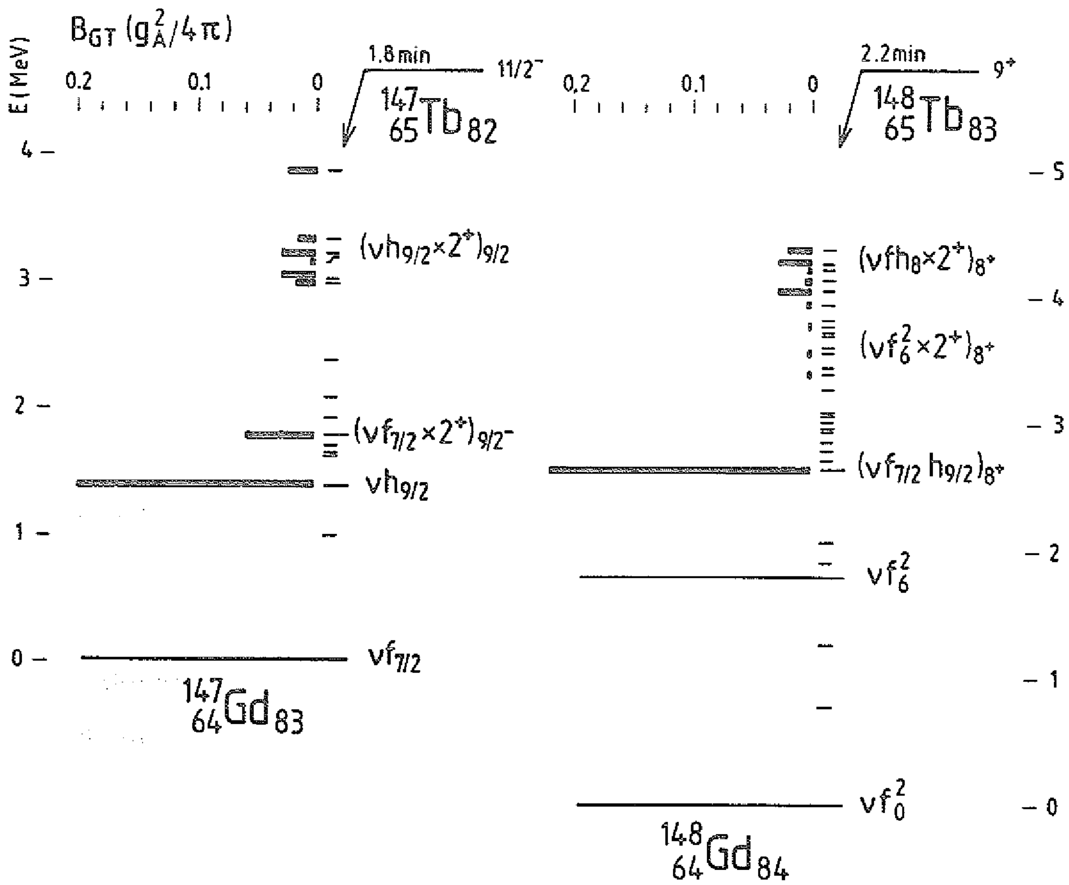

Fig.2.10 Gamow–Teller strength functions for ^{147}Gd (present work) and ^{148}Gd [COL 90, COL 91]. All levels observed in the decay of $^{147}Tb(11/2^-)$ and $^{148}Tb(9^+)$ are shown (thin lines). B_{GT}–values (heavy bars) are given when $B_{GT} > 2\cdot 10^{-3}\, g_A^2/4\pi$.

The population of these states with about 1/3 of the total decay strength suggests a rather large $(\nu h_{9/2}, \nu h_{9/2}\times 2^+)$ coupling matrix element. Since the two groups of $9/2^-$ levels are well separated in energy we estimate it within a two–state mixing formalism (eqs. 2.1 and 2.2) from their respective strengths and strength weighted energies to be of the order of 0.7 MeV. This coupling matrix element is rather large and indicates that the valence neutron in ^{147}Gd is very effective in inducing the excitation of the 2^+ core phonon. The same core polarization matrix element is also responsible for the unusually large neutron effective charge values at N=83 [PII 90]. Although this effect has quite early been recognized [KLE 79B, DAL 80] and was attributed to the dominant proton component in the ^{146}Gd 2^+ state, quantitative analysis even now is precluded, since pertinent experimental data are still not available, like for example an accurate ^{146}Gd B(E2)-value.

We mention here that similar results have been recently obtained in a high-sensitivity γ-spectroscopic study of ^{148}Gd populated in the decay of ^{148}Tb(9^+) [COL 90, COL 91]. The two decays are expected to be quite similar since the $\nu f_{7/2}$ spectator particle should have little influence on the β-decay. In both parent nuclei the $h_{9/2}$ neutron shell is completely empty as the valence neutron of ^{148}Tb in the 9^+ state occupies the $f_{7/2}$ orbital. Therefore, the total GT-decay strength should be the same in the two cases, which is essentially verified in experiment, where we find 0.37(2) and 0.32(1) $g_A^2/4\pi$ for the decays of ^{147}Tb($11/2^-$) and ^{148}Tb(9^+) respectively.

The comparison, shown in Fig.2.10, suggests a common interpretation of the high-lying β-strength found in both daughter nuclei. This is strongly supported by the $[(\nu f_{7/2}h_{9/2})_{8^+},(\nu f_{7/2}h_{9/2}\times 2^+)_{8^+}]$ matrix element which from the ^{148}Gd data is also found to be 0.7 MeV.

2.4.2.2 Pair scattering across Z=64.

The highest ^{147}Gd level, populated in ^{147}Tb $11/2^-$ decay, 3.872 MeV, is established from the firm 997–2875 keV $\gamma\gamma$-coincidence relationship. The β-feed excludes positive parity, and the level must therefore be $11/2^-$ or $13/2^-$. This state represents the only definite evidence for the presence of a $\pi h_{11/2}$ 0^+ pair in ^{147}Tb. We note however that, in contrast to simple expectation, a similar strength at that energy is not evident in ^{147}Tb $1/2^+$ decay. A likely explanation for this disappointement could be the different 3-quasiparticle configurations of the states fed. ^{147}Tb $11/2^-$ decay here proceeds to the $[\pi h_{11/2}(\pi h_{11/2}\nu h_{9/2})_{1^+}]$ configuration where both the strongly attractive $(\pi h_{11/2}\nu h_{9/2})_{1^+}$ and $(\pi h^2_{11/2})_{2^+}$ interactions can significantly contribute in the lowest $11/2^-$ state of the configuration. Only the $(\pi h_{11/2}\nu h_{9/2})_{1^+}$ coupling can be expoited in the $[\pi s_{1/2}(\pi h_{11/2}\nu h_{9/2})_{1^+}]_{1/2^+,3/2^+}$ states populated in $1/2^+$ decay, and consequently the lowest levels here could well lie a few hundred keV higher and thus escape detection.

Unfortunately, the observation of a single state populated in the decay of core–excited $h_{11/2}$ protons is not sufficient to provide quantitative estimate of pair scattering in ^{147}Tb since this state contains only an unspecified fraction of the total strength.

2.4.2.3 Gamow–Teller transition strength (Silver and Gold).

Since the observation of Gamow-Teller (GT) resonances [GOO 80] in charge-exchange reactions absolute transition rates for GT β–decay have been the subject of renewed interest. The GT^-–resonance* is however not accessible in β^-–decay but in the very proton–rich nuclei the proton single particle states are raised by the Coulomb repulsion and it becomes possible to excite the GT^+–resonance [KLE 85] whenever the proton and neutron Fermi energies are between the spin–orbit partners of a high–l orbit, such that the $j_> = l+1/2$ state is partly filled with protons whereas the neutron $j_< = l+1/2$ orbit is unoccupied. This condition is fulfilled for the N=82 nuclei above ^{146}Gd. Here, the $h_{11/2}$ proton of an even–even nucleus decays to the empty $h_{9/2}$ neutron shell proceeding as $(\pi h^2_{11/2})_{0^+} \longrightarrow (\pi h_{11/2}\nu h_{9/2})_{1^+}$ and in the ideal case should populate a single state in the odd–odd daughter which carries the entire strength. This specific structural property makes experimental studies of these decays attractive. Already in early investigations [NOL 82] it was consistently found that the GT–strength is ~7 times attenuated compared to the shell model prediction, whereas the charge–excange reaction results [GAA 83] gave an attenuation of the order of ~2.

Theoretical studies largely attribute this discrepancy to ground state correlations [TOW 85] which admix high–lying 0^+ excitations to the parent ground state thereby reducing the β–decay strength.

* We use the notation GT^- (or GT^+) for a state formed by the action of the operator $\sigma\tau_-$ (or $\sigma\tau_+$) on a given state.

Strength determinations from odd-Z (N=82) GT-decays are more difficult. In general, here both the valence particle $\pi h_{11/2} \rightarrow \nu h_{9/2}$ as well as the $0^{+} \rightarrow 1^{+}$ decay of the paired protons contribute. The latter decay leads to 3-quasiparticle states above ~3 MeV where the level density is high and the detection sensitivity low.

An exception is ^{147}Tb where, as we have shown above, essentially only the $h_{11/2}$ valence proton decay contributes to the observed strength. Moreover, the decay of the single $h_{11/2}$ proton into the empty $h_{9/2}$ neutron shell provides the GT single particle transition rate which our experiment has determined to be

$$B_{GT}(\pi h_{11/2} \rightarrow \nu h_{9/2}) = 0.37(2)\ g_A^2/4\pi.$$

Following the conclusions of the previous sections we obtain it as the summed strength to ^{147}Gd levels up to 3.5 MeV.

The prediction of the shell model for the total decay strength in N=82 nuclei is

$$B(GT) = n\ \frac{4l}{2l+1}\ \frac{g_A^2}{4\pi},$$

i.e. should be proportional to the number n of $h_{11/2}$ protons in the parent nucleus where the constant of proportionality is a function of the orbital angular momentum l of the decay partners. The early data mentioned above [NOL 82] have shown that this is approximately fulfilled for the decays of the even-even N=82 nuclei ^{148}Tb, ^{150}Er, and ^{152}Yb .

Our new result for the ^{147}Tb decay strength deviates substantially from this expectation. The decay of the two-valence proton nucleus ^{148}Dy has recently been measured with a γ-ray detection sensitivity of 10^{-4} per parent decay (at $E_\gamma = 2$ MeV excitation) giving the total decay strength as

$$B_{GT}(^{148}Dy \rightarrow {}^{148}Tb) = 0.47(3)\ g_A^2/4\pi,$$

where we have used a new Q_{EC}-value [KEL 91B]. With our result for $^{147}Tb(\pi h_{11/2})$ we obtain a strength ratio

$$\frac{B_{GT}(^{148}Dy)}{B_{GT}(^{147}Tb)} = 1.27(11),$$

far outside the expected value of 2.0. Such a deviation from the simple particle-number proportionality is predicted from the theory of ground state (g.s.) correlations, but was so far not established in experiment. I.S.Towner [TOW 85] has shown that the g.s. correlations are principally different in decay of paired or unpaired $h_{11/2}$ protons. Following his considerations the difference becomes obvious when considering the individual contributions, due to g.s. correlations, to the transition strengths which are presented in form of diagrams in Fig.2.11.

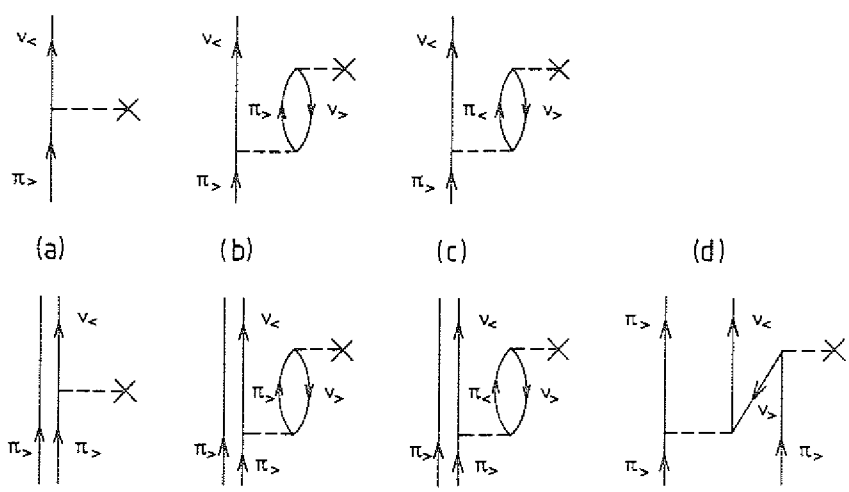

Fig2.11 First-order contributions to core polarization for closed-shell-plus-one (top) and closed-shell-plus-two nuclei taken from [TOW 85]. The following notation is used : $\pi_>$: proton in orbit $j_> = l+1/2$; $\nu_<$: neutron in orbit $j_< = l+1/2$.

The top row gives the single particle transition matrix element m_a (a) and the first-order core polarization contributions, m_b and m_c, for closed-shell-plus-one nuclei (b and c). For n protons in the parent state there are additional first-order corrections coming from two-body graphs shown below for closed-shell-plus-two nuclei. Whereas the diagrams (a), (b), and (c) are identical to the above one-particle case except for the additional non-interacting proton, the contribution (d), m_d, can only occur when a second proton is present. The contribution (d) contains the additional particle-particle matrix element

$$\langle \pi h_{11/2} \nu h_{9/2} | V_{pp} | \pi h_{11/2} \nu h_{11/2} \rangle,$$

which is of crucial significance for the GT-strength, and so far was taken exclusively from theory. This particle–particle interaction (V_{pp}), has been investigated in more detail in a number of recent theoretical studies [ENG 88, SUH 88, CIV 90] following Towner's original work [TOW 85]. These studies were primarily devoted to calculation of double β-decay rates where this interaction is of equal significance. Our data allow for experimental determination of it. With the above notation and the measured strength for the ^{147}Tb($11/2^-$) and ^{148}Dy(0^+) decays we write

$$\frac{B_{GT}(^{147}\mathrm{Tb})}{B_{GT}(^{148}\mathrm{Dy})} = \frac{(m_a - m_b - m_c)^2}{2(m_a - m_b - m_c - \sqrt{1/2}\, m_d)^2} = \frac{0.37(2)}{0.47(3)},$$

which with

$$\frac{1}{12}(m_a - m_b - m_c)^2 = 0.37(2)\, g_A^2/4\pi, \tag{2.4}$$

gives

$$m_d = 0.61(11)\, g_A/\sqrt{4\pi}. \tag{2.5}$$

This matrix element corresponding to the process represented by the diagram (d) in Fig.2.11 is equivalent to

$$m_d = \frac{\langle \pi h_{11/2} \nu h_{9/2}; 1^+ | V_{pp} | \pi h_{11/2} \nu h_{11/2}; 1^+ \rangle}{\varepsilon(\nu h_{9/2}) - \varepsilon(\nu h_{11/2})} \times \langle 0 | M_{GT} | \pi h_{11/2} \nu h_{11/2}^{-1}; 1^+ \rangle,$$

where M_{GT} is the GT-operator and the energy denominator of 5.8(5) MeV [VEJ 69] is given by the relative energy of $h_{9/2}$ and $h_{11/2}$ neutron single particle states. After application of the Wigner–Eckart theorem [EDM 57] this can be rewritten as

$$m_d = \frac{\langle V_{pp} \rangle}{\varepsilon(\nu h_{9/2}) - \varepsilon(\nu h_{11/2})} \times \sqrt{13/5}\ \langle \nu h_{9/2} || M_{GT} || \pi h_{11/2} \rangle.$$

The last term is the reduced single particle matrix element of the GT-decay m_a (diagram (a) in the top row of Fig.2.11). From the value of 1.7(3) for the ratio $[m_a/(m_a - m_b - m_c)]^2$, which has been calculated in [TOW 85] for different interactions and from (2.4) we obtain $m_a = 2.75(9)\, g_A/\sqrt{4\pi}$, and therefore, with (2.5), the off–

diagonal matrix element is

$$\langle V_{pp} \rangle = \sqrt{5/13} \times \frac{0.61}{2.75} \times 5.8\,\text{MeV} = 0.8(2)\ \text{MeV},$$

where the error essentially contains only the contributions from the experimental input data. This result can be compared to values obtained with the Schiffer-True parametrization [SCH 76] which gives 1.42 MeV with R_2=2.0 fm or 1.55 MeV with R_2=0.1 fm. The surface-delta interaction (SDI) with A_0 and A_1 parameters fitted for the ^{146}Gd region [WAL 89] gives a value of 1.44 MeV.

CHAPTER 3 : ^{149}Dy from the decays of ^{149}Ho $11/2^-$ and ^{149}Ho $1/2^+$.

3.1 Introduction and previous results.

Interest in the low–lying ^{149}Dy states fed in β–decay derives from similar motives as in ^{147}Gd. Also in ^{149}Dy one expects the same limited number of low–lying states formed by the single neutron–, the neutron two–particle one–hole–, and the $\nu f_{7/2} \times 3^-$ and 2^+ configurations, which so far are largely not known. Moreover it is of interest to study the GT–strength function which here, however, is expected to be more complex. Decay of ^{149}Ho, with three valence protons, can intensely feed high–lying 3–quasiparticle states in ^{149}Dy. Contrary to ^{147}Tb, GT–decay will here occur for both the $11/2^-$ and the $1/2^+$ parent activities.

Low–lying ^{149}Dy levels were first observed in an in–beam γ–experiment where its 0.5 sec $27/2^-$ isomer at 2.7 MeV excitation was identified [STE 76A, STE 76B], which in its γ–decay proceeds through the 1.073 MeV $13/2^+$ state of $\nu f_{7/2} \times 3^-$ character.

The original ^{149}Ho $11/2^-$ decay study [TOT 79] gave the $\nu h_{9/2}$ state at 1.091 MeV and a more weakly populated ^{149}Dy level at 1.583 MeV. An early experiment at GSI identified [SCH 84] the ^{149}Ho $1/2^+$ activity. These data, which will be discussed in more detail below, also located significant GT–strength to ^{149}Dy states near 3 MeV excitation in both the ^{149}Ho $11/2^-$ and $1/2^+$ decays.

3.2 Measurements and experimental results.

High–quality γγ–coincidence spectra for the two ^{149}Ho β–decays were measured in an experiment at ISOLDE, with 600 MeV protons on a Ta foil target where ^{149}Ho is produced with high yield. This experiment was primarily devoted to investigation of the 0.5 sec ^{149}Dy $27/2^-$ decay, to be discussed in chapter 4, but it also gave excellent data for the two ^{149}Ho decays. Coincidences were measured with two coaxial Ge–detectors (of 33% and 20% efficiency) placed at a relative angle of 40°, at 4 cm distance from the activity and shielded from each other by Pb. The Fig.3.1 gives examples of γγ–coincidence spectra.

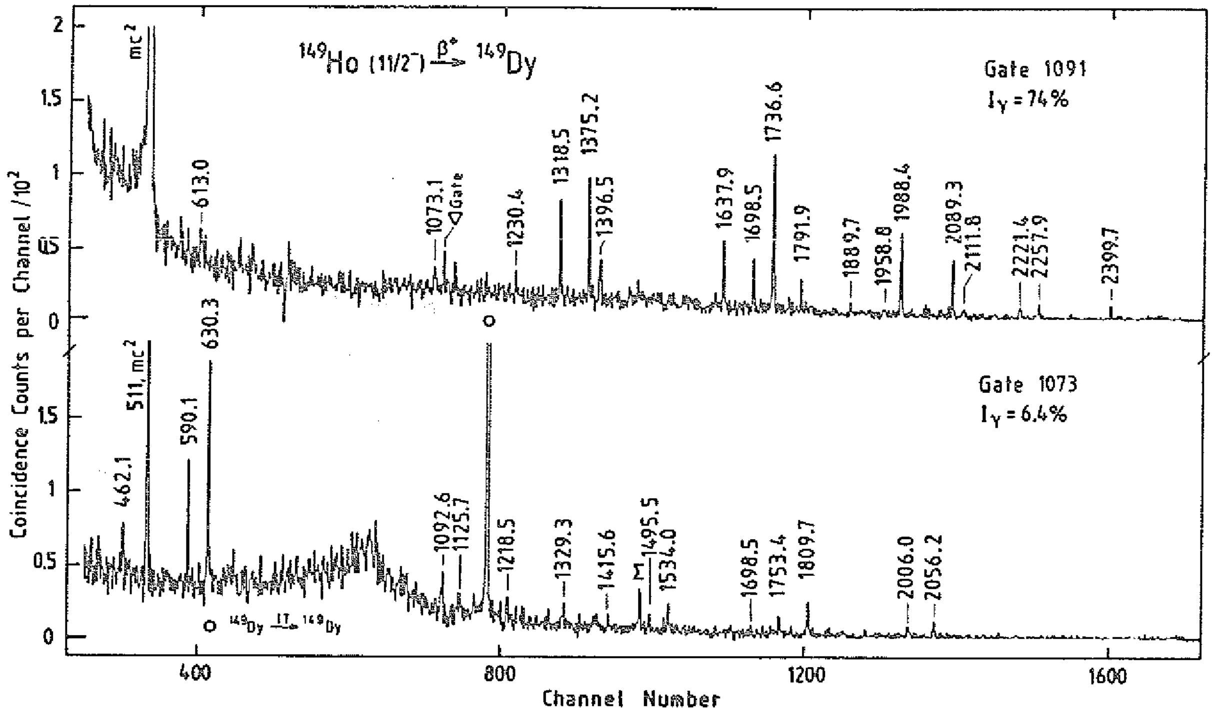

Fig.3.1 Gamma rays coincident with the 1091 and 1073 keV ground state transitions of ^{149}Dy observed in ^{149}Ho 11/2$^-$ decay. Gate transitions intensities are given per 10^2 parent decays.

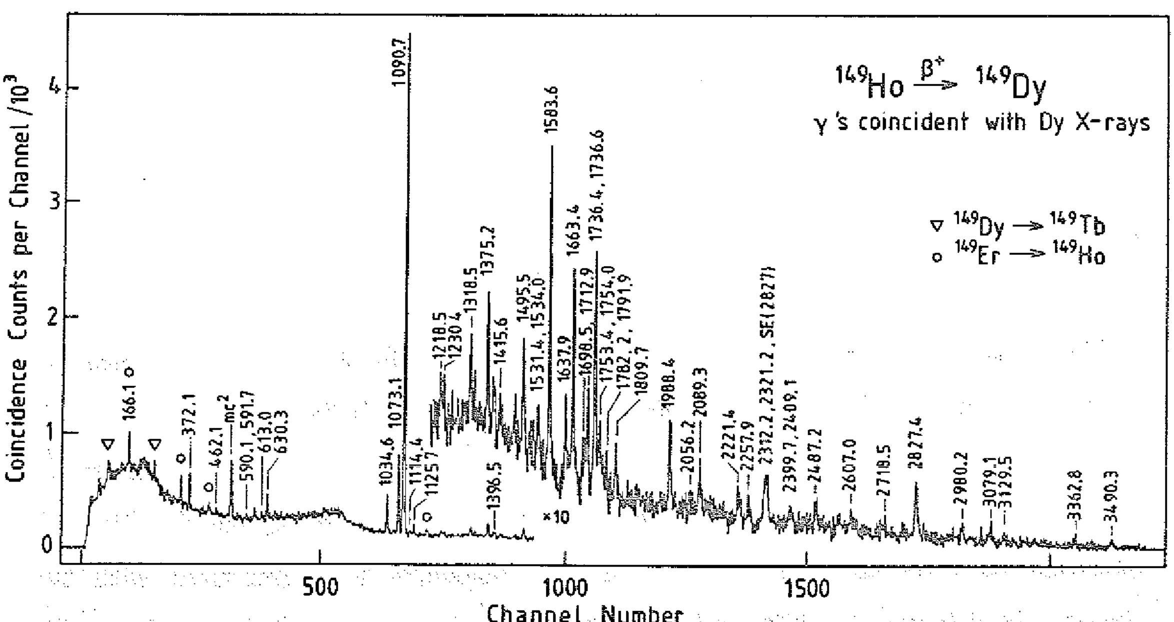

Fig.3.2 Gamma-ray spectrum coincident with Dy X-rays.

Table 3.1: Gamma rays emitted in decay of 21 s ^{149}Ho(11/2$^-$).

E_γ (keV)	I_γ [a]	Observed coincident transitions [b]	E_i (keV)	$I_i^\pi \rightarrow I_f^\pi$
462.1(3) [c]	2.3(6)	Dy X, 630, 1073	2165.5	$(13/2)^+ \rightarrow 11/2^+$
511(2)	5.2(15) [d]	—	1583.6	$(11/2^-) \rightarrow 13/2^+$
590.1(5) [c]	4.5(15) [d]	Dy X,1073,1416,1126,1035 [e]	1663.4	$(9/2^+) \rightarrow 13/2^+$
613.0(2)	1.9(4)	Dy X,1091	1703.4	$11/2^+ \rightarrow 9/2^-$
630.3(5) [c]	10.4(15)	Dy (Er) X,1073,462	1703.4	$11/2^+ \rightarrow 13/2^+$
694.5(6)	1.3(4) [d]	Tb (Dy) X,1663,1035 [e],(590)	2357.9	$\rightarrow (9/2^+)$
1073.1(2) [c]	63.7(7)	DyX,630,462,590,1810,2056, 2006, 1219, 1753, 1496, 1126, 1329,1534,1416,1546	1073.1	$13/2^+ \rightarrow 7/2^-$
1090.7(2)	744.3(15)	DyX,1737,1375,1988,1319, 2089,1397,1638,1699,1230, 1792,2400,1890,2221,2258,2112	1090.7	$9/2^- \rightarrow 7/2^-$
1114.8(3)	3.2(5)	DyX,1713	2827.5	$\rightarrow (9/2^-)$
1125.7(2)	11.5(5)	DyX,1663,590,1073	2789.1	$\rightarrow (9/2^+)$
1218.5(2)	4.5(5)	DyX,1073	2291.6	$\rightarrow 13/2^+$
1230.4(4)	2.6(11)	DyX,1091	2321.2	$\rightarrow 9/2^-$
1318.5(3)	13.0(5)	Dy(Ho)X,1091	2409.1	$\rightarrow 9/2^-$
1329.2(3)	2.2(4)	(Dy,Tb)X,1073	2402.3	$\rightarrow 13/2^+$
1375.2(3)	17.6(10)	DyX,1091	2466.2	$\rightarrow 9/2^-$
1396.5(2)	6.1(7)	DyX,1091	2487.2	$\rightarrow 9/2^-$
1415.6(3)	5.3(5)	DyX,1663,590,1073	3079.1	$\rightarrow (9/2^-)$
1495.5(2)	16.5(4)	DyX,1584,1073	3079.1	$\rightarrow (11/2^-)$
1534.0(5)	1.5(5)	—,1073,1035 [e],372 [e]	2607.0	$\rightarrow 13/2^+$
1545.9(2)	9.0(7)	DyX,1584,(1073)	3129.5	$\rightarrow (11/2^-)$
1583.6(2)	44.8(7)	DyX,1496,1546,1729	1583.6	$(11/2^-) \rightarrow 7/2^-$
1637.9(3)	10.6(4)	DyX,1091	2727.2	$\rightarrow 9/2^-$
1663.4(2)	35.3(7)	DyX,1126,1416,(695)	1663.4	$(9/2^+) \rightarrow 7/2^-$
1698.5(4)	8.6(8)	DyX,1091	2789.1	$\rightarrow 9/2^-$
1712.9(2)	19.7(4)	DyX,1115	1712.9	$(9/2^-) \rightarrow 7/2^-$
1729.0(3)	4.1(4)	—,1583	3312.4	$\rightarrow (11/2^-)$
1736.6(5)	38.0(75) [d]	DyX,1091,1035 [e]	2827.5	$\rightarrow 9/2^-$
1753.4(4)	6.0(15) [d]	DyX,1073,1035 [e]	2827.5	$\rightarrow 13/2^+$
1782.2(3)	3.3(6)	(DyX)	(1782.2	$(7/2^-) \rightarrow 7/2^-)$
1791.9(3)	4.6(5)	DyX,1091	2883.7	$\rightarrow 9/2^-$
1809.7(3)	7.9(11)	DyX,1073	2883.7	$\rightarrow 13/2^+$
1889.7(3)	3.4(6)	DyX,1091	2980.3	$\rightarrow 9/2^-$
1958.8(4)	4.7(7)	(DyX),1091	3049.5	$\rightarrow 9/2^-$
1988.4(2)	19.7(8)	DyX,1091	3079.1	$\rightarrow 9/2^-$
2006.0(5)	2.3(9)	—,1073	3079.1	$\rightarrow 13/2^+$
2056.2(5)	1.9(11)	DyX,1073	3129.5	$\rightarrow 13/2^+$
2089.3(2)	8.7(7)	DyX,1091	3180.0	$\rightarrow 9/2^-$
2111.8(3)	2.6(5)	(DyX),1091	3202.5	$\rightarrow 9/2^-$
2221.4(6)	4.0(16)	Dy(Ho)X,1091	3312.4	$\rightarrow 9/2^-$
2257.9(3)	4.6(7)	DyX,1091	3348.6	$\rightarrow 9/2^-$

Table 3.1: continued

E_γ (keV)	I_γ^a	Observed coincident transitions[b]	E_i (keV)	$I_i^\pi \rightarrow I_f^\pi$
2312.2(3)	7.0(7)	DyX	2312.2	$\rightarrow 7/2^-$
2321.2(3)	9.7(11)	DyX	2321.2	$\rightarrow 7/2^-$
2399.7(3)	3.9(7)	DyX,1091	3490.3	$\rightarrow 9/2^-$
2409.1(3)	3.9(8)	DyX	2409.1	$\rightarrow 7/2^-$
2467.4(6)	2.6(11)	DyX	(2466.2)	$\rightarrow 7/2^-$
2487.2(3)	8.7(6)	DyX	2487.2	$\rightarrow 7/2^-$
2607.0(3)	5.3(5)	DyX	2607.0	$\rightarrow 7/2^-$
2718.5(4)	2.2(7)	(DyX)	(2718.5	$\rightarrow 7/2^-)$
2827.4(3)	22.0(8)	DyX	2827.5	$\rightarrow 7/2^-$
2980.3(4)	4.5(8)	DyX	2980.3	$\rightarrow 7/2^-$
3014.2(4)	1.8(5)	(DyX)	(3014.2	$\rightarrow 7/2^-)$
3079.1(3)	6.2(6)	DyX	3079.1	$\rightarrow 7/2^-$
3129.5(4)	2.5(5)	(DyX)	3129.5	$\rightarrow 7/2^-$
3202.5(6)	1.5(6)	—	3202.5	$\rightarrow 7/2^-$
3362.8(4)	4.4(7)	DyX	3362.8	$\rightarrow 7/2^-$
3490.3(4)	3.1(6)	DyX	3490.3	$\rightarrow 7/2^-$

a) Intensities given per 10^3 $^{149}Ho(11/2^-)$ decays. Uncertainties reflect statistical error and spectral complexity.

b) For contaminated gate transitions only X-rays coincident with degenerate gate partner listed; contaminant γ-rays are omitted (except from $^{149}Ho(1/2^+)$ decay).

c) $\alpha_K(462) = 0.029(6) = 0.9(2)\alpha_K^{th}(M1)$; preliminary: $\alpha_K(630) = 0.011(3) = 0.7(2)\alpha_K^{th}(M1) = 1.6(4)\alpha_K^{th}(E2)$; $\alpha_K(1073)$ from: P.J.Daly et al.: Z. Phys. A298(1980)173.

d) Estimated from coincidence spectra.

e) Transition following $^{149}Ho(1/2^+)$ decay.

Decay-time information came from a measurement at the GSI on-line mass separator where ^{149}Ho was produced with ~5.4 MeV/A ^{58}Ni-beam on ^{94}Mo and ^{95}Mo targets leading to the $^{152}_{70}Yb_{82}$ and $^{153}_{70}Yb_{83}$ compound nuclei. Singles spectra, up to $E_\gamma = 4$ MeV, were recorded, during a β^+-endpoint measurement [KEL 91B], in 8×5 sec multispectral scaling mode after 40 sec activity collection time. For a few low-energy transitions conversion coefficients were obtained from electron spectra measured with a mini-orange spectrometer. Gamma-X ray coincidences, Fig.3.2, and additional $\gamma\gamma$-coincidence information came from a preliminary experiment with two coaxial Ge and a 1 cm^3 planar detectors.

The results of these measurements give the two decay schemes of Fig.3.3 and 3.4. The data are compiled in Table 3.1 and 3.2. The ^{149}Dy level properties are in Table 3.3 listed.

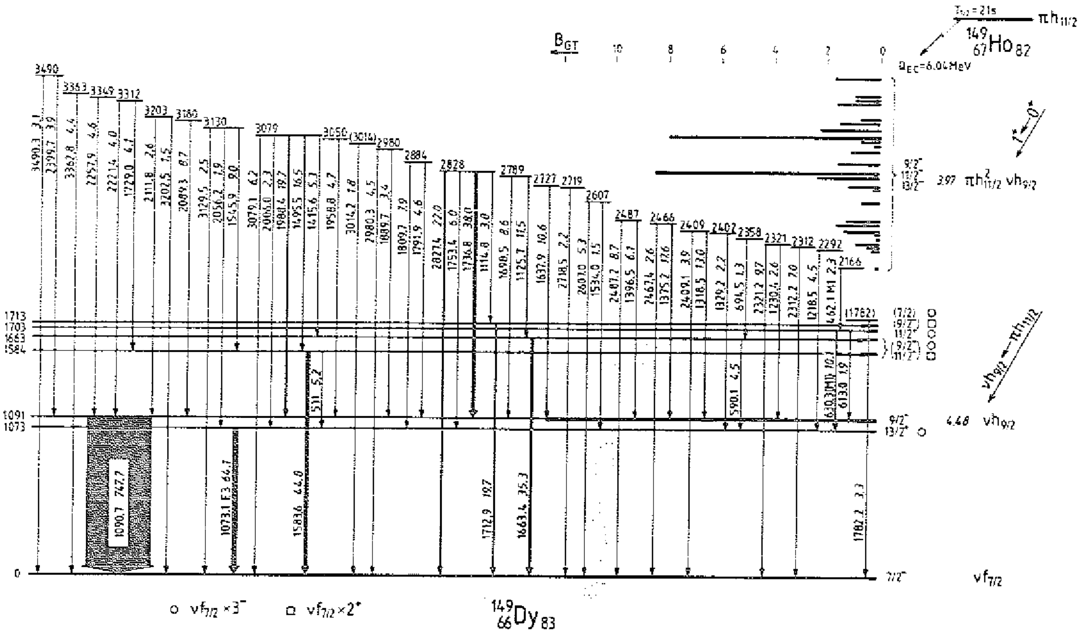

Fig,3.3 Decay scheme of 21 s ^{149}Ho $11/2^-$. Total transition intensities are given per 10^3 parent decays, and specified multipolarities are from α_K data. The GT–strengths drawn as bars to the right are given in units of $100 \cdot g_A^2/4\pi$.

Table 3.2: Gamma rays emitted in decay of 58 s ^{149}Ho($1/2^+$).

E_γ (keV)	I_γ^a	Observed coincident transitions^b	E_i (keV)	$I_i^\pi \rightarrow I_f^\pi$
94.3(3)^c	32(12)	(DyX),1035,372	1501.0	$(3/2)^+ \rightarrow 1/2^+$
166.1(2)^c	27(5)^d	(DyX),1035.372	1572.8	$(3/2)^+ \rightarrow 1/2^+$
372.1(2)^c	253(15)	DyX,1035,166,94,1531	1406.7	$1/2^+ \rightarrow 3/2^-$
591.7(5)^c	38(14)	—,1035	1626.3	$(5/2^+) \rightarrow 3/2^-$
692.9(6)	55(14)^d	Tb(Dy)X,1035,1663^e,(590)^e	1727.5	$(1/2^-) \rightarrow 3/2^-$
741.0(5)	15(10)	—,1035	1775.6	$(1/2^+) \rightarrow 3/2^-$
1034.6(2)	997(20)	DyX,372,1736,1754,166,94, 741,693,592	1034.6	$3/2^- \rightarrow 7/2^-$
1531.4(5)	30(12)^d	Ho(Dy)X,1035,372,1073^e	2938.1	$\rightarrow 1/2^+$
1736.4(6)	280(50)^d	DyX,1035,1091^e	2771.0	$\rightarrow 3/2^-$
1754.0(5)	190(60)^d	DyX,1035,1073^e	2788.6	$\rightarrow 3/2^-$

a) Intensities given per 10^3 ^{149}Ho($1/2^+$) decays. Uncertainties reflect statistical error and spectral complexity.

b) For contaminated gate transitions only X-rays coincident with degenerate gate partner listed; contaminant γ-rays are omitted (except from ^{149}Ho($11/2^-$) decay).

c) $\alpha_L(94) = 0.59(16) = 1.6(5)\,\alpha_L^{th}(M1)$; $\alpha_K(166) = 0.47(13) = 0.96(29)\,\alpha_K^{th}(M1)$; $\alpha_K(372) = 8.0(16)\cdot 10^{-3} = 0.95(19)\,\alpha_K^{th}(E1)$; $\alpha_K(592) < 5.0 \cdot 10^{-3} = 2\,\alpha_K^{th}(E1)$.

d) Estimated from coincidence spectra.

e) Transition following ^{149}Ho($11/2^-$) decay.

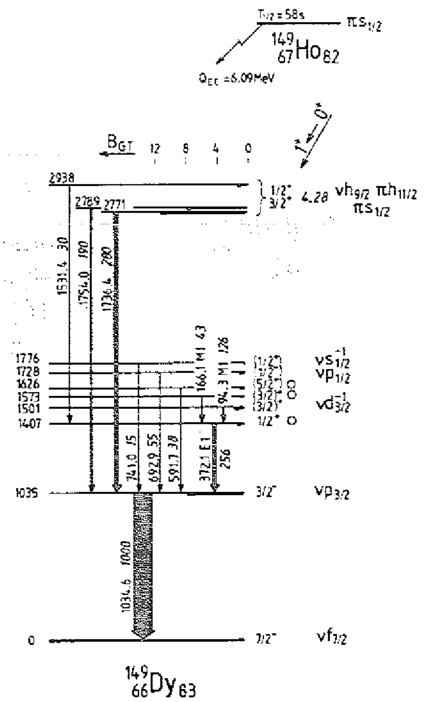

Fig.3.4 Decay scheme of 58 s ^{149}Ho $1/2^+$. Cf. caption to Fig.3.3.

3.3 Spin–parity and configuration assignements.

The ^{149}Dy ground state is surely $\nu f_{7/2}$, and as mentioned above the β–decay characterises the 1.091 MeV level as the $\nu h_{9/2}$ state and the 1.073 MeV state is firmly established as $(\nu f_{7/2}\times 3^-)_{13/2^+}$. The 1.035 MeV state, from the level energy systematics in the N=83 isotones, must almost certainly be $\nu p_{3/2}$; in ^{147}Gd it lies at 1.152 MeV. As discussed, one expects this state to couple to the $(\nu f_{7/2}\times 2^+)_{3/2^-}$ excitation, and one reason for the lower $p_{3/2}$ energy in ^{149}Dy might be the lowering of the 2^+ core state which drops from 1.972 MeV in ^{146}Gd to 1.678 MeV in ^{148}Dy. Possibly the 1.728 MeV level deexciting exclusively to the $\nu p_{3/2}$ state through the 693 keV γ–ray, and fed strongly in ^{149}Ho $1/2^+$ decay, could be the $\nu p_{1/2}$ excitation. Also the separation of the two spin–orbit partners is similar as in ^{147}Gd, but from the present data alone the assignement can only be tentative.

The three low–spin levels at 1.407, 1.501, and 1.573 MeV have firm even–parity and are therefore three of the four $1/2^+$ and $3/2^+$ states arising from the $\nu s_{1/2}^{-1}\, j_0^2$ and $\nu d_{3/2}^{-1}\, j_0^2$ two–particle one–hole excitations and the members of the octupole

Table 3.3 : Levels in ^{149}Dy populated in the decay of ^{149} Ho 1/2$^+$ and 11/2$^-$ isomers.

^{149}Ho 1/2$^+$					^{149}Ho 11/2$^-$				
E_x (keV)	I^π	‰feed	log ft^a	$B_{GT}^{a,b}$	E_x (keV)	I^π	‰feed	log ft^c	$B_{GT}^{c,b}$
1035	3/2$^-$	166(85)	5.53	1.2(6)					
					1073	13/2$^+$	18(4)	6.02	.4(1)
					1091	9/2$^-$	593(8)	4.49	13(2)
1407	1/2$^+$	57(51)	5.84	.6(5)					
1501	(3/2)$^+$	126(47)	5.45	1.4(5)					
1573	(3/2)$^+$	43(8)	5.89	.5(1)					
					1584	(11/2$^-$)	20(2)	5.75	.7(1)
1626	(5/2$^+$)	38(14)	5.92	.5(2)					
					1663	(9/2$^+$)	22(2)	5.69	.8(1)
					1703	11/2$^+$	10(2)	6.00	.4(1)
					1713	(9/2$^-$)	15.9(6)	5.80	.6(1)
1728	(1/2$^-$)	55(14)	5.71	.7(2)					
1776	(1/2$^+$)	15(10)	6.25	.2(1)					
					1782	(7/2$^-$)	3.3(6)	6.45	.10(2)
					2166	(13/2)$^+$	2.4(6)	6.41	.10(3)
					2292		4.5(5)	6.08	.30(5)
					2312		7.0(7)	5.89	.5(1)
					2321		12(2)	5.64	.9(2)
					2358		1.3(4)	6.61	.10(3)
					2402		2.2(4)	6.35	.20(4)
					2409		17(1)	5.46	1.3(2)
					2467		20.2(15)	5.36	1.7(2)
					2487		15(1)	5.49	1.3(2)
					2607		6.8(7)	5.76	.7(1)
					2719		2.2(7)	6.21	.2(1)
					2727		10.6(4)	5.51	1.2(1)
2771		280(50)	4.54	11(2)					
2789		190(60)	4.70	8(3)					
					2789		20.1(9)	5.21	2.4(3)
					2828		70(7)	4.65	8.6(14)
					2884		12.5(12)	5.38	1.6(2)
2938		30(12)	5.43	1.4(6)					
					2980		8(1)	5.53	1.1(2)
					3014		1.8(5)	6.16	.3(1)
					3050		4.7(7)	5.72	.7(1)
					3079		50(2)	4.68	8(1)
					3130		13(1)	5.23	2.3(4)
					3180		8.7(7)	5.40	1.5(2)
					3203		4.1(8)	5.72	.7(2)
					3312		8(1)	5.37	1.7(4)
					3349		4.6(7)	5.60	1.0(2)
					3363		4.4(7)	5.61	1.0(2)
					3490		7(1)	5.35	1.7(3)

a) $Q_{EC}[^{149}Ho(1/2^+)] = 6.09(5)$ [ALK 83 , FIR 89], $T_{1/2} = 58(3)$ sec [SCH 87].

b) in units of $100 \cdot g_A^2/4\pi$. Calculated as $B_{GT} = \frac{3880}{ft}\, g_A^2/4\pi$ corresponding to $(g_A/g_V)^2 = 1.26$.

c) $Q_{EC}[^{149}Ho(11/2^-)] = 6.04(5)$ [ALK 83], $T_{1/2} = 21(2)$ sec [TOT 79].

septuplet mixing with them. From the energy comparison with ^{147}Gd we suggest the assignements as given in the level scheme (Fig.3.4). The parity of the 1.776 MeV level is indetermined, the proposed $\nu s_{1/2}^{-1}$ assignement, based on energy systematics, is highly tentative. There is no experimental evidence for the speculative $5/2^+$ assignement for the 1.626 MeV state except for its energy.

The five states around 1.6 MeV populated in ^{149}Ho $11/2^-$ decay all lie within less than 0.1 MeV of the ^{148}Dy 2^+ and 3^- excitations at 1.678 and 1.688 MeV. Of these states only the 1.703 MeV level can be assigned as the $11/2^+$ member of the octupole septuplet. From their γ–deexcitation the 1.584 and 1.663 MeV states must be $11/2^-$ or $9/2^+$ that we assign as the $\nu f_{7/2}\times 2^+$ and $\nu f_{7/2}\times 3^-$ multiplet members but cannot distinguish them. Because of its higher β–strength we prefer $(\nu f_{7/2}\times 2^+)_{9/2^-}$ for the 1.703 MeV level. The observed β–strength to that state and the 1.091 MeV $\nu h_{9/2}$ level would suggest a coupling matrix element $m(\nu h_{9/2},\nu f_{7/2}\times 2^+)=0.13$ MeV, not too dissimilar from the 0.17 MeV value of ^{147}Gd. It is however not a priori clear whether that value should be the same because the microscopic structure of the 2^+ phonons in ^{146}Gd and ^{148}Dy could well be different. For the weakly fed 1.782 MeV state, also decaying only to the ground state a $7/2^+$ assignement would be possible.

3.3.1 The $\nu f_{7/2}\times 3^-$ particle–phonon multiplet.

An important result of previous octupole septuplet studies at N=83 is the systematic variation [KAD 89] of the coupling constant K for the q·Q interaction. This variation was attributed to the decrease of the (negative) quadrupole moment of the 3^- phonon with increasing proton number and is related to the dominant $\pi h_{11/2} d_{5/2}^{-1}$ particle–hole contribution to the phonon. When going from Gd, with small negative Q, to lower–Z nuclei the hole–character of the $d_{5/2}$ proton will gradually disappear and will become particle–like in ^{142}Nd causing a much larger negative Q, as is observed in experiment [KAD 89]. Similarly, with protons added in the nuclei above Gd the negative Q should further decrease and is eventually expected to change sign and become positive.

In Fig.3.5 we summarize the ^{149}Dy septuplet data and indicate the here apparent couplings to the $\nu i_{13/2}$ single particle state and to the $\nu s_{1/2}^{-1} j_0^2$ two-particle one-hole excitation. We compare the data with the curve obtained for a q·Q interaction, with the coupling constant K = −1.0 MeV estimated, as shown in Fig.3.5, from extrapolation of the experimental K-values for the four lower-Z isotones.

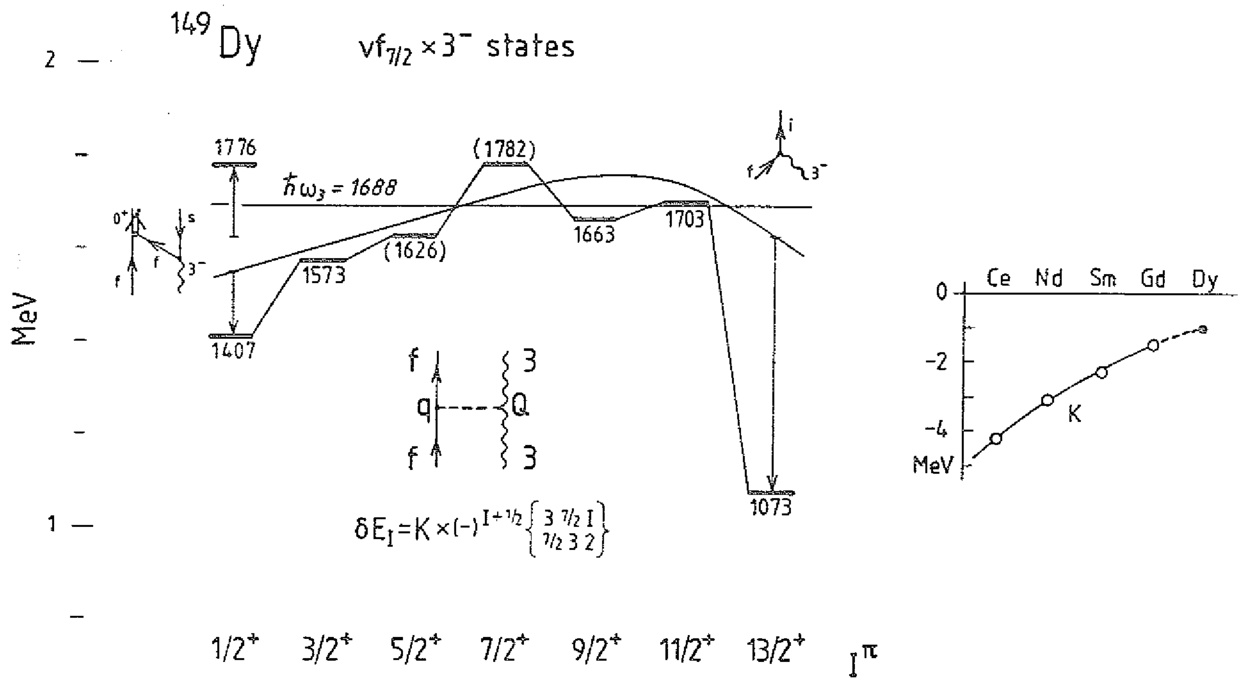

Fig.3.5 The $\nu f_{7/2} \times 3^-$ octupole septuplet in $^{149}Dy_{83}$. Excitation energies are given in keV, including those of tentatively assigned states, and couplings to close-lying neutron excitations are indicated. The smooth curve is calculated from the q·Q interaction with the coupling constant K = −1.0 MeV obtained by extrapolation from the values in lower-Z N = 83 isotones (inset to the right).

The data are in fair agreement with this prediction, and also the implied coupling matrix elements for the I = 1/2 and 13/2 states are in accord with systematics. In any case, the energy shifts shown in Fig.3.5 for the ^{149}Dy septuplet are significantly smaller than in the lower-Z N = 83 isotones.

Septuplet studies in ^{151}Er and ^{153}Yb should reveal the inversion of the phonon quadrupole moment. First evidence of this effect has been found in a study by Mc Neill et al. [McN 89] of ^{153}Yb who identified in this nucleus an $11/2^+$ state at 1.762 MeV, clearly lower than the 1.890 MeV ^{152}Yb 3^- phonon energy.

3.4 Gamow–Teller decay strength.

The β–decay of ^{149}Ho $11/2^-$ can be viewed as the superposition of the odd–proton decay in ^{147}Tb $11/2^-$, discussed above, and the 0^+ pair decay as it occurs in ^{148}Dy with B_{GT}=0.47(3) $g_A^2/4\pi$. The 1.091 MeV $\nu h_{9/2}$ level in ^{149}Dy receives however only B_{GT}=0.13(2) $g_A^2/4\pi$, half the strength to the two lowest $9/2^-$ states in ^{147}Gd. This may be understood as a result of mixing with 3–quasiparticle states that leads to a shift of the strength to higher excitation energies. The strength corresponding to ^{148}Dy $0^+ \longrightarrow 1^+$ decay occurs in ^{149}Dy above 2 MeV, where the total observed strength is B_{GT}= 0.41(2) $g_A^2/4\pi$. This value is essentially equal to ^{148}Dy decay, but does not show the expected increase from the $\nu h_{9/2}$ admixture. From the comparison it becomes clear that our experiment misses about 30% of the expected total strength as a result of the decreasing detection sensitivity at high energy.

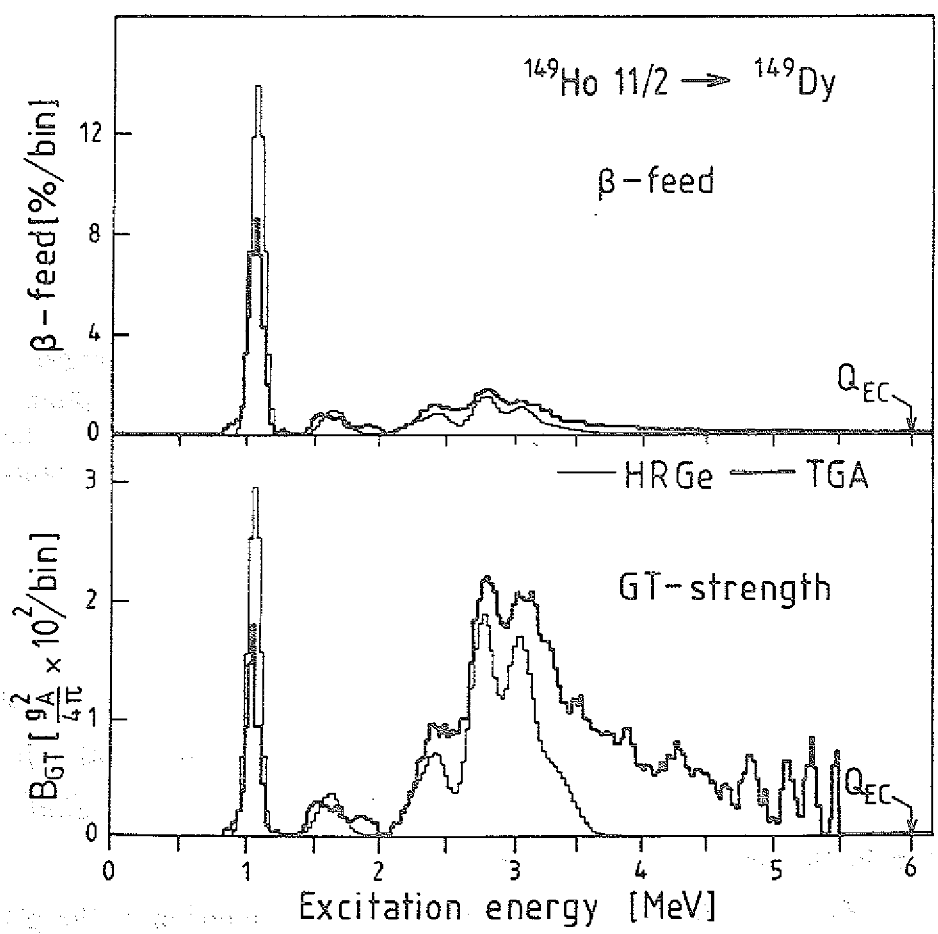

Fig.3.6 Beta–feeding distributions (top) and GT–strengths (bottom) for ^{149}Ho $11/2^-$ decay measured in the present work (HRGe) and by total absorption γ–ray spectroscopy (TGA) [ALK 90]. Energy bin 28.5 keV.

Independent support for this contention may come from the results of TGA-measurements of ^{149}Ho $11/2^-$ decay [ALK 90]. These data (Fig.3.6) suggest 8% β-feeding intensity from 3.5 to 5.5 MeV in ^{149}Dy, which apparently must feed levels with intensities below our sensitivity limit. However, also in this case the TGA data at low excitation present a problem. The 2% β-feed in the TGA data between 1.8 and 2.1 MeV excitation would require at least 6 unobserved levels in this energy range where we would firmly detect any state fed with 0.3% intensity. The total GT-strength determined in the TGA measurements, 1.13 $g_A^2/4\pi$, is nearly twice the value of 0.57(3) $g_A^2/4\pi$ from our high-resolution measurement, and also significantly above the expectation of 0.84(4) $g_A^2/4\pi$ based on the ^{147}Gd $11/2^-$ and ^{148}Dy 0^+ decay data.

For ^{149}Ho $1/2^+$ decay one expects a B_{GT}= 0.47 $g_A^2/4\pi$, as in ^{148}Dy. The apparent strength of B_{GT}= 0.21(4) $g_A^2/4\pi$ to high-lying $1/2^+$ and $3/2^+$ 3-quasiparticle states reflects the here yet more limited detection sensitivity. The 1035 keV ground state transition should represent nearly the total decay, and its intensity suggests that the GT-strength to the 3-quasiparticle states should be doubled, which brings it into close agreement with the ^{148}Dy result.

The above considerations on ^{149}Ho decay reemphasize the severe experimental difficulties in β-strength determinations for the odd-A N=82 nuclei, which for higher-Z parent nuclei will certainly aggreviate further. That the situation is much more favorable for the decays of the doubly-even parent nuclei is a specific feature of this region, which we will discuss below.

CHAPTER 4 : Gamow–Teller decay of the 0.5 s $27/2^-$ high–spin isomer in $^{149}_{66}Dy_{83}$ and the $\pi h_{11/2} \nu h_{9/2}$ residual interaction.

4.1 Introduction

For analysis of GT–decays in nuclei above ^{146}Gd knowledge of the $\pi h_{11/2} \nu h_{9/2}$ proton–neutron residual interaction is of vital importance. In general the two–nucleon residual interactions are calculated from theory, but rarely such theoretical values can quantitatively describe the observed energy spectra in heavy nuclei. Alternatively, one can in principle obtain the two–body interactions from experiment by locating the two–body multiplets in the respective odd–odd nuclei in single–nucleon transfer experiments on target nuclei with one valence nucleon. These experiments however can only be done for nuclei close to stability and are limited to cases where targets are available and to two–body multiplets involving the target ground state nucleon.

In nuclei far off stability the two–body multiplets, in general, cannot be selectively excited. Rather, they must be identified in γ–ray measurements following unspecific excitation processes like compound nucleus– or β–decay. For example, in–beam γ–ray studies with modest angular momentum transfer or neutron capture experiments have been used to identify such states [ERC 83, STY 88].

In unstable nuclei the only possible means for configuration–selective excitation is allowed β–decay. In the nuclei above Gd GT–decay studies of odd–odd parent nuclei identified several multiplet members of $\pi\pi$ and $\nu\nu$ character [STY 88, TAI 89], but only the 1^+ coupling of the $\pi\nu$ multiplet formed by the GT–partners is accessible in ground state decay of even–even parent nuclei. In this way, GT–decay of ^{148}Dy [KLE 85], which in its ground state is largely $(\pi h^2_{11/2})_{0^+}$, populates in ^{148}Tb the $(\pi h_{11/2} \nu h_{9/2})_{1^+}$ level at 0.620 MeV. From this energy, one obtains the strongly attractive 1^+ residual interaction as

$$V_{\pi h_> \nu h_<,1} = E_{\pi h_> \nu h_<,1} - E_0 = -1.360 \text{ MeV} \tag{4.1}$$

with

$$E_0 = E^{147Tb}_{\pi h_>} + E^{147Gd}_{\nu h_<} - M_{146Gd} - M_{148Tb} + M_{147Tb} + M_{147Gd} = 1.980 \text{ MeV}, \tag{4.2}$$

where E is the excitation energy and the M–values are ground state masses (Table 4.2).

The remaining nine multiplet members, with I = 2 to 10, are expected to lie more than 1 MeV above the ^{148}Tb yrast line and were so far not known. High-spin members of this multiplet would be populated in β-decay of the well known $(\pi h^2_{11/2})_{10^+}$ state of ^{148}Dy, but its much faster $10^+ \rightarrow 8^+$ E2 decay precludes a β-decay branch. However, in the neighbouring N = 83 nuclei the half-life of the corresponding $(\pi h^2_{11/2} \nu f_{7/2})_{27/2^-}$ isomer is about 0.5 sec, and here a 5% GT-decay branch has been recently observed for the ^{151}Er $(\pi h^4_{11/2} \nu f_{7/2})_{27/2^-}$ 5qp-state [BAR 88], and indications of a similar but much weaker GT-decay branch for the ^{149}Dy 27/2$^-$ 3qp-isomer have also been reported. In contrast to ^{151}Er, this latter decay populates $\pi h_{11/2} \nu h_{9/2} \nu f_{7/2}$ 3qp-states in the $^{149}_{65}$Tb$_{84}$ daughter nucleus, which can provide information on the searched for high-spin $\pi h_{11/2} \nu h_{9/2}$ residual interaction.

The γ-decay of the 0.5 s ^{149}Dy 27/2$^-$ isomer was well known from the early work of Stefanini et al. [STE 76A], and also the high-spin states in the β-decay daughter ^{149}Tb have been studied [NDS 85]; recent high-sensitivity OSIRIS measurements with ^{7}Li beam identified important additional ^{149}Tb levels [LAC 91] which we will discuss below together with the ^{149}Dy 27/2$^-$ GT-decay results.

4.2 Experiments and results.

The 27/2$^-$ ^{149}Dy activity was produced at ISOLDE in spallation reactions of tantalum with 600 MeV protons. It was collected on tape for 200 ms and was measured for 1 sec with the Ge-detector set up as described in the previous chapter. The singles spectra were recorded in eight 0.125 sec subgroups for γ-ray half-life identification. In our singles spectra ^{149}Dy 27/2$^-$ accounted for approximately 1/6 of the decays. The ^{149}Dy ground state (4.1 min) and ^{149}Ho 11/2$^-$ (21 sec) contributed 2.5 and 1.5 times more decays. The ^{149}Tb 11/2$^-$ (4.2 min) had about the same intensity as the ^{149}Dy 27/2$^-$ isomer while ^{149}Ho 1/2$^+$ (58 sec) and ^{149}Tb 1/2$^+$ (4.1 h) were 20 and 4 times weaker. It is clear that under these conditions study of a weak GT-decay branch of the ^{149}Dy 27/2$^-$ isomer is difficult, but the very high statistics obtainable at ISOLDE allowed to investigate it with good accuracy.

The results of our measurements on the ^{149}Dy $27/2^-$ decay are shown in Fig.4.1 and 4.2, and are summarized in Table 4.1. The coincidence data clearly show a cascade of 5 γ-rays and their apparent decay half-life of 0.5 sec demonstrates that they are emitted following the $27/2^-$ decay. Coincidences with annihilation radiation conclusively characterise them as γ-rays in the β-decay daughter ^{149}Tb. All these ^{149}Tb γ-rays have previously been observed in in-beam yrast experiments [OGA 77, SIN 79] and the associated energy levels up to $27/2^-$ and their configurations were well known.

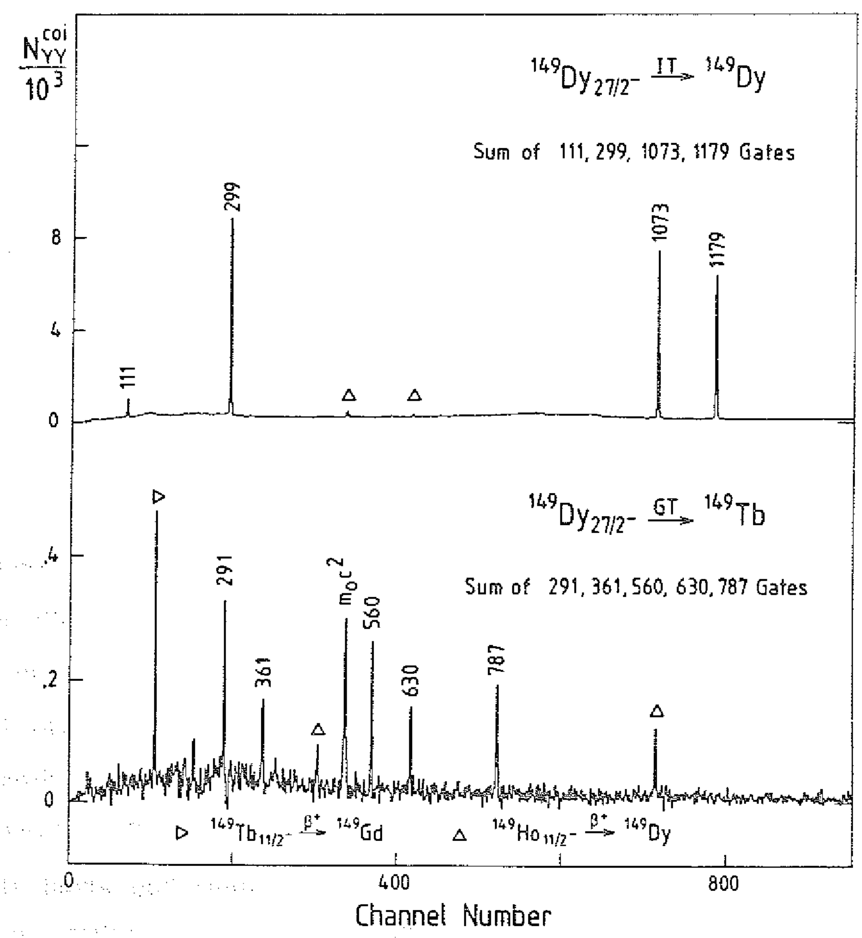

Fig.4.1 Gamma-gamma coincidence spectra in the decay of the 0.5 s ^{149}Dy $(\pi h_{11/2}^2 \nu f_{7/2})\,27/2^-$ isomer at 2.661 MeV excitation. Top: internal transition decay. Bottom: GT-decay branch to the $(\pi h_{11/2} \nu h_{9/2} \nu f_{7/2})\,25/2^-$ state in ^{149}Tb.

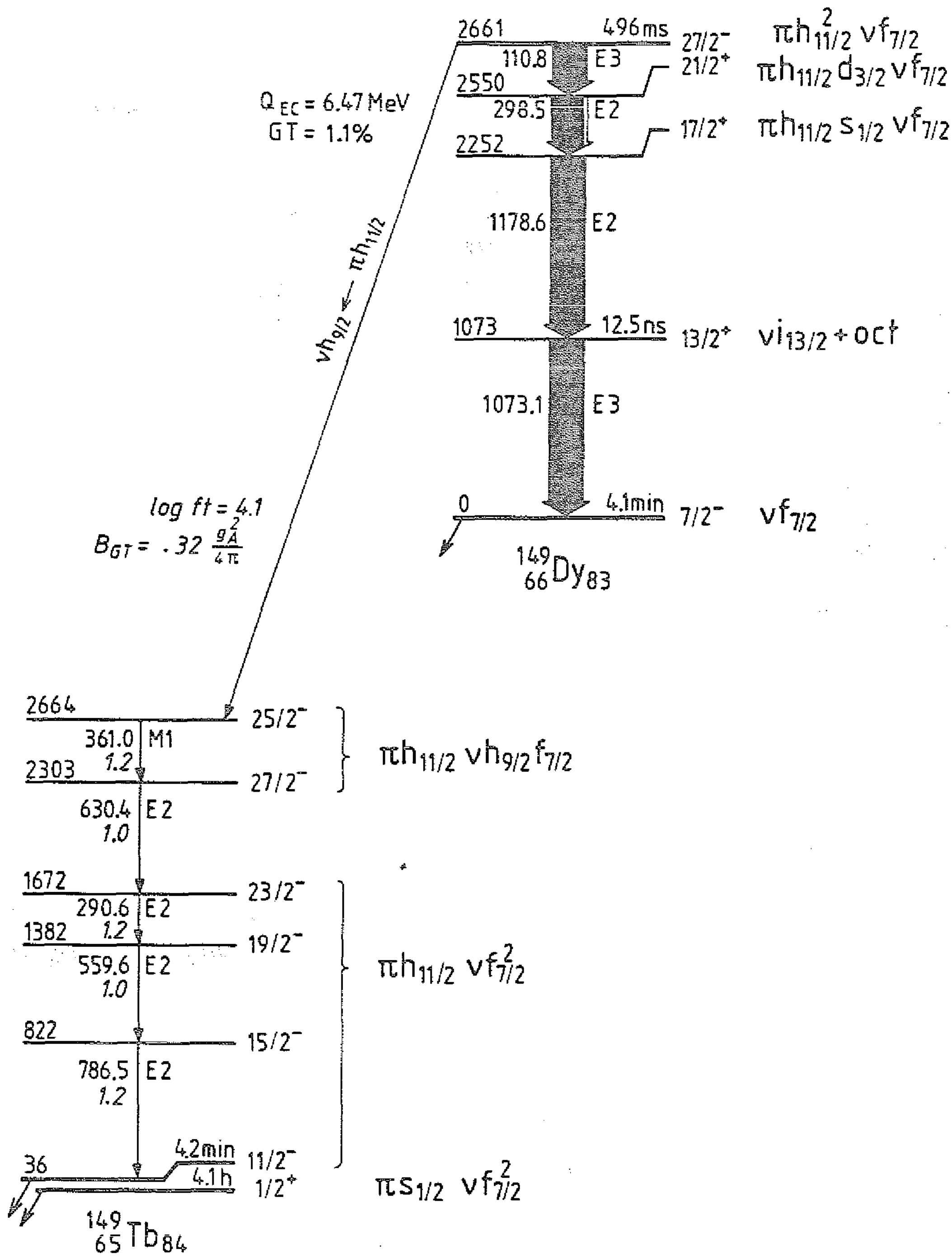

Fig.4.2 The decay scheme of the $27/2^-$ isomer in ^{149}Dy.

Table 4.1 Gamma–transitions following IT– and β–decay of 0.5 s ^{149}Dy 27/2$^-$.

E_γ(keV)	Multi–polarity [a]	I_γ [b]	I_{tot} [b]	$T_{1/2}$ (sec)
		Transitions in ^{149}Dy		
110.8(2)	E3	3.38	97	0.55(9)
298.5(2)	E2	99	105	0.50(2)
1073.1(2)	E3	97 [c]	97 [c]	0.50(3) [c]
1178.6(2)	E2	96	96	0.49(2)
		Transitions in ^{149}Tb		
290.6(2)	E2	1.08(19)	1.15(20)	0.5(3)
361.2(2)	M1	1.11(19)	1.18(20)	– [d]
559.6(2)	E2	1.03(20)	1.04(20)	0.48(13)
630.2(3) [e]	E2	1.0(3) [e]	1.0(3) [e]	– [f]
786.5(4)	E2	1.2(4) [e]	1.2(4) [e]	0.6(2) [g]

a) From in–beam studies [OGA 76, SIN 79, DAL 80].
b) Given per 10^2 isomer decays. Errors are 5% unless specified. I_{tot} calculated with tabulated α_{tot}–values [RÖS 78].
c) Corrected for 18% contribution from 21 s ^{149}Ho 11/2$^-$ decay.
d) Complex peak in singles spectra.
e) Extracted from coincidence data.
f) Obscured in singles spectra by about 8 times stronger 630.9 keV ^{149}Gd line and by about twice stronger 630 keV ^{149}Dy line.
g) Resolved with difficulty from 52 times stronger 789.4 keV line in ^{149}Tb.

For the 2.664 MeV state $I^\pi = 25/2^-$ or $29/2^-$ was previously suggested [SIN 79], but our data firmly establish it to be a $(\pi h_{11/2} \nu h_{9/2} f_{7/2})_{25/2^-}$ state. Within the accuracy of our data, the five ^{149}Tb γ–rays have equal intensities, indicating that the β–decay proceeds entirely to this 25/2$^-$ state. From the γ–intensities of Table 4.1, the β–decay branch

$$\frac{I_{GT}}{I_{IT}+I_{GT}} = 1.12(10)\%$$

results. Our timing data give the isomer half–life as

$$T_{1/2}(27/2^-) = 496(14) \text{ ms},$$

in excellent agreement with the early [STE 76A] value. The ^{149}Dy ground state Q_{EC}–value has recently been measured as $Q_{EC}(^{149}\text{Dy},7/2^- \longrightarrow {}^{149}\text{Tb},1/2g) = 3.812(10)$

MeV [KEL 89]. Using the pertinent excitation energies, the measured half-life and the decay branch we obtain

$$\log ft\ (^{149}Dy,27/2^{-} \longrightarrow {}^{149}Tb,25/2^{-}) = 4.08(2) \quad \text{or}$$

$$B_{GT} = 0.32(2)\ g_A^2/4\pi\,.$$

This B_{GT}-value is only two thirds of the ^{148}Dy ground state decay. The quantitative interpretation of the GT-strength would however need more detailed theoretical analysis.

4.3 The $\pi h_{11/2} \nu h_{9/2}$ residual interaction.

The ^{149}Dy $27/2^-$ decay data clearly identify the $(\pi h_{11/2}\nu h_{9/2}\nu f_{7/2})$ $25/2^-$ and $27/2^-$ states in ^{149}Tb. Their energies allow to extract the 10^+ and 9^+ $\pi\nu$ residual interaction for these $\pi h_{11/2}\nu h_{9/2}$ couplings. This is possible since the other two two-body couplings contributing to the ^{149}Tb 3qp-states, $\pi h_{11/2}\nu f_{7/2}$ and $\nu f_{7/2}\nu h_{9/2}$ are known from in-beam studies of the respective two-valence particle nuclei ^{148}Tb and ^{148}Gd [STY 87, PII 90]. These data are compiled in Fig.4.3, together with other two-body multiplets used in later discussions.

The ^{149}Tb $27/2^-$ state straightforwardly gives the fictitious $(\pi h_{11/2}\nu h_{9/2})10^+$ ^{148}Tb excitation energy from the relation

$$\begin{aligned} E^{148Tb}_{\pi h_> \nu h_<,10} &= E^{149Tb}_{\pi h_> \nu h_< \nu f_>,27/2} - E^{148Tb}_{\pi h_> \nu f_>} - E^{148Gd}_{\nu h_< \nu f_>,8} + \\ &\quad + E^{147Gd}_{\nu f_>} + E^{147Gd}_{\nu h_<} + E^{147Tb}_{\pi h_>} - S = 1.483 \text{ MeV}, \end{aligned}$$

where S contains the ground state masses of the six pertinent nuclei and is

$$S = -M_{149Tb} + M_{148Gd} + 2M_{148Tb} - M_{147Tb} - 2M_{147Gd} = -0.516 \text{ MeV},$$

with the masses given in Table 4.2. From the calculated 10^+ excitation energy the residual interaction follows from eq.(4.2) as -0.497 MeV.

Table 4.2 : Input data used in the present shell model calculations.

Nucl.	Config.	I^{π}	E_x(keV) or Mass excess	Ref.
^{146}Gd		0^+	−76095	86Ru
^{147}Gd	$\nu f_{7/2}$	$7/2^-$	−75366	86Ru
	$\nu h_{9/2}$	$9/2^-$	1397	78Le
^{148}Gd	$\nu f_{7/2}^2$	0^+	−76278	86Ru
		2^+	784	90Pi
		4^+	1416	90Pi
		6^+	1811	90Pi
	$\nu f_{7/2}\nu h_{9/2}$	8^+	2694	90Pi
		7^+	2935	90Pi
		6^+	2783	90Pi
		5^+	(2860)	*
		4^+	(2839)	*
		3^+	(2870)	*
		2^+	(2746)	*
		1^+	(2850)	*
^{147}Tb	$\pi s_{1/2}$	$1/2^+$	−70767	86Ru,87Li
	$\pi h_{11/2}$	$11/2^-$	51	87Li
^{148}Tb	$\pi d_{3/2}\nu f_{7/2}$	2^-	−70570	86Ru,87St
	$\pi h_{11/2}\nu f_{7/2}$	9^+	90	87St
		8^+	406	87St
		7^+	328	87St
		6^+	426	87St
		5^+	351	87St
		4^+	375	87St
		3^+	281	87St
		2^+	178	87St
	$\pi h_{11/2}\nu h_{9/2}$	10^+	(1484)	91St
		9^+	(1723)	91St
		8^+	(1654)	*
		7^+	(1690)	*
		6^+	(1610)	*
		5^+	(1670)	*
		4^+	(1550)	*
		3^+	(1570)	*
		2^+	(1130)	*
		1^+	620	78Le
^{149}Tb	$\pi s_{1/2}$	$1/2^+$	−71498	86Ru,90Ma
	$\pi h_{11/2}$	$11/2^-$	36	84De
^{148}Dy	$\pi h_{11/2}^2$	0^+	−67898	86Ru
		2^+	1678	80Da
		4^+	2428	80Da
		6^+	2732	80Da
		8^+	2834	80Da
		10^+	2919	80Da
^{149}Dy	$\nu f_{7/2}$	$7/2^-$	−67772	86Ru
^{150}Dy		0^+	−69320	86Ru

* Estimated energy.

78Le: Table of isotopes [LED 78], 80Da: P.J.Daly et al. [DAL 80], 84De: D.J.Decman et al. [DEC 84],86Ru: B.Rubio et al. [RUB 86], 87Li: C.F.Liang et al. [LIA 87], 87St: J.Styczen et al. [STY 87], 90Ma: L.G.Mann et al. [MAN 90], 90Pi: M.Piiparinen et al. [PII 90], 91St: J.Styczen et al. [STY 91].

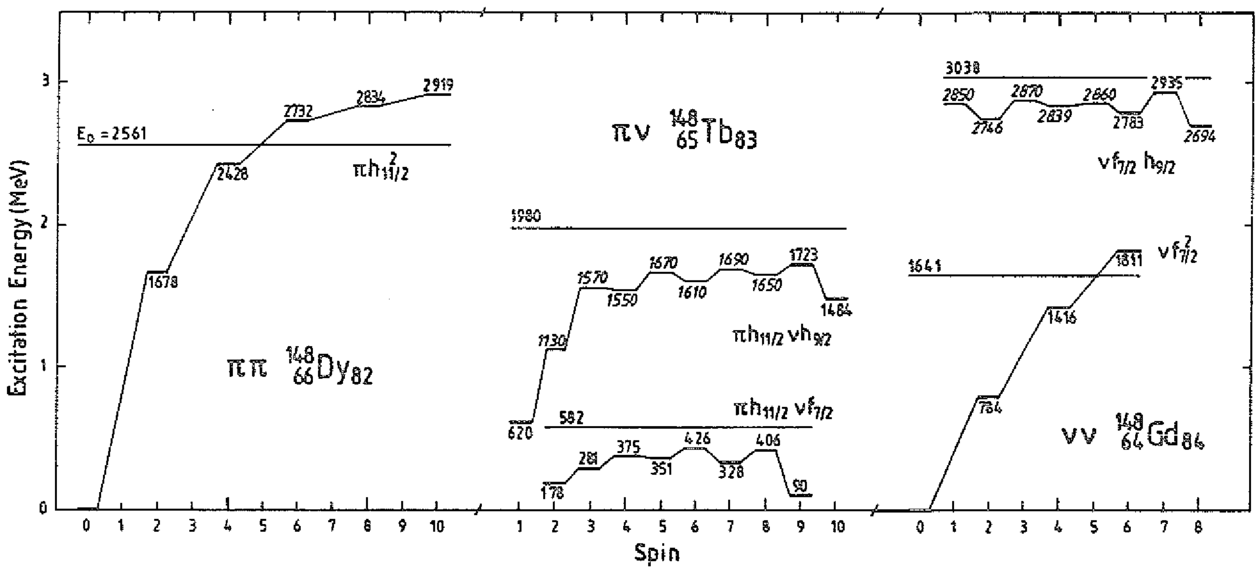

Fig.4.3 Two-nucleon multiplets in ^{148}Dy, ^{148}Tb, and ^{148}Gd specifying the two-body interactions used in the shell model calculations. Observed excitations are given in keV, in skew numbers when estimated.

The $\pi h_{11/2}\nu h_{9/2}\nu f_{7/2}$ 3qp-configuration can form two $25/2^-$ states which, in a recoupling calculation [BRU 77], result as the eigenvalues of a 2×2 matrix. By appropriate choice of the coupling order the off-diagonal matrix elements are specified from the $(\pi h_{11/2}\nu f_{7/2})_{8^+,9^+}$ and $(\nu f_{7/2}\nu h_{9/2})_{7^+,8^+}$ interactions alone which are known, and of the diagonal matrix elements only one contains the unknown $\pi h_{11/2}\nu h_{9/2}$ 9^+ energy whereas the other one can be calculated with the known 10^+ energy. Our measured $25/2^-$ excitation therefore fully specifies the $\pi h_{11/2}\nu h_{9/2}$ 9^+ energy as 1.682 MeV. The second $25/2^-$ state of the configuration is naturally also fixed by this 9^+ interaction and results at 2.751 MeV excitation. This state has been observed in the recent high-sensitivity in-beam experiment [LAC 91], at 2.763 MeV.

With this knowledge we reanalized the in-beam data of ^{144}Sm(^{7}Li,3n)^{148}Tb experiment [STY 87,STY 91] where the primary two-body $\pi h_{11/2}\nu h_{9/2}$ high-spin multiplet members could have been weakly excited. We could identify ^{148}Tb levels at 1.484 and 1.723 MeV, within ~40 keV of the expected 10^+ and 9^+ energies, with decay properties consistent with these spin-values. Although the data for these very weakly populated ^{148}Tb levels cannot provide definite I^π assignements we include them in Fig.4.3. The excellent consistency of the observed (10^+) and (9^+) states with the $\pi h_{11/2}\nu h_{9/2}\nu f_{7/2}$ 3qp–energies in ^{149}Tb supports these tentative two–body configuration identifications in ^{148}Tb.

The remaining 2^+ to 8^+ multiplet members are not known and there are at present no experimental data which could specify any individual of these energies. However, the spin–averaged $\pi h_{11/2}\nu h_{9/2}$ interaction determines the variation of the low–lying $\nu h_{9/2}$ state in the N=83 nuclei when $h_{11/2}$ proton pairs are added above Gd. The state is observed in the isotones up to ^{153}Yb and its energy decreases regularly from 1.397 MeV in ^{147}Gd down to 0.567 MeV in ^{153}Yb.

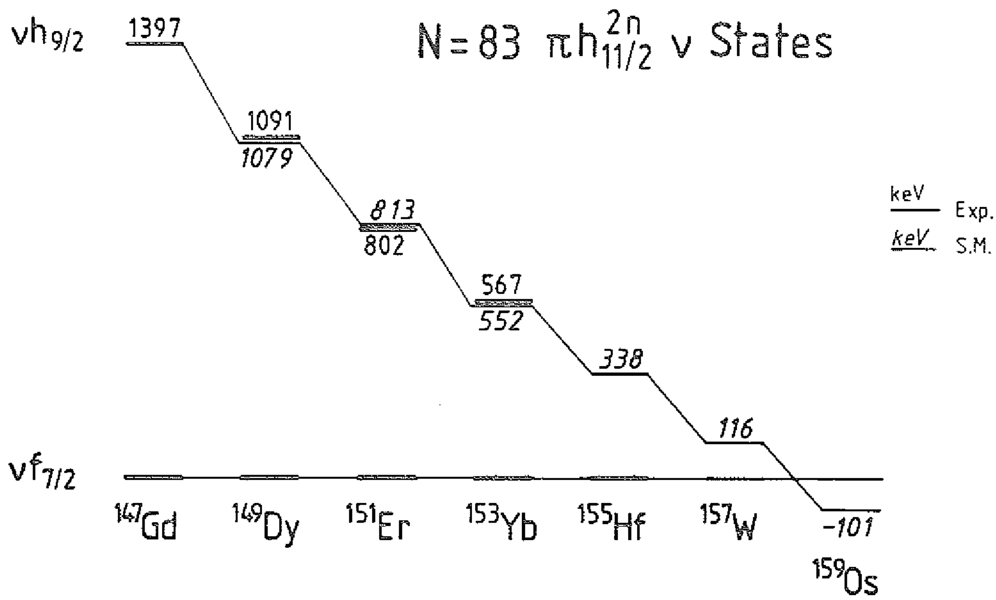

Fig.4.4 The $\nu h_{9/2}$ excitation energy in N=83 isotones compared with calculated results (italic numbers).

The estimated 2^+ to 8^+ energies shown in Fig.4.3 reproduce the three known $\nu h_{9/2}$ excitations above Gd within less than 15 keV (Fig.4.4). The calculated $9/2^-$ excitation energies are obtained from multiparticle recoupling calculations as the relative energy of the lowest $(\pi h_{11/2}^{2n}\nu h_{9/2})_{9/2^-}$ and $(\pi h_{11/2}^{2n}\nu f_{7/2})_{7/2^-}$ states, using the 1.397 MeV $\nu h_{9/2}$ single particle energy from ^{147}Gd. Such calculations naturally also give the yet lower $h_{9/2}$ energies for the N=83 nuclei above Yb. They predict that latest $^{159}_{76}Os_{83}$ should have an $\nu h_{9/2}$ ground state.

The adopted $\pi h_{11/2}\nu h_{9/2}$ interactions as shown in Fig.4.3 will be used in all further shell model calculations.

CHAPTER 5 : Yrast energies and GT–strength functions from shell model calculations with empirical two–body interactions.

The shell model describes nuclear states in terms of angular momentum coupled many–particle configurations. In heavy nuclei its application is limited to regions in the near vicinity of closed shells, where a few valence particles move in well defined orbitals. A particular nuclear state in general will be a mixture of many configurations, but in cases where it is well separated from other levels with the same spin and parity a single configuration might be dominant. Such states will most likely occur along the yrast line because here the level density is low. These pure configuration excitations are well suited for shell model analysis with empirical interactions. It has been shown that yrast states in the neighbourhood of ^{208}Pb are reproduced with high accuracy [BLO 79] when the shell model input data – ground state masses, single particle energies and two–nucleon residual interactions – are taken from experiment. More recently it was noticed that such shell model analyses are also quite successful in nuclei around ^{146}Gd [BLO 83,LAC 91], where however lack of the experimental input data often limited them.

5.1 Yrast states.

In the nuclei above ^{146}Gd, with one or two valenve neutrons, the yrast states are largely formed by the couplings of protons in the $h_{11/2}$ shell and neutrons in either $f_{7/2}$ or $h_{9/2}$. (The only remaining high–j particle – $\nu i_{13/2}$ – has much higher single particle energy and therefore is not active at the beginning of the yrast line.) With the disclosure of the $\pi h_{11/2}\nu h_{9/2}$ two–body multiplet it is now possible to calculate the yrast states of these configurations in the N=83 and 84 nuclei and compare them with experimental results.

In the following we present a few examples of yrast line calculations where we will use this new $\pi h_{11/2}\nu h_{9/2}$ interaction. As mentioned, the remaining $\pi h_{11/2}\pi h_{11/2}$, $\pi h_{11/2}\nu f_{7/2}$, $\nu f_{7/2}\nu h_{9/2}$, and $\nu f_{7/2}\nu f_{7/2}$ multiplets were identified in previous studies (Fig.4.3 and Table 4.2). In our analysis of these nuclei, which include up to ten valence particles, we decided to decompose the complex configurations into the full set of two-body interactions in order to keep the ambition of the calculation on the same level in all cases. Moreover, alternate reductions into larger substructures, which might well be more successful, are precluded since sufficient pertinent data are not available. We note here that our shell model calculations reduce to pure angular momentum recoupling calculations since the radial part of the interactions is included in the experimental matrix elements. Moreover, it is clear from the above that our calculations will not include configuration mixing.

Before presenting the full results, we calculate, as a simple example, the energy of the maximally aligned $(\pi h_{11/2} \nu f_{7/2} \nu h_{9/2}) 18^{+}$ state in ^{150}Dy which is experimentally observed [LUN 79] at 5.071 MeV. It is

$$E^{150Dy}_{\pi h^2_> \nu f_> h_<, 18} = E^{148Dy}_{\pi h^2_>, 10} + \frac{31}{20} E^{148Tb}_{\pi h_> \nu h_<, 10} + \frac{9}{20} E^{148Tb}_{\pi h_> \nu h_<, 9} + \frac{29}{18} E^{148Tb}_{\pi h_> \nu f_>, 9} +$$

$$+ \frac{7}{18} E^{148Tb}_{\pi h_> \nu f_>, 8} + E^{148Gd}_{\nu f_> \nu h_<, 8} - E_o = 5.105 \text{ MeV},$$

where the fractions are angular momentum recoupling coefficients [EDM 57] and E_o contains the pertinent single particle energies and ground state masses, compiled in Table 4.2, as

$$E_o = 4\, E^{147Tb}_{\pi h_>} + 2\, E^{147Gd}_{\nu f_>} + 2\, E^{147Gd}_{\nu h_<} - (3\, M_{146Gd} - 4\, M_{147Gd} + M_{148Gd} +$$

$$- 4\, M_{147Tb} + 4\, M_{148Tb} + M_{148Dy} - M_{150Dy}) = 3.887 \text{ MeV}.$$

The non-stretched yrast states involve a rapidly increasing number of contributing two-body couplings. We obtain them with the angular momentum recoupling part of a shell model code.

5.1.1 Low-lying states in odd-odd N=83 nuclei.

The Fig.5.1 gives the calculated level energies for low-lying high-spin states in the odd-odd N=83 isotones compared to experimental data known up to ^{154}Lu. The data for ^{148}Tb which provide our two-body interactions are also included. The states in ^{150}Ho, ^{152}Tm, and ^{154}Lu were observed [McN 86, McN 90] in the decay of a $(\pi h_{11/2}^{2n+1} \nu f_{7/2})17^+$ isomer at ~2.6 MeV excitation. Also included in the figure is the lowest $(9^+ \times 3^-)11^-$ octupole excitation, which is a pronounced yrast state and explains why in ^{150}Ho the $(\pi h_{11/2} \nu h_{9/2})9^+$ and 10^+ states were not seen.

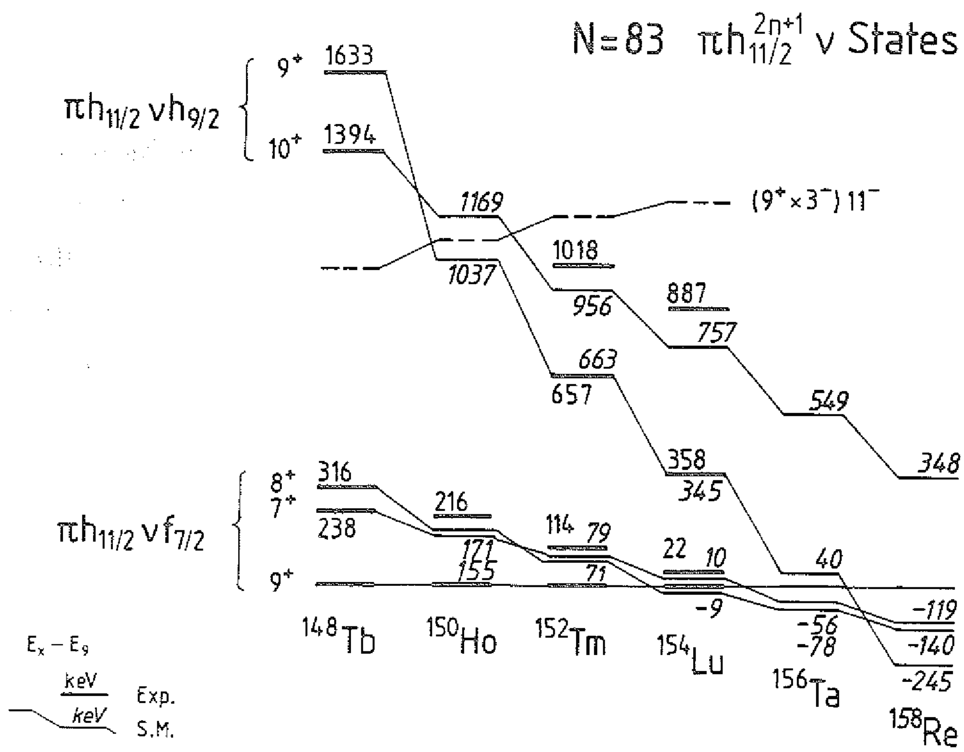

Fig.5.1 Experimental and calculated (italic numbers) low-lying high-spin states of the configurations $\pi h_{11/2}^{2n+1} \nu f_{7/2}$ and $\pi h_{11/2}^{2n+1} \nu h_{9/2}$ in doubly odd N = 83 isotones. All energies (in keV) are relative to the $(\pi h_{11/2}^{2n+1} \nu f_{7/2})9^+$ state. From experiment the levels at 216 keV (Ho) and 114 keV (Tm) are assigned as 8^+, in ^{154}Lu as 22 keV (8^+) and 0 keV (9^+). References to the data are given in the text.

The $\pi h_{11/2} \nu f_{7/2}$ configuration in experiment and calculation shows the typical compression with increasing proton number when the $h_{11/2}$ shell is filled. The calculation predicts the 8^+ coupling in ^{150}Ho and ^{152}Tm slightly too low, and gives already for ^{154}Lu an 8^+ ground state, 9 keV below the 9^+ coupling, whereas experiment suggests an (8^+) state 22 keV above the (9^+) ground state. Spin 8^+ is probably more firmly predicted for the ground state of the still undiscovered ^{156}Ta nucleus, whereas the even more exotic ^{158}Re should again have a 9^+ ground state but of different configuration.

The drastic lowering of the $\pi h_{11/2}\nu h_{9/2}$ states largely reflects the afore mentioned similar energy decrease of the $\nu h_{9/2}$ single particle excitation with the filling of the $h_{11/2}$ proton shell. There are two remarkable features for this configuration, namely the inversion of the 10^+ and 9^+ states already in ^{150}Ho, which is much below the middle of the shell, and the much larger predicted 10^+ to 9^+ separation at the upper end of the shell in ^{158}Re compared to the two-particle situation in ^{148}Tb. Both effects are related to the very large attraction of −1.4 MeV in the 1^+ coupling of the configuration (Fig.4.3).

The inversion of the 10^+ and 9^+ states has been discussed by McNeill et al. [McN 86] who have identified these levels in Tm and Lu. The inversion is caused by the presence of a $\pi h_{11/2}$ 0^+ pair and should first occur in Ho. In the 10^+ coupling the two odd particles are fully aligned, and therefore the m = 11/2 proton substate (third component of the j = 11/2 angular momentum) is occupied, preventing a proton of a pair to form the 1^+ coupling with the $h_{9/2}$ neutron. In 9^+, the $h_{11/2}$ proton or the $h_{9/2}$ neutron occupy the m = j − 1 substate which allows to form the strongly attractive $(\pi h_{11/2}\nu h_{9/2})1^+$ coupling. In the higher-Z nuclei the effect is enhanced as more protons will contribute to the 1^+ coupling.

5.1.2 Yrast states in even-Z N = 84 nuclei.

The Fig.5.2 compares the observed and calculated yrast states in N = 84 nuclei of the $\pi h^{2n}_{11/2}\nu f^{2}_{7/2}$ and $\pi h^{2n}_{11/2}\nu f_{7/2}h_{9/2}$ configurations. The data for ^{150}Dy are from an early (α,6n) study [LUN 79] by the group. The ^{152}Er yrast states up to 18^+ were first reported by [BAS 80]; we here also include the 15^+ and the second 16^+ levels identified by Kuhnert et al. [KUH 88] in a recent high-sensitivity OSIRIS experiment at the HMI-Berlin. The nucleus ^{154}Yb [RAT 84] is presently reinvestigated by the group [ZHA 91], also in an OSIRIS experiment with ^{54}Fe beam on ^{106}Cd. A recent ^{154}Lu β-decay study [VIE 88] established the ^{154}Yb 8^+ excitation at 2.047 MeV, which in turn determines the level energies above the 8^+ state as shown in Fig.5.2. In ^{156}Hf, only the 8^+ excitation is known from α-decay data [HOF 79] as 1.977(18) MeV. Accurate ground state masses necessary for the calculation are only known for ^{150}Dy (Table 4.2), whereas in the other nuclei we normalize our calculated excitation energies to a specific state marked in the figure by an asterisk.

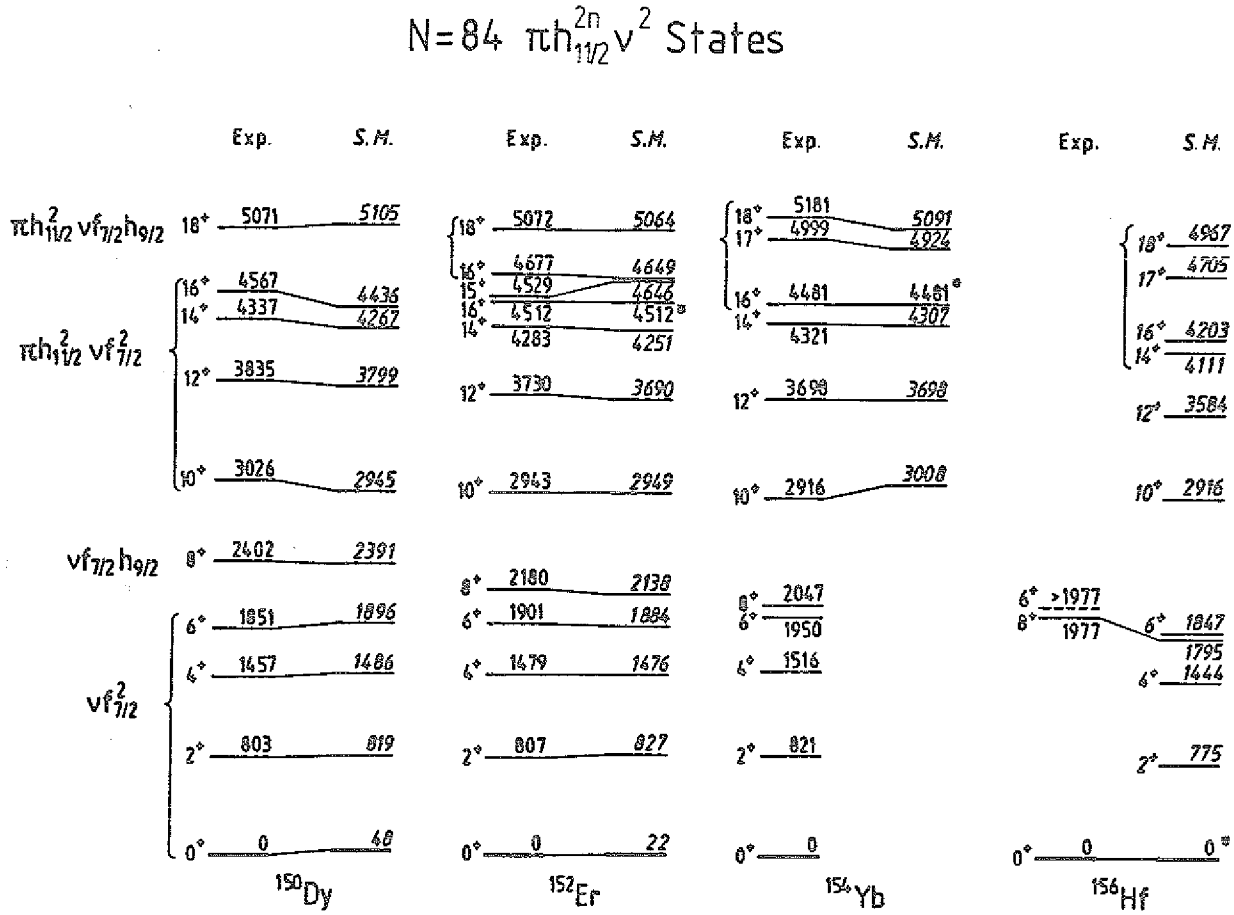

Fig.5.2 Yrast states in even-A N=84 nuclei of $\pi h_{11/2}^{2n} \nu f_{7/2}^{2}$ and $\pi h_{11/2}^{2n} \nu f_{7/2} h_{9/2}$ configurations. Level energies (in keV) calculated from the shell model (S.M.) with experimental two-body interactions are given in italic and connected to the corresponding observed states (to the left). Calculated excitation energies in ^{152}Er, ^{154}Yb, and ^{156}Hf are normalized to the state marked by an asterisk. The ground state masses used to calculate the excitation energies in ^{150}Dy are listed in Table 4.2. References to the experimental data are given in the text.

Also in these N=84 nuclei the decrease of the $\nu h_{9/2}$ single particle energy complicates the structure of the yrast line in the heavier isotones. While in Dy the two configurations are well separated, they move closer in Er and begin to overlap in Yb. Up to $I^{\pi} = 8^{+}$, the protons do not contribute to the spin. Consequently the energy spectra are essentially determined by the $\nu f_{7/2}^{2}$ and $\nu f_{7/2} h_{9/2}$ interactions, which is already apparent from the very similar 0^{+} to 6^{+} spacings of the $\nu f_{7/2}^{2}$ configuration. Also the 8^{+} energy is quantitatively described by the lowering of the $\nu h_{9/2}$ energy in the N=83 isotones. In fact the relative $(\nu f_{7/2} h_{9/2}) 8^{+}$ and

$(\nu f_{7/2}^2)6^+$ two–neutron interaction, that can be extracted from the 8^+ and 6^+ energies at N = 84 and the $9/2^-$ excitation in the respective N = 83 isotopes, results for the three nuclei as −540 (^{150}Dy), −523 (^{152}Er), and −470 keV (^{154}Yb). Most dramatically the $(\nu f_{7/2}h_{9/2})8^+$ lowering becomes evident in ^{156}Hf, where the state drops below the $(\nu f_{7/2}^2)6^+$ level giving rise to the 0.57 ms $\Delta l = 8$ α–decay isomer [HOF 79]. The occurance of this isomer is correctly predicted by our calculations.

In contrast to the 8^+ energy variation, which similar as the $9/2^-$ lowering is caused only by interaction with 0^+ proton pairs, unpaired protons contribute to the $\pi h_{11/2}^2 \nu f_{7/2} h_{9/2}$ high–spin states, and consequently the energy shifts are here strongly affected by the Pauli principle. The effect is analogous as in the $\pi h_{11/2} \nu h_{9/2}$ configuration in the odd–odd N = 83 isotones, where in the 9^+ (I_{max}–1) coupling the $\pi h_{11/2}$ m = 11/2 substate is vacated and therefore the $(\pi h_{11/2} \nu h_{9/2})1^+$ attraction can be exploited. Since in the ^{150}Dy 18^+ state the $\pi h_{11/2}$ m = 11/2 and 9/2 substates are both occupied, only the $I_{max}-2$ state will significantly drop in ^{152}Er, where it occurs 395 keV below the 18^+ excitation. This energy lowering, but less pronounced, occurs also for the other lower spin couplings, and the 17^+ state 182 keV below 18^+ in ^{154}Yb is of this origin.

5.1.3 Yrast states in odd–Z N = 84 nuclei.

Yrast data for the odd–Z N = 84 isotones are compiled in Fig.5.3. In these nuclei the analogous configurations, but coupled to the odd $h_{11/2}$ proton, have only been recognized up to $27/2^-$ at ~2.3 MeV, corresponding to the $(\pi h_{11/2}^{2n} \nu f_{7/2} h_{9/2})8^+$ states in the even isotones at similar energy.

The ^{149}Tb results are from the ^{149}Dy $27/2^-$ GT–decay (chapter 4) and from a recent in–beam study [LAC 91]. The ^{151}Ho was studied by Gizon et al. [GIZ 81], but we have in two cases reinterpreted levels (1.694 and 2.685 MeV) where the data were ambiguous. Additional information about configuration assignements comes from data [BAR 88] on the ^{151}Er $27/2^-$ GT–decay. The ^{153}Tm data are still quite limited [RAT 84], with tentative I^π assignements above 1.8 MeV.

The evident message of Fig.5.3 is again the decreasing excitation of the configuration involving the $h_{9/2}$ neutron, which apparently will make level assignements in Tm delicate. In contrast to the 8^+ state at even–Z, where the spin originates from the two valence neutrons alone, the odd $h_{11/2}$ proton at odd-Z will also contribute to the spin and therefore the addition of a proton pair activates the 1^+ attraction for the (I_{max}-1) $25/2^-$ coupling. This becomes manifest in experiment where the low $25/2^-$ state drops from 316 keV above $27/2^-$ in Tb to 229 keV below $27/2^-$ in Ho. In both nuclei the low $25/2^-$ state is strongly fed in GT-decay and consequently is dominated by the $(\pi h_{11/2}\nu h_{9/2})9^+$ coupling, whereas the higher-lying $25/2^-$ state, not observed in GT-decay, contains largely the $(\pi h_{11/2}\nu h_{9/2})10^+$ amplitude. The different Z-dependence for the two $25/2^-$ energies thus reflects the similar behaviour of the $(\pi h_{11/2}\nu h_{9/2})10^+$ and 9^+ states in the odd-odd N = 83 nuclei.

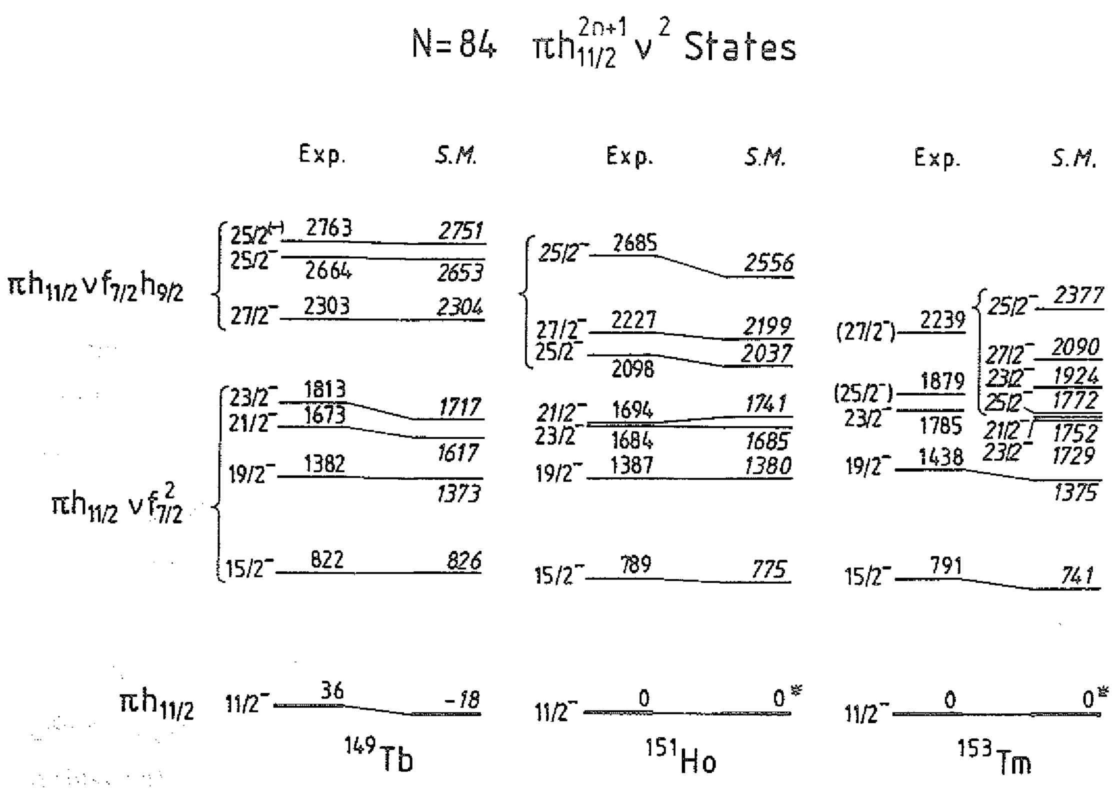

Fig.5.3 Experimental (left) and calculated (S.M., right) yrast levels in N = 84 odd-Z nuclei of the configurations $\pi h_{11/2}^{2n+1}\nu f_{7/2}^{2}$ and $\pi h_{11/2}^{2n+1}\nu f_{7/2}h_{9/2}$. In ^{151}Ho and ^{153}Tm the energies calculated relative to the ground state (*) are given, for ^{149}Tb ground state masses from Table 4.2 have been used. References to the experimental data are given in the text where also the $21/2^-$ and $25/2^-$ level assignements in ^{151}Ho are discussed. (cf. caption to Fig. 5.2.)

5.2 Gamow–Teller strength.

An important application of the $\pi h_{11/2}\nu h_{9/2}$ interaction is the calculation of β–strength functions. In this region (N ≥ 82) the only allowed decay is the $\pi h_{11/2} \rightarrow \nu h_{9/2}$ GT–transition, and for the N = 82 parents the strength function can be calculated from the $\pi h^2_{11/2}$ and $\pi h_{11/2}\nu h_{9/2}$ interactions alone. In contrast to the above discussed yrast states, where the squared amplitudes of individual two–body couplings largely specify the level energies, the strength functions are significantly more sensitive to the detailed properties of the two–body interactions since they are governed by the amplitudes of the contributing couplings. Moreover, here all states with a given spin must be considered. They will in general lie above the yrast line and might well occur in regions of high level density where configuration mixing is significant.

As we have discussed in section 2.4.2, extraction of the total experimental strength for a particular GT–transition is of high theoretical interest, but in general the determination of this value is beset with serious experimental difficulties.

The reduced phase space for β–decay to levels in the daughter at high excitation, where configuration mixing further reduces the feeding to an individual state, together with the increased branching of the successive γ–decay all will contribute to the difficulties to identify the strength. An additional elementary problem is the distribution of the strength relative to the Q_β–value, which can only be taken from theory. For these reasons useful quenching factors can only be obtained in cases where the strength function is simple and preferably concentrated at low excitation energy.

Previous experiments have indicated [NOL 82] that this occurs in the $0^+ \rightarrow 1^+$ decays of the doubly even N = 82 isotones above Gd, where the $\pi h_{11/2} \rightarrow \nu h_{9/2}$ GT–decay almost exclusively proceeds to a single low–lying 1^+ state in the odd–odd daughter. These results are summarized in Fig.5.4. In each case the pertinent detection sensitivity is also shown, and it becomes evident that e.g. in ^{152}Tm half of the strength could have been missed even in the unlikely case that it were concentrated in a single state lying 1.2 MeV below the parent state.

The experimental data [KLE 88] for GT–decays of ^{150}Er and ^{152}Yb in the figure also include additional results from a current analysis of new data. The decay of ^{148}Dy was studied earlier [KLE 85], with much superior sensitivity than the other two, since the production of ^{150}Er and ^{152}Yb isotones is more difficult.

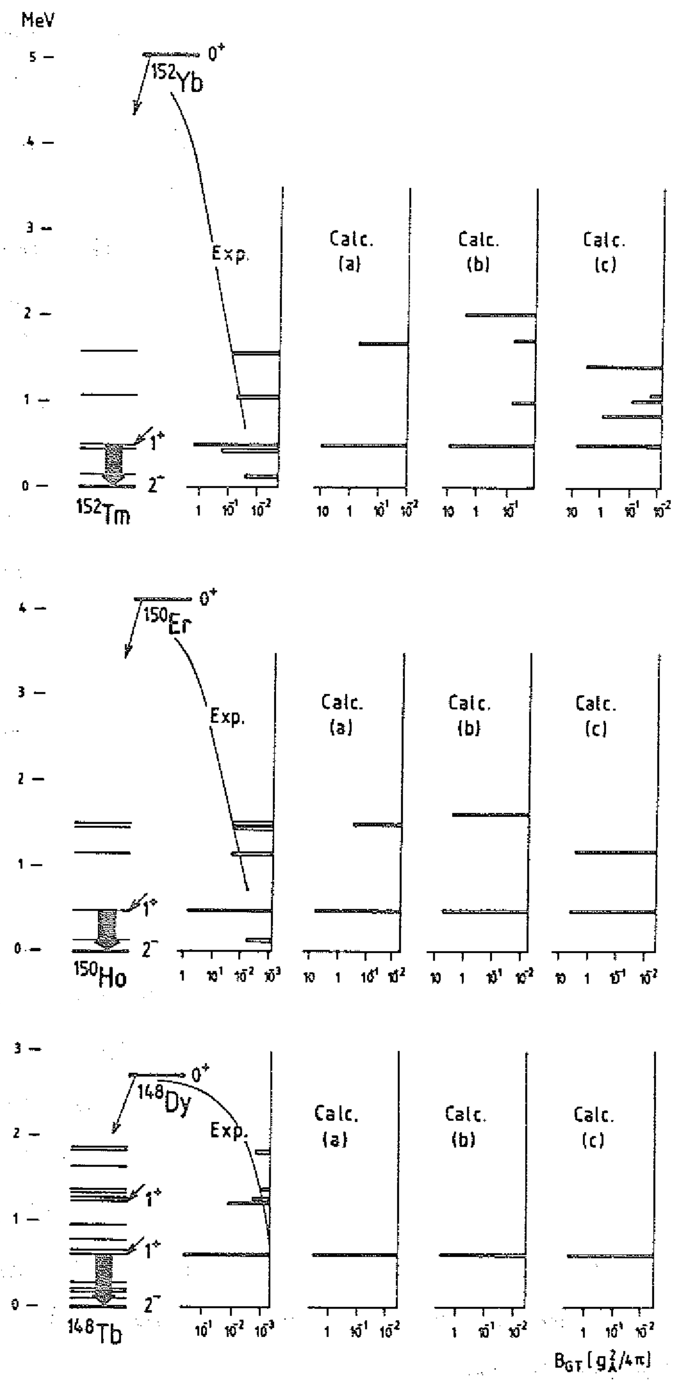

Fig.5.4 Measured GT strength functions for $0^+ \longrightarrow 1^+$ decays of doubly even N = 82 nuclei compared to results calculated with (a) the empirical $\pi h_{11/2} \nu h_{9/2}$ and $\pi h^2_{11/2}$ two-body interactions, (b) Schiffer-True interactions ($R_2 = 0.1$ fm), and (c) surface delta interactions ($A_0 = 0.429$ MeV, $A_1 = 0.106$ MeV [WAL 89]). The sensitivity limit for detection of an individual level is given. Open strength bars are drawn for levels with unclear spin-parity. Theoretical level energies are relative to the lowest experimental 1^+ state. Reference to the data are given in the text.

To demonstrate the strong dependence of the calculated strength function on the detailed properties of the two-body interactions we show for each case the results obtained with three different interactions, namely (a) our empirical $\pi h_{11/2}^{2}$ and $\pi h_{11/2}\nu h_{9/2}$ interactions, (b) the Schiffer–True interaction [SCH 76], and (c) with a surface delta (SDI) interaction [WAL 89]. We calculate the strength functions, with the OXBASH shell model code [BRO 86], where we restrict the configuration space to $\pi h_{11/2}^{2n}$ in the parent nucleus and to $\pi h_{11/2}^{2n-1}\nu h_{9/2}$ in the daughter nucleus. In the figure, the calculated 1^+ energies are normalized to the lowest experimental 1^+ state.

The result for ^{148}Tb is trivial, because the $\pi h_{11/2}\nu h_{9/2}$ configuration has only one 1^+ state. The $\pi h_{11/2}^{3}\nu h_{9/2}$ configuration of ^{150}Ho forms five 1^+ levels which all lie below 3.8 MeV excitation, but the lowest two receive, in the three calculations, more than 99% of the total decay strength. It is however obvious, from Fig.5.4, that only the calculation (a) is compatible with experiment, whereas for (b) and (c) the second 1^+ state should clearly have been seen in experiment.

The calculated results for ^{152}Tm feature even more pronounced variation. The configuration forms thirteen 1^+ levels, but again the calculated states shown carry $>99\%$ of the total strength. Also here it is evident that only the calculation with empirical two-body interactions is in accord with experiment. We note in passing that the second 1^+ state of calculation (a) lies close in energy, in ^{150}Ho and ^{152}Tm, to an experimental state with similar properties, where the data are compatible with a 1^+ assignement but cannot definitely establish it.

One significant aspect of the present analyses is the good agreement with experiment for the calculation (a) in all three cases, which demonstrates the optimal quality of the empirical two-body interactions also in the delicate problem of strength function calculations.

Even more important is their significance for determination of the GT reduction factor. Experimental strength reduction factors naturally derive always from the observed strength, and therefore tend to have rather small uncertainty, determined only by the errors of Q_β, $T_{1/2}$, and feeding fractions. But in general undetected β–feeding may well give rise to much larger, and in any case not controlled uncertainty.

The present results strongly suggest that in the three N = 82 decays considered the full strength is observed in experiment, and that losses due to configuration mixing should here be much less likely than in many other cases where the decay strength lies at high excitation energy.

CHAPTER 6 : Synopsis.

In the present work we report on results of β-decay measurements of N=82 and 83 nuclei above the doubly magic ^{146}Gd, namely the decays of the $1/2^+$ and $11/2^-$ isomers in ^{147}Tb and ^{149}Ho, and on the unusual β-decay of the $27/2^-$ 3-quasiparticle isomer in ^{149}Dy at 3 MeV excitation. For these nuclei the only allowed β-decay is the $\pi h_{11/2} \rightarrow \nu h_{9/2}$ GT-transition.

The data provide new information on several nuclear structure aspects. Among these are the absolute GT-transition strength, and the distribution of the $\nu h_{9/2}$ orbital in the daughter nucleus. The β-decay data firmly identify specific one- or few-nucleon configurations at low excitation in the daughter nucleus, and moreover, the γ-decay of the primary β-populated states can excite low-lying above yrast levels that cannot be reached by other techniques and are of particular interest for understanding of the nuclear structure in the nuclei of this region.

Results of the latter type include the identification of particle-phonon multiplets in the N=83 nuclei, formed by the couplings of the $\nu f_{7/2}$ valence particle with the respective N=82 core phonon. The ^{149}Ho decay data have disclosed the octupole septuplet in ^{149}Dy which exhibits smaller anharmonicities than found in the lower-Z isotones. This result therefore indicates a further decrease of the negative 3^- phonon quadrupole moment, in accord with expectations based on its microscopic structure. The decay data of ^{147}Tb gave new results on the $\nu f_{7/2} \times 2^+$ quintet in ^{147}Gd, suggesting a positive quadrupole moment for the ^{146}Gd 2^+ particle-hole phonon. Also this result can be anticipated from the microscopic composition of the ^{146}Gd 2^+ state.

The $\pi s_{1/2}$ ^{147}Tb ground state cannot decay by an allowed transition. Our data have shown that the decay predominantly proceeds to the $\nu p_{1/2}$ state in ^{147}Gd via the $\pi s_{1/2} \rightarrow \nu p_{1/2}$ first forbidden pseudoscalar transition, which here however is found to be 8 times slower than the same transition as observed in ^{207}Tl β^--decay. This reduction can be attributed to high-lying $[\pi s_{1/2}(\pi^{-1}\nu^{+1})_{0^-}]_{1/2^-}$ states in ^{147}Gd that screen the transition to the low-lying $\nu p_{1/2}$ state. Such particle-hole excitations are precluded in ^{207}Pb.

The comparison of the ^{147}Tb($1/2^+$) and ^{147}Tb($11/2^-$) decays strongly suggests that pair scattering of protons across Z = 64 is essentially not contributing to the β-decay. Consequently, the considerable fraction of GT-decay strength to high-lying states in ^{147}Gd must be attributed to decay of the odd $h_{11/2}$ valence proton, and in fact their γ-decay is consistent with $I^{\pi} = 9/2^{-}$. These levels are interpreted as $(\nu h_{9/2} \times 2^{+}_{146Gd})9/2^{-}$ excitations, and the results give quantitative information on the quadrupole core polarization at N = 83 which is responsible for the unusually large neutron effective charge values found in these nuclei, e.g. in atomic spectroscopy with collinear laser beams.

Since $\pi h_{11/2}$ pairs do not contribute to ^{147}Tb $11/2^{-}$ decay, the data provide an accurate value of the $\pi h_{11/2}$ Gamow-Teller single particle transition strength. From the shell model expectation of a decay strength proportional to the number of $h_{11/2}$ protons in the parent nucleus one would anticipate twice the strength for the ^{148}Dy two-particle nucleus, but instead we find the ratio to be only $B_{GT}^{148Dy}/B_{GT}^{147Tb} = 1.27(11)$. This reduced decay strength for paired protons is theoretically predicted as a specific feature of two-body core polarization, which is here for the first time verified in GT-decay. The effect is of crucial significance in current analyses of GT-quenching and of double β-decay rates.

For theoretical interpretation of the GT-strength function data, knowledge of the $\pi h_{11/2} \nu h_{9/2}$ two-body residual interaction is necessary, and previously only the 1^{+} coupling was known from experiment. The GT-decay of the ^{149}Dy $(\pi h^{2}_{11/2} \nu f_{7/2})27/2^{-}$ isomer allowed to determine the 10^{+} and 9^{+} $\pi h_{11/2} \nu h_{9/2}$ residual interactions from the decomposition of three nucleon excitations in ^{149}Tb populated in this decay. With these results, and the remaining 2^{+} to 8^{+} residual interactions estimated from other data, we have calculated the yrast states in N = 83 and 84 nuclei with up to ten valence particles in $\pi h_{11/2}$, $\nu f_{7/2}$, and $\nu h_{9/2}$, and we find detailed agreement with experimental energies. These parameter-free calculations exploit exclusively angular momentum symmetries as the dynamic quantities - two-body interactions, single particle energies, and, where available, ground state masses - are taken from experiment.

We also have calculated the GT-strength functions for the decays of the ^{150}Er and ^{152}Yb doubly-even nuclei. These $0^{+} \rightarrow 1^{+}$ decays are of particular interest for experimental determination of the reduction of the GT-transition rate. In experiment they are observed to populate only a single low–lying 1^+ state in the daughter nucleus, whereas the $\pi h^3_{11/2}\nu h_{9/2}$ and $\pi h^5_{11/2}\nu h_{9/2}$ configurations allow respectively five and thirteen 1^+ states. The data cannot exclude feeding into 1^+ levels at high excitation, where the detection sensitivity inevitably is reduced. However, the strength functions calculated with our empirical two–body interactions give the important result that more than 95% of the total $\pi h^{2n}_{11/2}$ decay strength is concentrated in the observed lowest–lying 1^+ level, a result which for these decays provides high reliability of the quenching factor derived from the strength observed in experiment.

LIST OF REFERENCES

AFA 71 V.P.Afanasiev, I.I.Gromova, G.Iskhakov, V.V.Kuznetsov, M.Ya.Kuznetsova, N.A.Lebedev: Izv. Akad. Nauk SSSR Ser. Fiz. 35(1971)719 [transl.: Bull. Akad. Sci. USSR, Phys. Ser. 35(1971)659].

ALK 83 G.D.Alkhazov, M.A.Mezilev, Yu.N.Novikov, N.Ganbaatar, K.Ya.Gromov, V.G.Kalinnikov, A.Potempa, E.Sieniawski, F.Tarkanyi: Z. Phys. A 310(1983)247.

ALK 89 G.D.Alkhazov, L.H.Batist, A.A.Bykov, V.D.Wittmann, S.Yu.Orlov, S.D.Payziev, A.G.Polyakov, V.K.Tarasov: Preprint LIYaF–1513, Leningrad 1989, [transl. in German in GSI–tr–90–08, July 1990].

ALK 90 G.D.Alkhazov, L.H.Batist, A.A.Bykov, V.N.Fedoseyev, V.S.Letokhov, V.I.Mishin, S.Yu.Orlov, Sh.D.Payziev, V.N.Pantaleyev, S.K.Sekatsky, V.K.Tarasov, V.D.Wittmann: Preprint LNPI–1651, Leningrad 1990.

BAR 88 R.Barden, A.Plochocki, D.Schardt, B.Rubio, M.Ogawa, P.Kleinheinz, R.Kirchner, O.Klepper, J.Blomqvist: Z. Phys. A 329(1988)11.

BAS 80 G.Bastin, A.Peghaire, J.P.Thibaud, S.Andre, D.Barneoud, C.Foin, P.Aguer: Nucl. Phys. A 345(1980)302.

BLO 79 J.Blomqvist: Proc. Symp. on High–Spin Phenomena in Nuclei, Argonne 1979, ANL/PHY–79–4, p.155.

BLO 83 J.Blomqvist, P.Kleinheinz, P.J.Daly: Z. Phys. A 312(1983)27.

BOH 75 A.Bohr and B.R.Mottelson: Nuclear Structure (W.A.Benjamin Inc., Reading, Mass., 1975), Vol. II, Ch. 6, p. 569ff.

BOW 73 W.W.Bowman, D.R.Haenni, T.T.Sugihara: Phys. Rev. C 7(1973)1686.

BRO 86 B.A.Brown, A.Etchegoyen, W.D.M.Rae: OXBASH, the Oxford–Buenos–Aires–MSU Shell–Model code, MSUCL Report 524, unpublished.

BRU 77 P.J.Brussaard, P.W.M.Glaudemans: Shell–model applications in nuclear spectroscopy (Amsterdam, North–Holland, 1977).

CHU 69 Y.Y.Chu, E.M.Franz, G.Friedlander: Phys. Rev. 187(1969)1529.

CIV 90 O.Civitarese, A.Faessler, J.Suhonen, X.R.Wu: Departement of physics, University of Jyväskylä, preprint 23/90, 1990.

COL 90 R.Collatz: Diplomarbeit, Universität zu Köln, 1990.

COL 91 R.Collatz, R.Menegazzo, R.Broda, C.T.Zhang, P.Kleinheinz, J.Rico, J.Blomqvust: Verhandl. DPG(VI)26, Darmstadt 1991, p.490.

DAL 80 P.J.Daly, P.Kleinheinz, R.Broda, S.Lunardi, H.Backe, J.Blomqvist: Z. Phys. A 298(1980)173.

DEC 84 D.J.Decman, L.G.Mann, G.L.Struble, D.H.Sisson, C.M.Henderson, H.J.Scheerer, P.Kleinheinz, K.E.Thomas, H.A.O'Brein: Proc. 7th Int. Conf. on Atomic Masses and Fundamental Constants, AMCO-7, Darmstadt-Seeheim 1984, O.Klepper (ed.), p.220.

deS 61 A.de Shalit: Phys. Rev. 122(1961)1530.

EDM 57 A.R.Edmonds: Angular Momentum in Quantum Mechanics (Princeton University Press, Princeton, N.J., 1957).

ENG 88 J.Engel, P.Vogel, M.R.Zirnbauer: Phys. Rev. C 37(1988)731.

ERC 83 A.Ercan, R.Broda, M.Piiparinen, P.Kleinheinz, J.Blomqvist: Proc. Int. Conf. on Nuclear Physics, Florence 1983, p.154.

FIR 89 R.B.Firestone, J.M.Nietschke, P.A.Wilmarth, K.Vierinen, J.Gilat, K.S.Toth, Y.A.Akovali: Phys. Rev. C 39(1989)219.

GAA 83 C.Gaarde: Nucl. Phys. A 396(1983)127c.

GIZ 81 J.Gizon, A.Gizon, S.Andre, J.Genevey, J.Jastrzebski, R.Kossakowski, M.Moszynski, Z.Preibisz: Z. Phys. A 301(1981)67.

GOO 80 C.D.Goodman, C.A.Goulding, M.B.Greenfield, J.Rapaport, D.E.Bainum, C.C.Foster, W.G.Love, F.Petrovich: Phys. Rev. Lett. 44(1980)1755.

GOV 71 G.B.Gove, M.J.Martin: Nucl. Data Tables 10(1971)205.

HOF 79 S.Hofmann, W.Faust, G.Münzenberg, W.Reisdorf, P.Armbruster, K.Güttner, H.Ewald: Z. Phys. A 291(1979)53.

KAD 89 H.Kader, G.Graw, F.J.Eckle, G.Eckle, P.Schiemenz, P.Kleinheinz, B.Rubio, G.de Angelis, T.N.Massey, L.G.Mann, J.Blomqvist: Phys. Lett. B 227(1989)325.

KEL 89 H.Keller, R.Kirchner, O.Klepper, E.Roeckl, K.Rykaczewski, D.Schardt, R.S.Simon, P.Kleinheinz, W.Meczynski, R.Menegazzo, C.F.Liang, P.Paris, J.Zylicz: GSI, Darmstadt, Scientific Report 1989, p.19.

KEL 91A H.Keller: Doktorarbeit, TH Darmstadt, GSI Report, GSI-91-06, 1991.

KEL 91B H.Keller, D.Schardt, E.Roeckl, R.S.Simon, O.Klepper, R.Kirchner, P.Kleinheinz, R.Menegazzo, C.F.Liang, P.Paris, K.Rykaczewski, J.Zylicz: Z. Phys. A, in press.

KLE 75 P.Kleinheinz, M.R.Maier, R.M.Diamond, F.S.Stephens, R.K.Sheline: Phys. Lett. 53B(1975)442.

KLE 79A P.Kleinheinz, R.Broda, P.J.Daly, S.Lunardi, M.Ogawa, J.Blomqvist: Z. Phys. A 293(1979)279.

KLE 79B P.Kleinheinz: Proc. Symp. on High-Spin Phenomena in Nuclei, Argonne 1979, ANL/PHY-79-4, p.125.

KLE 81 P.Kleinheinz: Phys. Scr. 24(1981)236.

KLE 85	P.Kleinheinz, K.Zuber, C.Conci, C.Protop, J.Zuber, C.F.Liang, P.Paris, J.Blomqvist: Phys. Rev. Lett. 55(1985)2664.
KLE 88	P.Kleinheinz, R.Barden, R.Kirchner, O.Klepper, A.Plochocki, E.Roeckl, B.Rubio, D.Schardt: Inst. f. Kernphysik, KFA Jülich, Annual Report 1988, p.34, and R.Menegazzo, P.Kleinheinz, B.Rubio, D.Schardt: preliminary results.
KLE 91	P.Kleinheinz, G.de Angelis, B.Rubio, H.J.Scheerer: to be published.
KOM 83	T.Kommpa, R.Komu, M.Kortelahti, J.Muhonen, A.Pakkanen, M.Piiparinen, I.Prochazka, J.Blomqvist: Z. Phys. A 314(1983)33.
KUN 88	A.Kuhnert: Doktorarbeit, Universität und HMI Berlin, 1988, and A.Kuhnert, K.H.Meier, H.Kluge, H.Grawe, H.Hübel, F.S.Stephens, M.A.Delaplangue: HMI Berlin, Preprint 1988.
LAC 91	M.Lach, P.Kleinheinz, M.Piiparinen, M.Ogawa, S.Lunardi, M.C.Bosca, J.Styczen, J.Blomqvist: Z. Phys. A, in press.
LED 78	Table of Isotopes, 7th Edn., C.M.Lederer, V.S.Sherley (Eds.), (Wiley, New York, 1978).
LIA 87	C.F.Liang, P.Paris, P.Kleinheinz, B.Rubio, M.Piiparinen, D.Schardt, A.Plochocki, R.Barden: Phys. Lett. B 191(1987)245.
LUN 79	S.Lunardi, M.Ogawa, H.Backe, M.Piiparinen, Y.Nagai, P.Kleinheinz: Proc. Symp. on High Spin Phenomena in Nuclei, Argonne 1979, ANL-PHY-79-4, p.403.
MAN 88	L.G.Mann, K.H.Maier, A.Aprahamian, J.A.Becker, D.J.Decman, E.A.Henry, R.A.Meyer, N.Roy, W.Stöffl, G.L.Struble: Phys. Rev. C 38(1988)74.
MAN 90	L.G.Mann, D.J.Decman, H.E.Martz, T.N.Massey, G.L.Struble, P.Kleinheinz, H.J.Scheerer, D.G.Burke, G.Kajrys: Z. Phys. A 337(1990)301.
McN 86	J.H.McNeill, R.Broda, Y.H.Chung, P.J.Daly, Z.W.Grabowski, H.Helppi, M.Kortelahti, R.V.F.Janssens, T.L.Khoo, R.D.Lawson, D.C.Radford, J.Blomqvist: Z. Phys. A 325(1986)27.
McN 89	J.H.McNeill, A.A.Chisti, P.J.Daly, M.A.C.Hotchkis, M.Piiparinen, B.J.Varley: Z. Phys. A 332(1989)105.
McN 90	J.H.Mcneill, J.Blomqvist, A.A.Chisti, P.J.Daly, W.Gelletly, M.A.C.Hotchkis, M.Piiparinen, B.J.Varley, P.J.Woods: Z. Phys. A 335(1990)241.
NAG 81	Y.Nagai, J.Styczen, M.Piiparinen, P.Kleinheinz, D.Bazzacco, P.v.Brentano, K.O.Zell, J.Blomqvist: Phys. Rev. Lett. 47(1981)1259.
NDS 85	J.A.Szücs, M.W.Johns, B.Singh: Nuclear Data Sheets 46(1985)1.
NEW 74	E.Newman, K.S.Toth, D.C.Hensley, W.D.Schmidt-Ott: Phys. Rev. C 9(1974)674; Erratum Phys. Rev. C 12(1975)346.

NOL 82 E.Nolte, G.Korschinek, Ch.Setzensack: Z. Phys. A 309(1982)33.

OGA 77 M.Ogawa, S.Lunardi, M.R.Meier, P.Kleinheinz: Proc. Int. Symp. on high-spin States and Nuclear Structure, Dresden 1977, ZfK-336, L.Funke (ed.), p.31; and Inst. f. Kernphysik, KFA Jülich, Annual Report 1976, p.38.

PII 84 M .Piiparinen, P.Kleinheinz, K.Zuber, D.Schardt, O.Klepper, R.Kirchner, E.Roeckl, J.Blomqvist: Institut für Kernphysik, KFA Jülich, Annual Report 1984, p.110.

PII 90 M.Piiparinen, P.Kleinheinz, S.Lunardi, M.Ogawa, G.de Angelis, F.Soramel, W.Meczynski: Z. Phys. A 337(1990)387.

RAT 84 G.E.Rathke: Diplomarbeit, Technische Universität München, 1984.

RÖS 78 F.Rösel, H.M.Fries, K.Adler, H.C.Pauli: Atomic Data and Nuclear Data Tables 21(1978)110.

RUB 86 B.Rubio, A.Ercan, G.de Angelis, P.Kleinheinz, J.L.Tain, B.Brinkmöller, D.Paul, J.Meissburger, L.G.Mann, D.J.Decman, T.N.Massey, G.L.Struble, H.J.Scheerer, J.Blomqvist: Z. Phys. A 324(1986)27.

SCH 84 D.Schardt, P.O.Larsson, R.Kirchner, O.Klepper, V.T.Koslowsky, E.Roeckl, K.Rykaczewski, K.Zuber, N.Roy, P.Kleiheinz, J.Blomqvist: Proc. 7^{th} Int. Conf. on Atomic Masses and Fundamental Constants, AMCO-7, Darmstadt-Seeheim 1984, O.Klepper (ed.), p.222.

SCH 87 D.Schardt, R.Barden, R.Kirchner, O.Klepper, A.Plochocki, E.Roeckl, P.Kleinheinz, M.Piiparinen, B.Rubio, K.Zuber, C.F.Liang, P.Paris, A.Huck, G.Walter, G.Marguier, H.Gabelmann, J.Blomqvist: Proc. 5^{th} Int. Conf. on Nuclei far from Stability, Rosseau Lake 1987, I.S.Towner (ed.), (New York: AIP Conf. Proc. 164), p. 477.

SCH 76 J.P.Schiffer, W.W.True: Rev. of Mod. Phys. 48(1976)191.

SIN 79 N.C.Singhal, M.W.Johns, J.V.Thompson: Can. J. Phys. 57(1979)1959.

STE 76A A.M.Stefanini, P.Kleinheinz, M.R.Maier: Phys. Lett. 62B(1976)405.

STE 76B A.M.Stefanini, P.J.Daly, P.Kleinheinz, M.R.Maier, R.Wagner: Nucl. Phys. A 258(1976)34.

STY 81 J.Styczen, P.Kleinheinz, M.Piiparinen, J.Blomqvist: Proc. 4^{th} Int. Conf. on Nuclei far from Stability, Helsingor, (Denmark 1981), CERN 81-09, p.548.

STY 87 J.Styczen, P.Kleinheinz, W.Starzecki, B.Rubio, G.de Angelis, H.J.Hähn, C.F.Liang, P.Paris, R.Reinhardt, P.von Brentano, J.Blomqvist: Proc. 5^{th} Int. Conf. on Nuclei far from Stability, Rosseau Lake 1987, I.S.Towner (ed.), (New York: AIP Conf. Proc. 164), p.489.

STY 88 J.Styczen, P.Kleinheinz, M.Piiparinen, B.Rubio, H.Güven, W.Starzecki, D.Schardt, G.Walter, A.Huck, G.Marguier, J.Blomqvist and ISOLDE collaboration: Inst. f. Kernphysik, KFA Jülich, Annual Report 1988, p.30.

STY 91 J.Styczen, P.Kleinheinz, M.Lach, R.Menegazzo, W.Meczynski, H.Güven, J.L.Tain, G.Walter, A.Huck, G.Marguier, D.Schardt, J.Blomqvist: Inst. f. Kernphysik, KFA Jülich, preprint 1991.

SUH 88 J.Suhonen, T.Taigel, A.Faessler: Nucl. Phys. A 486(1988)91.

TAI 89 J.L.Tain, B.Rubio, P.Kleinheinz, D.Schardt, R.Barden, J.Blomqvist: Z. Phys. A 333(1989)29.

TOT 79 K.S.Toth, C.R.Bingham, D.R.Zolnowski, S.E.Cala, H.K.Carter, D.C.Sousa: Phys. Rev. C 19(1979)482.

TOT 87A K.S.Toth, D.C.Sousa, J.M.Nitschke, P.A.Wilmarth: Phys. Rev. C 35(1987)310.

TOT 87B K.S.Toth, D.C.Sousa, J.M.Nitschke, P.A.Wilmarth: Phys. Rev. C 35(1987)620.

TOW 85 I.S.Towner: Nucl. Phys. A444(1985)402.

TRA 89 L.Trache, A.Clauberg, C.Wesselborg, P.v.Brentano, J.Wrzesinski, R.Broda, A.Berinde, V.E.Iacob: Phys. Rev. C 40(1989)1006.

VEJ 69 C.J.Veje in A.Bohr and B.R.Mottelson: Nuclear Structure (W.A.Benjamin Inc., Reading, Mass., 1969), Vol. I, Ch. 2, p.239.

VIE 88 K.S.Vierinen, A.A.Shihab-Eldin, J.M.Nitschke, P.A.Wilmarth, R.M.Chasteler, R.B.Firestone, K.S.Toth: Phys. Rev. C 38(1988)1509.

VYL 72 Ts.Vylov, K.Ya.Gromov, I.I.Gromova, G.I.Iskhakov, V.V.Kuznetsov, M.Ya.Kuznetsova: Kiev Report 1972.

WAL 89 N.R.Walet, P.Stoop, P.W.M.Glaudemans: Z. Phys. A 332(1989)9.

YAT 86 S.W.Yates, R.Julin, P.Kleinheinz, B.Rubio, L.G.Mann, E.A.Henry, W.Stöffl, D.J.Decman, J.Blomqvist: Z. Phys. A 324(1986)417.

ZHA 91 C.T.Zhang, R.Broda, R.Menegazzo, K.H.Maier, H.Grawe, P.Kleinheinz, M.Lach, R.Collatz: to be published.

ACKNOWLEDGEMENT

I acknowledge with sincere thanks the generosity of the Forschungszentrum Jülich and Prof. Otto Schult who supported fully my three years work at the Institut of Nuclear Physics, KFA Jülich.

I am grateful to Dr. Peter Kleinheinz for his invaluable and continuous help and perceptive criticism during my stay in his group, where I have enjoyed the privilege of having collaborated with Prof. Jan Blomqvist and Prof. Jan Styczen, from all of whom I have learned a great deal in many revealing discussions.

I wish to thank Wojtek Starzecki and Mardi Karnadi for the assistance they gave me with computer programming, Rüdiger Collatz, Rafał Broda, Cheng Teng Zhang, and Patrick Daly who contributed friendly support, as well as valuable suggestions, and Peter Wieder for accurately drawing many of the figures of this thesis.

I would like to express my gratitude to Karin Luft, Helga Paffen, and Claudia Strauch who solved many everyday problems.

FORSCHUNGSZENTRUM JÜLICH GmbH

KFA

Jül-2529
September 1991
ISSN 0366-0885